FACTORS AFFECTING THE INSULATION OF UHV SYSTEMS

A MASTER THESIS

SUBMITTED TO THE DEPARTMENT OF ELECTRICAL ENGINEERING
AND THE COMMITTEE ON FACULTY OF ENGINEERING
OF MIDDLE EAST TECHNICAL UNIVERSITY
IN PARTICAL FULFILLMENT OF THE REQUIREMENTS

FOR THE DEGREE OF
MASTER OF SCIENCE

by

Kesut Büyüközer

August, 1978

I certify that I have read this thesis and that in my opinion it is fully adequate, in scope and quality, as a thesis for degree of Master of Science.

.....

Supervisor

Asst.Prof.Dr.Nevzat Özay

I certify that this thesis satisfies all the requirements as a thesis for the degree of Master of Science.

.....

Chairman of the Department

Examining Committee in Charge

Murahan Hilal ....

Prof. Ertaş ....

Güder Aşan ....

Assoc. Prof. Dr. Ahmet Kumeli ....

Committee Chairman

ABSTRACT

FACTORS AFFECTING THE INSULATION OF

UHV SYSTEMS

Mesut Büyüközer
M.S. in E.E.
Supervisor: Asst.Prof.Dr.Nevzat Özay
August, 1978: 124 pages

Energization and reenergization overvoltages are the primary factors in establishing power system insulation level. As these overvoltages are generated by the closing operation of the circuit breaker which can be controlled to produce the minimum surge, then insulation level can be reduced for economic system design. However other causes of overvoltages (steady state, fault, fault clearing) which are not controllable other than initial system design may produce sufficiently high voltages wiping out the savings made.

In the thesis, the cause and maximum overvoltages produced during the normal operation, fault and fault clearing which would indicate the lower limits of surge reduction by the adjustment of circuit breaker are investigated and the measures to control these overvoltages are examined.

Key words: Circuit breaker, Transient recovery voltage, Rate of rise of recovery voltage, Opening resistor, Shunt reactor, Fault, Trapped charge.

ÖZET

ÇOK YÜKSEK GERİLİM SİSTEMLERİNİN İZOLASYONUNA ETKİ EDEN FAKTÖRLER

Mesut Büyüközer
Yüksek Lisans Tezi: Elektrik Mühendisliği Bölümü
Tez Yöneticisi: Asst.Prof.Dr.Nevzat Özay
Ağustos, 1978 : 124 sayfa

Enerjileme ve tekrar enerjilemeden dolayı meydana gelen aşırı gerilimler, enerji sistemlerinin izolasyon seviyesinin tesbitinde en önemli faktördür. İzolasyon seviyesini düşürerek ekonomik bir sistem tasarımı yapabilmek için kesicilerin kapanmasından doğan bu aşırı gerilimleri, kesicileri kapanma anında kontrol ederek azaltmak mümkündür. Bununla beraber, ancak ilk sistem tasarımı sırasında kontrolü mümkün olabilen diğer aşırı gerilim sebebleri (durgun rejim, arıza, arıza temizlenmesi), kesici kontroluyla elde edilebilen kazancı yokedebilecek derecede aşırı gerilimlere sebeb olabilirler.

Bu tezde, kesici kontrolüyle aşırı gerilimlerin düşürülebilecoği alt limiti tayin eden durgun rejim, arıza ve arıza temizlenmesinden doğan aşırı gerilimlerin sebebleri, maksimum değerleri, kontrol çareleri araştırılmaktadır.

Anahtar kelimeler: Kesici, Geçici rejim düzelme gerilimi, Düzelme geriliminin yükselme oranı, açma direnci, şönt reaktör, Arıza, Kalıcı yük.

ACKNOWLEDGEMENTS

The author wishes to express his gratitude to his supervisor, Asst.Prof.Dr.Nevzat Özay, for the opportunity to study under his guidance, for constant encouragement and helpful suggestions. He would like to thank technical staff of Research and Development Division of Turkish Electricity Authority for their interest and sincere suggestions. The author is also grateful to Miss Suna Gebizli for her nice typing.

TABLE OF CONTENTS

TABLE OF CONTENTS (CONTINUED)

TABLE OF CONTENTS (CONTINUED)

LIST OF TABLES

LIST OF FIGURES

LIST OF FIGURES (CONTINUED)

LIST OF FIGURES (CONTINUED)

CHAPTER I

INTRODUCTION

1.1 General

It is well known that proper insulation coordination is an important factor in the economic design of transmission system. Once the maximum operating voltage is established, the insulation requirements are basically determined by the overvoltages that can occur on the system.

Overvoltages can be classified in two primary categories:

1. External Overvoltages: These are caused by atmospheric discharges (lightning) and are independent of system operating voltage.

2. Internal Overvoltages: These are due to system faults and switching operations (connection or disconnection of load, interruption of circuit elements), and transient and steady state voltage variations.

The overvoltages due to lightning are essentially independent of voltage class neglecting moderate increase with the height of the tower since heights are much less than proportional to operating voltage. Lightning overvoltages will generall be dominant factor for insulation of the systems operating below 300 kv, where the system insulation levels are comperable.(36)

In the systems operating between 300-500 kv, if adequate shielding of the lines and low tower footing resistance are provided, the overvoltages produced by closing and reclosing (i.e. closing on trapped charge) become the deciding factor for the choice of insulation.(3)

If no special precautions are taken to limit switching surge magnitude, overvoltages as high as 4 times nominal line to neutral (crest) voltage are possible, where a value of 3.5 p.u. may be used as an approximate mean values.[3, 31] It should be observed that the 60 Hz and switching surge flashover strength of insulators do not increase in direct proportion to the number of insulator units and gap spacing, but saturate as the voltage level increases (Fig. 1.1)[2]

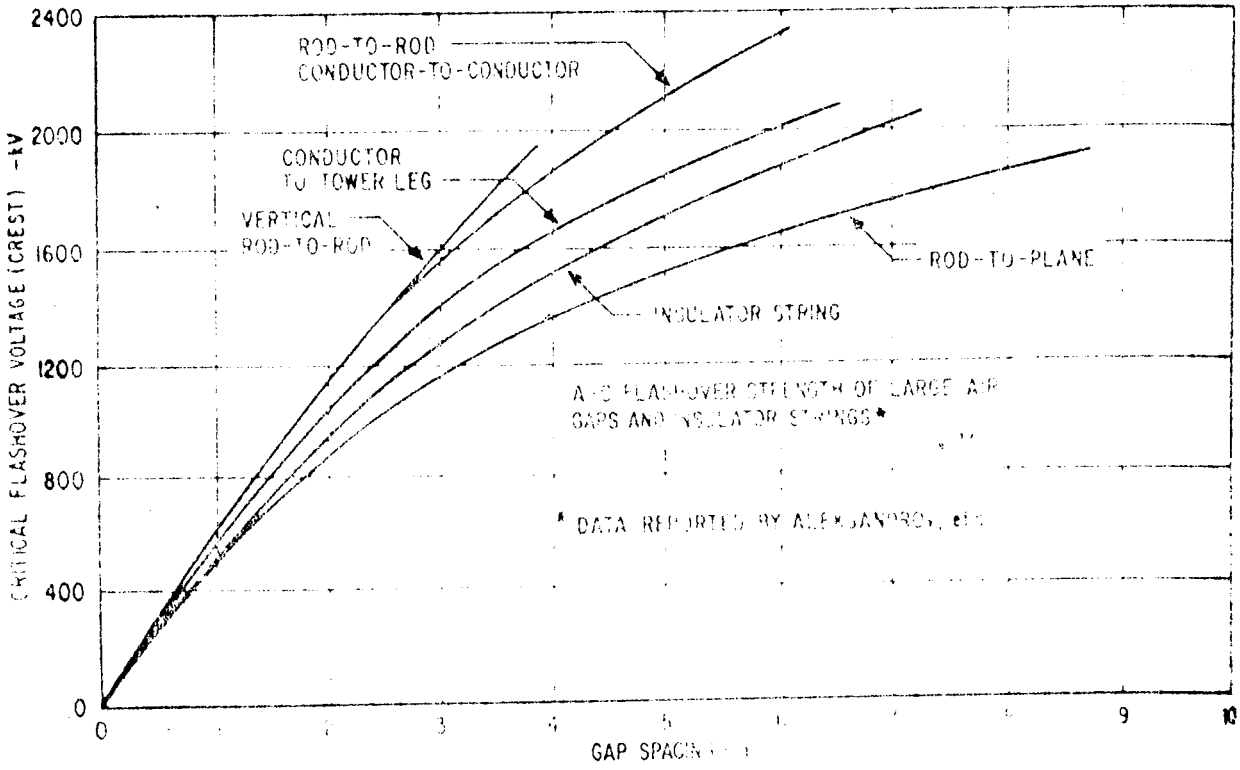

Fig.1.1 A-C flashover strength of large air gaps and insulator string as reported by Aleksandrov.[2]

Due to the saturation characteristics of air and porcelain dielectrics, it has become necessary to take steps to limit switching surges due to line energization and reenergization to less than 2.5 p.u at EHV and UHV system levels in order to make them economically feasable. As these surges are generated by the closing operation of the circuit breaker (CB) which can be adjusted to produce the minimum surge, then solution of the problem becomes straight forward. Effective switching surge control can be gained by synchronous closing of the circuit breaker by controlling the timing of breaker contact closing, by inserting one or more resistors across the breaker contacts, or by combination of these methods.[26,27] By using these various control methods, nearly all energizing and reenergizing transients can be reduced to 1.5 p.u or less, the more the reduction, the costlier the CB becoming.

If the overvoltage levels due to line energization and reenergization are reduced below 2 p.u. (infact, UHV system voltages are only feasible if this is so), then other overvoltage causes, in particular faults, load rejection, fault clearing must be taken into consideration. These latter causes, in general produce overvoltages somewhere between 1.0 p.u and 2.0 p.u of the system nominal voltage depending upon system conditions. However, as these causes, contrary to the case of energization, are not controllable other than by initial system design, they must be checked out first to see if further savings are possible by reducing the insulation level less than 2.0 p.u.

1.2 Purpose and Scope of the Thesis.

The purpose of this thesis is to investigate the causes and maximum overvoltages produced during the normal operation, fault and fault clearing which would indicate the lower limits of surge reduction by the adjustment of CB.

In Chapter 2, steady state overvoltages and measures to reduce them are examined. Overvoltages due to faults on transmission lines are analysed in Chapter 3. Chapter 4 presents the transient overvoltages due to load dropping and fault clearing. The influence of system configurations and measures to control overvoltage magnitudes are also briefly examined. Finally, in Chapter 5, the behaviour of lines after its disconnection from the power source and preparation of line to re-energization are studied.

In all cases, first a theoretical study of the problem is made using single phase system, then the system is simulated on the digital computer using the already developed Transients Analysis Program, the outline of which are given in Appendix C. The digital computer results are compared with the theoretical derivations.

CHAPTER II

STEADY STATE OVERVOLTAGES

2.1. Introduction

Generally, overvoltages in the steady state period occur on a transmission line that is either connected to the system at only one end, with the receiving end being disconnected or loaded below its surge impedance loading. Such situations arise during normal operations and can continue from several seconds to many minutes.(1)

External insulation design of EHV transmission systems is largely determined by switching surge and in some rare cases by lightning requirements.(2) If the insulation is designed on the basis of these requirements, the strength for power frequency voltages and clean insulators even in wet conditions is normally very high, being more than double the stress.(3) This also can be considered sufficient to withstand power frequency overvoltages (steady state overvoltages).

However, insulation failures may occur due to steady state overvoltages in wet weather conditions and are caused by contamination of the insulator-surface.(2)

Contamination flashovers on transmission systems are initiated by the deposition of airbone particles on the insulators. These particles may be of natural origin or generated by artificial pollution which mostly is a result of industrial activities. It should be noted that these deposits themselves do not decrease the insulation strength when they are dry. The loss of strength is caused only by the combination of two factors: contaminants and moisture. Infact, moisture is always necessary to

produce a conductive layer on contaminated insulator surfaces.

Contamination problems are beyond the scope of the thesis. Furthermore it should be noted that according to a report by CESI,[4] pollution does not seem to be a problem in Turkey for the time being.

2.2. Loadings of the Line

A newly constructed EHV transmission system usually have line loading well below surge imedance loading for both normal and emergency conditions in the early years. In the long range, the line loading eventually will reach to normal magnitude associated with EHV transmission system.

A line will show different characteristics under different loading arrangement resulting in different overvoltage magnitudes.

a) Underloaded case at receiving end:

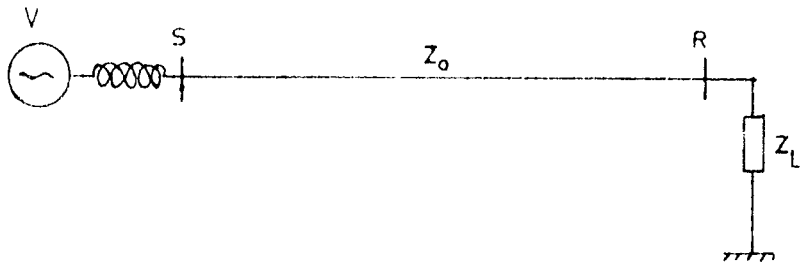

Fig.2.1 Single phase line

When the load at the receiving end is below the surge impedance loading (Fig. 2.1), load impedance Z_L is greater than line surge impedance Z_o.

$$Z_L > Z_o$$

Using the equation A.19 developed in the Appendix A, sending end voltage V_S can be written interms of receiving end voltage V_R, line surge impedance and load impedance as follows:

$$V_S = V_R \left[\cos \beta l + j \frac{Z_o}{Z_L} \sin \beta l \right] \qquad (2.1)$$

As the ratio Z_o/Z_L is less than 1, then

$$\left| \text{Cos}\,\beta l + j \frac{Z_o}{Z_L} \text{Sin}\,\beta l \right| < 1 \qquad (2.2)$$

This implies that, receiving end voltage magnitude V_R is greater than sending end voltage magnitude V_S, that is,

$$|V_S| < |V_R|$$

If receiving end is open, then $Z_L = \infty$

$$V_S = V_R \text{ Cos}\,\beta l \qquad (2.3)$$

This is the well known Ferranti effect.

A physical explanation of the phenomena is as follows: As Z_L is greater than Z_o, then the capacitive line charging power V_R^2 / X_C is greater than that of used by the line inductances $I_R^2 X_L$ where X_C and X_L line capacitance and inductive admittance. This surplus reactive power causes the voltage rises at the receiving end.

Shunt reactors are normally installed at the EHV substations to

absorb the additional reactive power produced. Shunt reactors and their effects will be discussed later.

b) Surge impedance loading at receiving end:

When line is terminated with its characteristic impedance, the power delivered is known as the surge impedance loading (SIL). From equation (2.1) with

$$\text{LOAD} = \text{SIL} \qquad \text{and} \qquad Z_L = Z_o,$$

$$V_S = V_R \left[\cos\beta l + j \sin\beta l \right] \tag{2.4}$$

Hence

$$|V_S| = |V_R|$$

For lossless line under SIL condition the reactive power absorbed by the line is equal to the reactive power generated i.e.

$$\frac{V_R^2}{X_C} = I_R^2 X_L \tag{2.5}$$

$$\frac{V_R}{I_R} = Z_o = \sqrt{X_L X_C} = \frac{\sqrt{JwL1}}{\sqrt{JwC1}} = \frac{\sqrt{L}}{\sqrt{C}} \tag{2.6}$$

where L and C are line inductance and capacitances respectively for per unit length.

l is the total line length.

At SIL, V and I are in phase and there will be no charging current. Therefore optimum transmission condition is obtained.

c) Overloaded case at receiving end:

In this case,

$$\text{LOAD} > \text{SIL} \quad , \quad Z_L < Z_o$$

$$V_S = V_R \left[\cos \beta l + j \frac{Z_o}{Z_L} \sin \beta l \right]$$

$$|V_S| = |V_R| \left[\cos^2 \beta l + \left(\frac{Z_o}{Z_L} \right)^2 \sin^2 \beta l \right]^{1/2} \qquad (2.7)$$

$$\text{Since} \quad \frac{Z_o}{Z_L} > 1 \implies \left| \cos \beta l + j \frac{Z_o}{Z_L} \sin \beta l \right| > 1 \qquad (2.8)$$

$$\text{Hence} \quad |V_S| > |V_R|$$

The inductive loss of the line $I_R^2 X_L$ is greater than that generated by the line capacitances V_R^2 / X_C and the insufficient amount of reactive power causes the voltage drop at the receiving end. In order to maintain the reactive power equilibrium for regulation of voltage levels, shunt capacitors are used to generate the additional reactive power. An infeed of reactive power into a line rises the line voltage, and this is most pronounced near the point of infeed.

2.3. Saturation Effects[6,7,8]

As it is explained in section 2.2., for the line loading below SIL, the excess line charging currents (reactive power) flow into reactive loads and machines located on lower voltage facilities from transmission lines. This line charging current flowing during light load condition causes voltage rises from the system source to the sending end of the

line and from sending end to receiving end. When the voltage rise across the system inductance is high enough to make the transformer operate above the knee of its magnetization curve, the nonlinearity of the curve generated harmonics which can result in increased overvoltages.

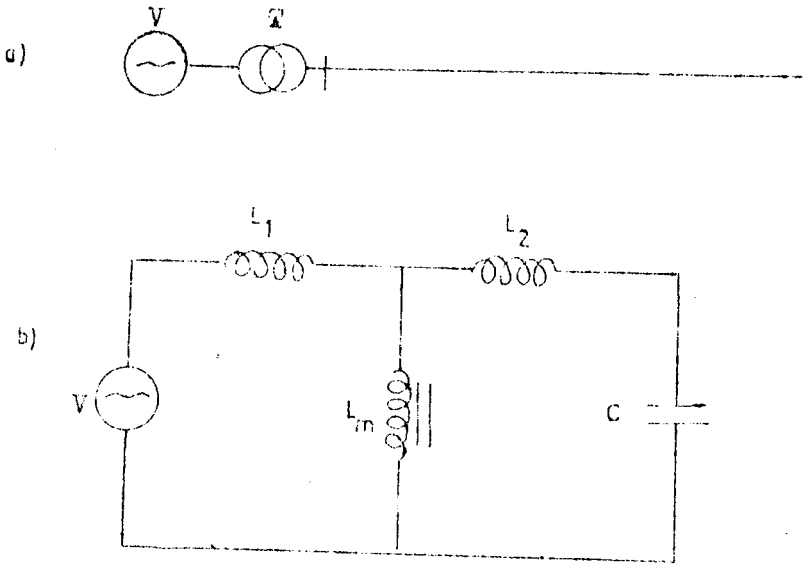

L_1, L_m - short circuit and magnetizing inductance of the transformer

L_2, C - Inductance and capacitance of the line.

Fig. 2.2 Circuit in which the occurrence of resonance phenomena at higher harmonic is possible.

Fig.2.2 shows a typical circuit with its equivalent to be considered in the study of saturation effect of the transformer. If the transformer is in saturation (operation voltage is above the knee point of the transformer magnetizing curve), the magnetizing current flowing through the nonlinear inductance L_m contains a fundamental frequency component and components of odd higher harmonics.[7] If the natural frequency of the linear part of the circuit i.e.,

$$f_o = \frac{1}{2\pi\sqrt{(L_1 + L_2)\ C}} \qquad (2.9)$$

is equal to one of the higher harmonic frequencies, higher odd harmonic

overvoltages will be caused at various points in the actual network. If the transformer has one of the winding delta connected only the 5th and higher harmonics can cause overvoltages in the actual network, the third harmonics being reduced by delta winding.

It is well known fact that in linear series circuit of L, R and C, extremely high voltages can occur across L and C components, particularly if the natural frequency of L and C is near the source voltage frequency.

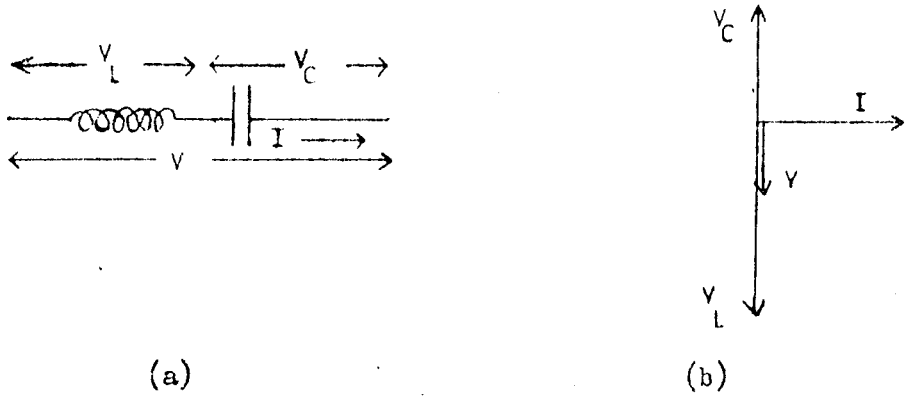

Fig.2.3. Simple series resonance.

From Fig. 2.3.b, it is evident that the voltages V_L and V_C add give the applied voltage V. But, because the voltage across the inductor leads the current in phase by 90°, and the capacitor voltage lags the current by the same amount, the phasor diagram appears as in Fig. 2.3.b. It is seen that both V_L and V_C can far exceed V. Voltage condition of this kind can be sustained when the power frequency is near to circuit natural frequency. Therefore, under certain circumstances the capacitance of power circuit can come into series resonance with the circuit inductance to produce excessive voltages. This phenomenon is called ferro-resonance if a saturable transformer is present.

Consider a line with an unloaded autotransformer connected to its receiving end and fed by a power source as shown in Fig. 2.4. The system is simulated

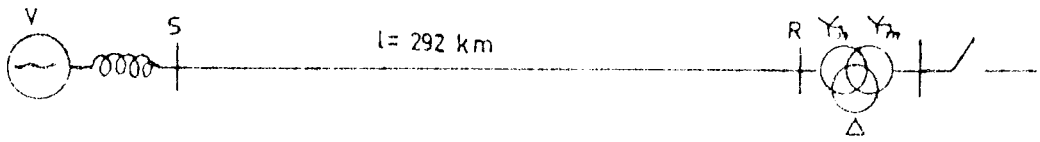

Fig. 2.4 EHV system studied for transformer saturation effect.

in the Transient Analysis Program and the line is energized from its sending end. The obtained voltage waveform shows that after the transients due to switching had died out due to line losses, there are still over-voltages (2.4 p.u) caused by the harmonics appearing on the waveforms (Fig. 2.5). These harmonics are created by the transformer saturation effect.

2.4. Reduction of Steady State Overvoltages with Shunt Reactors[9][10][11][12]

2.4.1. General

When the initial loading of transmission system is less than surge impedance loading, excess charging current will appear on the line terminals. This results voltage increase on the system. By compensating a portion of charging current, shunt reactos are used to control the voltage rises and to maintain a flat voltage profile on EHV systems.

Decreasing of charging current by means of shunt reactors is an important factor to control the steady state overvoltages due to transformer saturation. As it was explained in the previous section, ferro-resonance

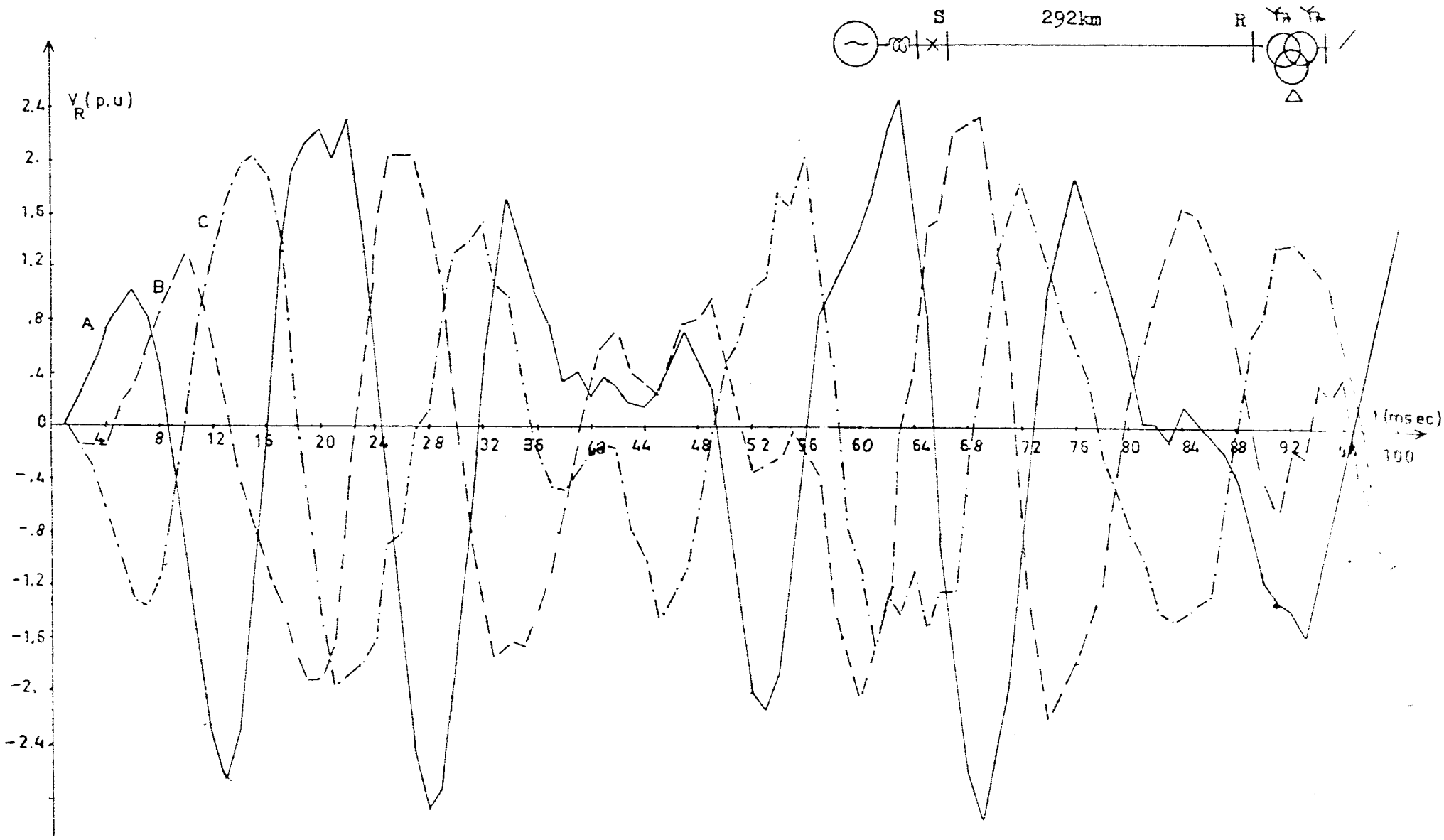

Fig.2.5. Receiving end voltage waveforms after three phase line energization (unloaded autotransformer at the receiving end)

oscillations occur between line capacitance and nonlinear transformer magnetizing impedance. When voltage level reaches to nonlinear part of transformer magnetizing curve. By using shunt reactors, operating voltages are reduced below the saturation region of transformer. Thus, any ferro-resonance oscillations are prevented. Reactors should of course have linear magnetizing characteristics up to a voltage level specified according to calculated temporary overvoltages, inorder to reduce the risk of ferro-resonances caused by themselves.

2.4.2. Determination of Reactor Requirements and Method of Connection.[10]

The reactive compensation determined during load flow studies under normal and contingency conditions (peak and light load conditions for summer and winter) are also included in steady state.

There are two alternative methods of connecting reactors to the system.

1. To connect directly to the EHV transmission lines.
2. To connect to the tertiary of the step-down transformer bank.

In evaluating these methods, several factors are considered including relative equipment cost, amount of reactor capacity required, effect on open circuit voltages and quality of voltage control. Usually, the EHV reactor is permanently connected to the transmission line to avoid the added expense of an EHV breaker. The reactor is size for the reactive requirement at maximum loading. This may be from 20 to 100 percent of total compensation required, the remaining percentage being located as switched dry-type reactors on the tertiary winding of an EHV autotransformer.[10]

The effects of shunt reactors after line dropping and fault clearing will be analysed in more detail in Chapter 5.

In general, reactors connected to EHV lines are either directly grounded, or in some cases grounded through a resistor to help decaying of trapped charges. If grounding resistors are used, they produce excessive losses as given below.

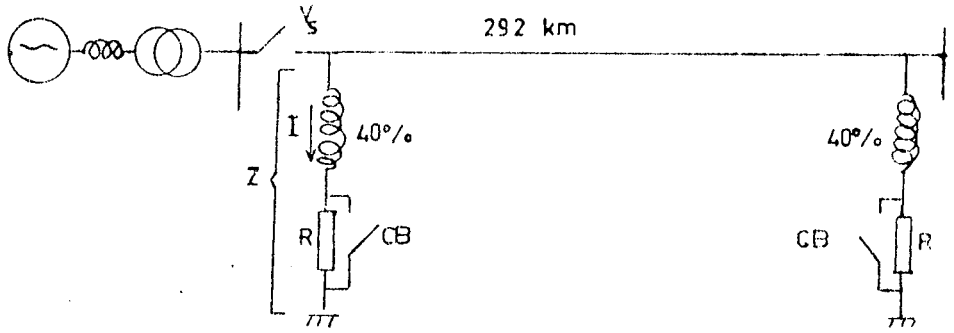

Fig. 2.6. Resistor insertion in the neutral of shunt reactors.

For the power system shown in Fig. 2.6. which has the characteristics given in Appendix D, an optimal grounding resistor of 153 Ω as calculated in view of the principals discussed in Chapter 5, is inserted.

The complex power absorbed by reactor together with 153 ohms series resistor is

$$S = V_s I^* = \frac{|V_s|^2}{Z^*} \qquad (2.10)$$

where $Z = Z_R + R = 0.111 + j\ 1.666$ p.u

$V_s = 1$ p.u.

in 100 MVA and 380 kv bases.

then

$$S = 0.01327 + j\ 0.19852 \text{ p.u.}$$

and $$S = P + j\ Q = 1.327 + j\ 19.852 \text{ MVA} \qquad (2.11)$$

If the system is in operation for 8766 hours in one year and the price of electricity is 0.57 TL/kwh, the power loss due to series resistor costs 6.66 million TL. in a year. Therefore, grounding of shunt reactors through a resistor is very costly one interms of system losses.

To avoid the power loss, the resistance is short circuited by a circuit breaker under normal service condition (Fig. 2.6). This breaker will, for example, be switched off after interruption of the unloaded line by an underfrequency relay which is energized by line oscillation and the resistance will damp the oscillation between line capacitance and reactive inductance in such a manner that after 0.4 seconds no remanent charge will be present on the line. Directly before closing the line, the resistor is short circuited and line is reenergised without trapped charge on it.[13] The voltage and current rate of CB connected across the resistor are calculated as 13.9 kv and 52 A respectively for the system shown in Fig. 2.6 under normal service conditions. Hence either a medium voltage circuit breaker or a power sectionalizing breaker which is much cheaper can be used for this purpose.

CHAPTER III

OVERVOLTAGES DUE TO FAULTS

3.1. Introduction

As the insulation levels are decreased, transients that are usually considered negligible take on added significance. Prime examples are transients associated with fault initiation.[14][15][16] Because of random nature of fault occurence, control is extremely difficult. The ultimate minimum insulation level may possibly be determined by these transients, making control of switching surge academic.

After all, when a fault occurs on a transmission line, it is usually cleared by the operation of the circuit breaker. So, if the line flashovers occur due to the overvoltages created by the faults it does not seem to be so important. This is certainly true for a single UHV line feeding a lower voltage transmission system which will have normally high level of insulation.

However, for interconnected UHV lines a fault overvoltage may easily be transmitted to other lines, causing flashovers in these lines and forcing them to open.

3.2. Modal Derivation of Different Types of Faults on Lines

A theoretical investigation is carried out in parallel with the computer study to understand the cause of overvoltages. This study explains the travelling waves of two different modes (ground and aerial), each having its surge impedance and speed of travel.

3.2.1. Simulation of the Faults.[14]

Faults can be represented by suddenly applied voltage to the line

at the fault point. The applied voltage is equal and opposite to that existing on the conductor at that time. The line to ground voltages at the point of fault may be found by applying superposition principle i.e. the act of voltage injection and the influence of the source are treated separately.

$$\left[\begin{array}{c}\text{Resultant}\\ \text{Voltage}\end{array}\right] = \left[\begin{array}{l}\text{Whose which would}\\ \text{have existed if}\\ \text{the fault doesn't}\\ \text{initiated}\end{array}\right] + \left[\begin{array}{l}\text{Those due}\\ \text{to cancelation}\\ \text{voltages}\end{array}\right]$$

Before occurrence of the fault, there are balanced three phase sinusoidal line to ground voltages at the fault point. Therefore, the voltage components due to system source are three phase balanced sinusoidal voltages. However, the cancellation voltages will be different for the different type of faults.

3.2.1.1. Single Line to Ground Faults.

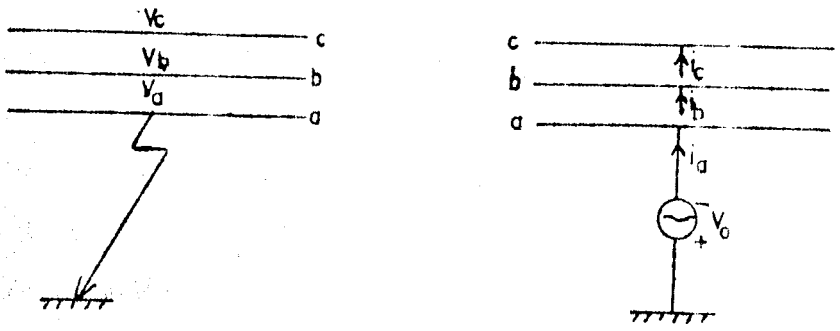

Fig. 3.1. SLG Fault on the line and its equivalent circuit.

Consider a 380 kv line which has modal characteristics given Table 3.I. To find the transient voltage due to SLG fault on the line,

hence

$$V_a = V \cos \omega t \tag{3.4}$$

$$V_b = \frac{Z_{21}}{Z_{11}} V \cos \omega t \tag{3.5}$$

$$V_c = \frac{Z_{31}}{Z_{11}} V \cos \omega t \tag{3.6}$$

The values V_a, V_b, V_c correspond to initial transietns at t=0 and cause initial jumps on the voltage waves.

The modal component of the injected voltages can be calculated by using formula C.19

$$V_{mode} = Q^{-1} V_{phase} \tag{3.7}$$

$$V_{mode} = \begin{bmatrix} \frac{1}{2} & -\frac{1}{2} & 0 \\ \frac{1}{3} & \frac{1}{3} & \frac{1}{3} \\ \frac{1}{6} & \frac{1}{6} & -\frac{1}{3} \end{bmatrix} \begin{bmatrix} V_a \\ V_b \\ V_c \end{bmatrix} \tag{3.8}$$

$$V_{mode} = \begin{bmatrix} \frac{V_a}{2} - \frac{V_b}{2} \\ \frac{V_a}{3} + \frac{V_b}{3} + \frac{V_o}{3} \\ \frac{V_a}{6} + \frac{V_b}{6} - \frac{V_c}{3} \end{bmatrix} \begin{matrix} \text{mode 1} \\ \text{mode 2} \\ \text{mode 3} \end{matrix} \tag{3.9}$$

The aerial modes 1, 3 corresponds to positive and negative sequences modes, the ground mode 2 corresponds to zero sequence mode.

The phase voltage at the fault point interms of the modal components are

$$V_{phase} = Q V_{mode} \tag{3.10}$$

3.2.1.3. Three Phase to Ground Fault

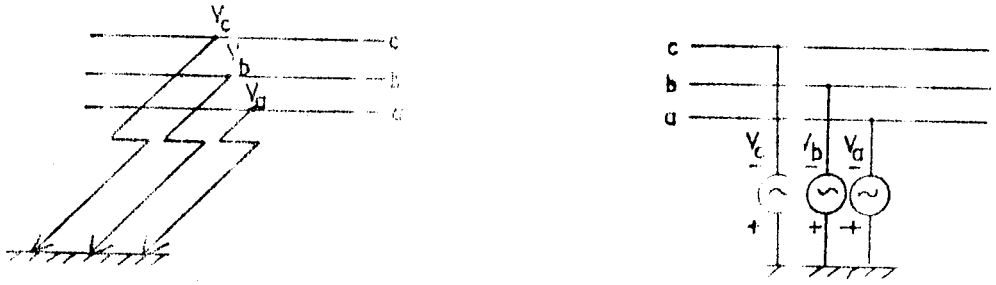

Fig. 3.4 3ϕG fault on the line and its equivalent circuit.

To simulate the 3 phase to ground fault, pre fault voltages V_a, V_b, V_c are injected to each phases respectively where

$$V_a = V \text{ Cos } wt \qquad (3.18)$$

$$V_b = V \text{ Cos } (wt-120) \qquad (3.19)$$

$$V_c = V \text{ Cos } (wt-240) \qquad (3.20)$$

Since the injection voltages at the fault point are symmetrical, from the equation (3.11), ground mode (mode 0) is zero and only aerial mode (mode 1 and 2) will travel. Hence no overvoltage is produced.

3.3. Effect of System Parameters.

a) Terminating impedance of the line (short circuit MVA) :

As the terminating impedance of the line at both ends decreases (hight short circuit MVA), the produced overvoltages increase due to increase in the negative reflection. The worst termination is zero impedance (infinite bus), which is approximated by a bus having several other lines.

b) The line length:

The surge travel times after occurrence of the faults depend on the line length. The period of surge pulses on the Sine waves are determined by the travel time. Therefore, crest overvoltage depends on the line length. If the first pulse appears on the crest of the Sine wave of the unfaulted phase, the crest overvoltage is maximum.

c) The fault location:

The maximum overvoltage crest occurs when the fault is at the mid-point of the line. Because, on the unfaulted phases, the reflected waves return to the midpoint from the both ends at the same time. The current waves cancel one another and the voltage waves combine to double the voltage.

d) The time of occurrence of the fault:

The crest overvoltage due to the fault is maximum when the fault occurs at the crest voltage of the phase to be faulted. In simulation of the fault, if the injected voltage to the faulty phase at the fault point is maximum, the induced voltages on the healthy phases will also be maximum. Therefore the travelling surge waves will have maximum magnitudes and this causes higher crest overvoltages.

3.4. Computer Results for a Fault.

The study was made on Transient Analysis Program by simulating power system shown in Fig. 3.5. To determine the maximum fault initiation transients, faults were applied at critical points on the basic system.

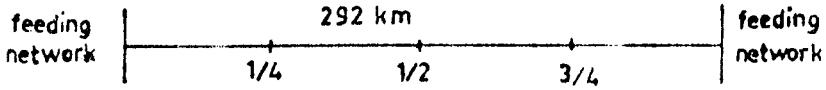

Fig. 3.5 Scheme of transmission system.

Variables in the study include fault location, source configuration, line length, line termination. The following paragraphs describe the most significant results.

A series of studies was made for different fault locations on the line with SLG fault. The line was fed by two infinite buses from the both ends. The crest overvoltage varied from 1.72 to 1.84 p.u as shown in Table 3.I. The worst fault location is at the midpoint of the line, and the maximum overvoltage is at that point. The voltage waveform is shown in Fig. 3.6. for this case.

In the other study, the line length is decreased to 146 km. and the overvoltages were calculated with SLG fault at its midpoint. The crest overvoltage is increased to 1.87 p.u.

As the source short circuit MVA increases, the overvoltage due to SLG fault is increased. The maximum crest voltage 1.84 p.u is obtained when the source short circuit MVA is infinite. Line sources connected, decrease the overvoltages due to SLG fault. Also, as the source impedance increases, overvoltage seen on the busbars reaches to 1.63 p.u.

For the line with infinite sources connected to its both end,

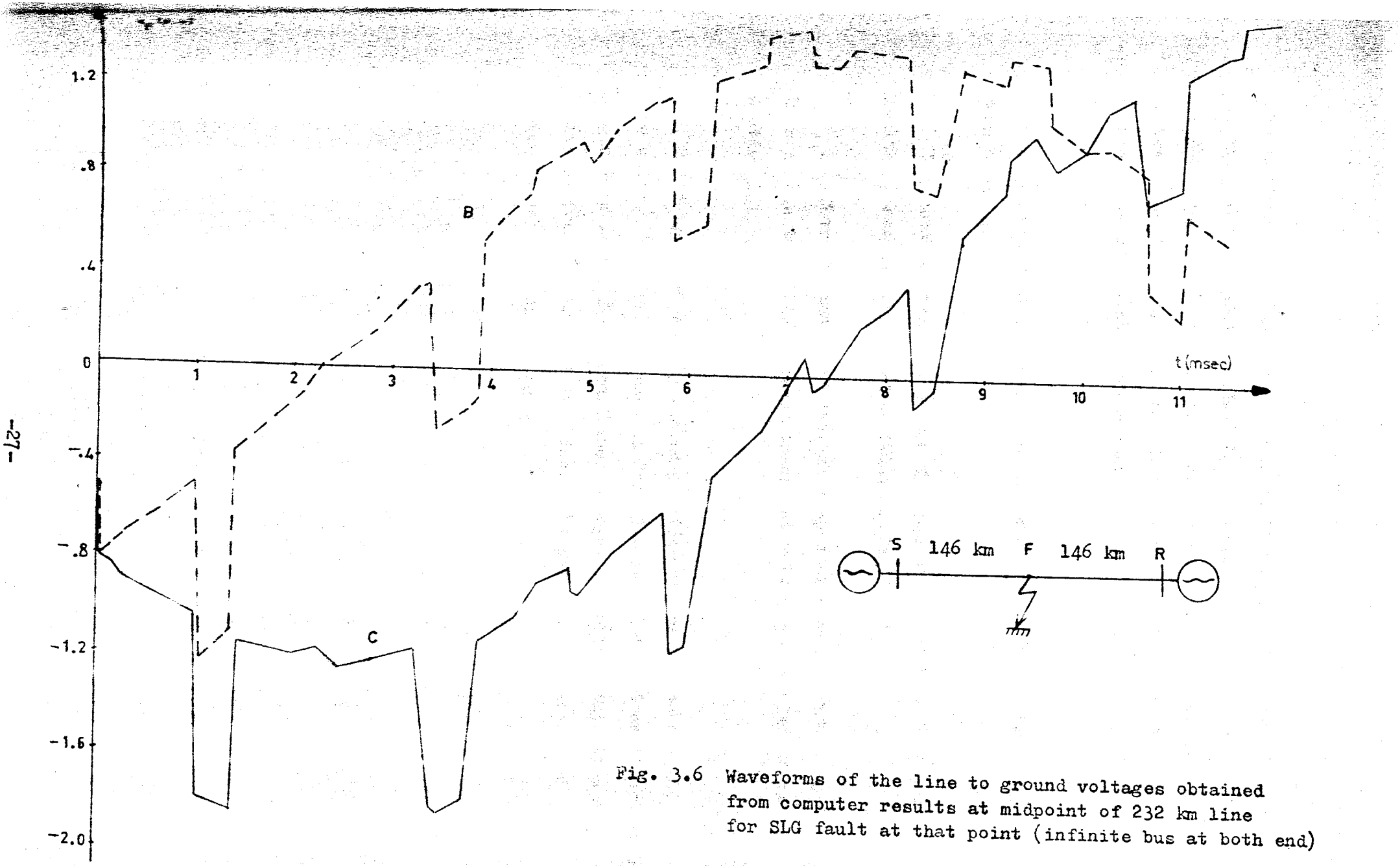

Fig. 3.6 Waveforms of the line to ground voltages obtained from computer results at midpoint of 232 km line for SLG fault at that point (infinite bus at both end)

the maximum overvoltage is calculated by varying the time of occurrence of the SLG fault at the midpoint. The maximum crest voltage of 1.87 p.u. is obtained when this time is 1 msec. after the crest voltage of the phase to be faulted. The minimum crest voltage 1.37 is obtained when the voltage of the phase to be faulted is zero just before the fault occurrence.

The results of studied cases are summarized on the Table 3.II on the following page.

The notable characteristics of waves of the voltage on the unfaulted phase can be stated as follows (Fig.3.6.)

1. There is immediate initial step increase of about 0.3 p.u. This is due to initial induced transient voltages as explained in section 2.1.1.

2. A train of equally spaced positive pulses are superposed on Sine waves. These pulses seen in Fig. 3.6 result from travelling waves originating at the fault point due to negative voltage injection and reflected from the ends of the line. The periods are determined by the travel time of the modes.

Table 3.II Transient Overvoltages caused by SLG Fault on the transmission line for different system parameters.

Source type Sending end	Source type Receiving end	line length (km.)	fault location	Time of the occurance of the fault after crest voltage (msec)	Fault type	The crest overvoltage along the line (p.u.) 0	l/4	l/2	3l/4	l
infinite bus	infinite bus	292	l/2	0	SLG	1	-	1.84	-	1
inductive source 20000 MVA	inductive source 20000 MVA	292	l/2	0	SLG	1.42	-	1.84	-	1.42
inductive source 3000 MVA	inductive source 3000 MVA	292	l/2	0	SLG	1.63		1.66		1.63
1 line S + inductive source 3000 MVA	inductive source 3000 MVA	292	l/2	0	SLG	1.25	-	1.52	-	1.39
4 line S + inductive source 3000 MVA	inductive source 3000 MVA	292	l/2	0	SLG	1.23	-	1.58	-	1.39
infinite bus	infinite bus	292	l/2	1	SLG	1.	-	1.87	-	1.
infinite bus	infinite bus	292	l/2	2	SLG	1.	-	1.76	-	1.
infinite bus	infinite bus	292	l/2	3	SLG	1.	-	1.50	-	1.
infinite bus	infinite bus	292	l/2	4	SLG	1.	-	1.41	-	1.
infinite bus	infinite bus	292	l/2	5	SLG	1.	-	1.37	-	1.
infinite bus	infinite bus	292	l/4	0	SLG	1.	1.74	1.65	1.61	1.
infinite bus	infinite bus	292	3l/4	0	SLG	1.	1.58	1.58	1.72	1.
infinite bus	infinite bus	146	l/2	0	SLG	1.	-	1.87	-	1.

CHAPTER IV

OPENING OF THE CIRCUIT BREAKER

4.1. General Principles Involved,[17, 18, 19,20]

The act of opening circuit breakers is a source of overvoltages. Most common reasons for opening are load interruption, line dropping and fault clearing. The overvoltages due to switch opening and problems of HV circuit breaker (CB) for successful operations are studied in this chapter.

Circuit interruption after the current zero is a race between the increase of dielectric strength of the switch and recovery voltage. Namely successful interruption depends upon whether the breakdown insulation strength within the gap exceeds the transient recovery voltages produced by the circuit (Fig. 4.1). The Transient Recovery Voltage is the voltage transient that occurs across the terminals of a pole of a circuit switching device upon interruption of the current, usually designated as TRV[18]. The capability limits of HV circuit interrupting devices are determined largely by transient recovery voltages.

The waveform of transient recovery voltage varies according to the arrangement of acutal circuits. The recommendations of IEC[20] on circuit breakers specify the methods for describing the TRV. The following parameters are used for representation of rated TRV (Fig.4.2)

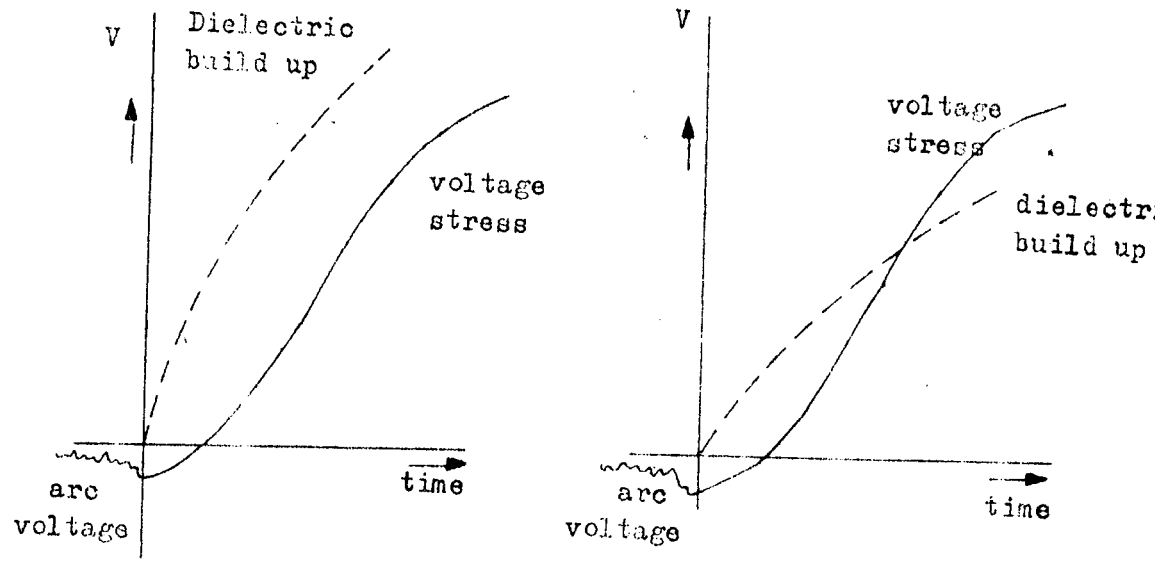

a) INTERRUPTION MAINTAINED

b) INTERRUPTION FOLLOWED BY DIELECTRIC FAILURE

F.g. 4.1. Build up of dielectric strength and voltage stress between circuit breaker contacts from the instant of current zero.

U_c = reference voltage (TRV peak value), in kv.

t_3 = time to reach voltage U_c, in μsec .

U_c/t_3 = rate of rise of recovery voltage (RRRV), kv/ μsec

Furthermore a time delay (t_d), in μsec , is introduced to show the influence of terminal capacitances, which are always present in a system

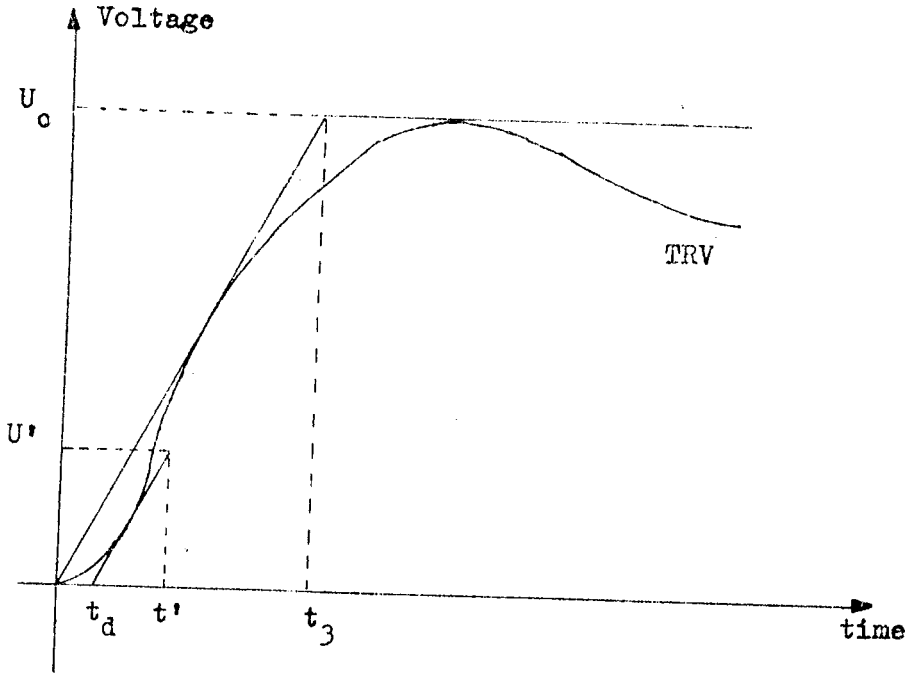

Fig. 4.2 - Representation of a specified TRV by a two-parameter reference line and a delay line.

4.2. Analysis of Different Modes of Operation of the Circuit Breaker.

For rough calculations, the mathematical analysis of three phase representation is more complex due to the mutual coupling between the phases, the sequential opening of switches, nonlinear components etc. Therefore, it becomes practical to study the behaviour of switching surges by means of a digital computer (Appendix C). However, mathematical analysis of some simple networks can be made by using hand calculations (Appendix B) for establishing an insight and to feel for the nature of opening surges.

4.2.1. Load Rejection[7]

In the following subsections, the different kinds of single phase

load rejections are studied to get an idea of switching transient and TRV.

4.2.1.1. Purely Resistive Load Rejection

Consider the elementary network in Fig. 4.3. which represents a transmission line and has purely resistive load at receiving end.

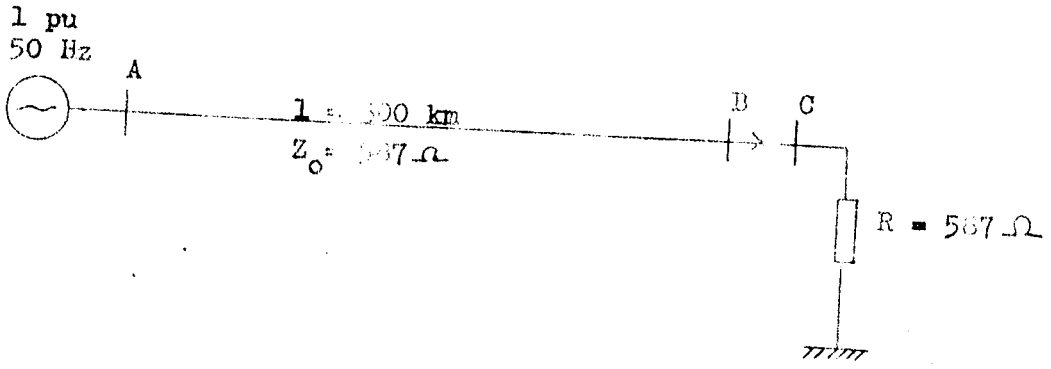

Fig.4.3 Single phase line with resistive load

The characteristics of the system is given. For simplicity R is chosen to represent SIL condition.

The response at the receiving end after load rejection may be found by applying superposition principle; i.e., the act of switching and the influence of source are treated separately.

$$\left[\begin{array}{l}\text{Resultant voltage}\\ \text{and current}\end{array}\right] = \left[\begin{array}{l}\text{Those which could}\\ \text{have existed if the}\\ \text{switch was not}\\ \text{operated}\end{array}\right] + \left[\begin{array}{l}\text{Those due to}\\ \text{cancellation}\\ \text{current or}\\ \text{voltage}\end{array}\right]$$

To represent switch opening, a current is injected through the circuit breaker opposite in sign with the current flowing before switching. The cancellation current may be taken as $i = Iwt$ for transient time since

the contacts of CB are usually open at current zero and I Sin wt ≅ Iwt. In coodinates of time vs. distance, Fig. 4.4. shows the travelling waves due to current injection, representated by straight lines (Appendix B).

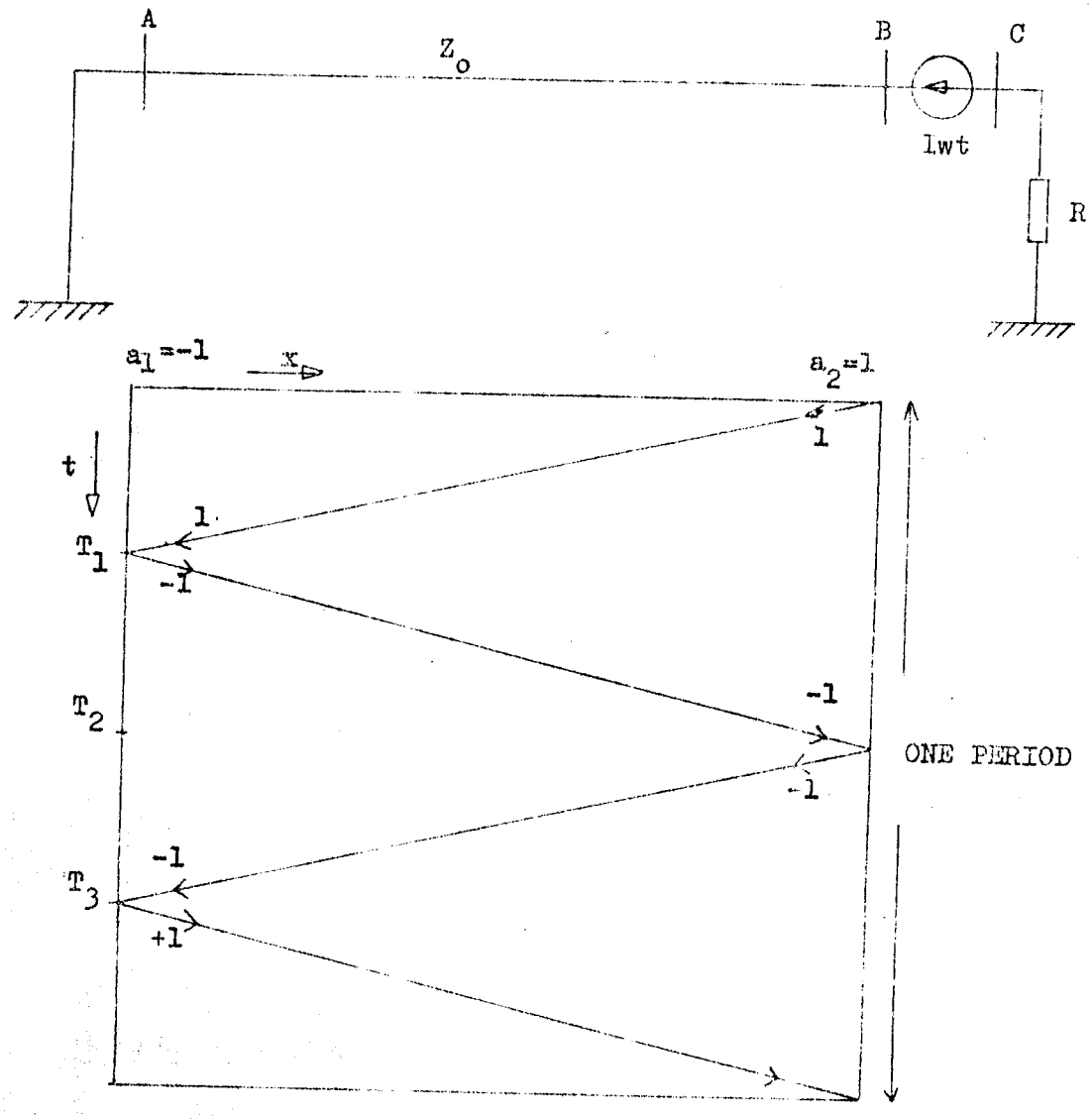

Fig. 4.4. - The lattice diagram for voltage V_{B2} after current i = Iwt injection.

Voltage wave V_{B2} derived from Fig. 4.4. is given in Fig. 4.5. In actual cases since the line has resistance, the voltage V_{B2} eventually becomes negligible due to resistive losses. By superimposing voltage wave V_{B2} to the voltage wave V_{B1} which would have existed if the switch were not operated, the transient voltage wave V_B is calculated at the point B after load rejection.(Fig. 4.5). Then, TRV accross CB contacts $V_B - V_C$ will be voltage at the line side of CB i.e V_B since the load side voltage V_C is equal to zero.

The waveforms V_B and V_C are also calculated by using the Transient Analysis Program on digital computer for the same elementary network Fig 4.6 (Appendix C). It can be seen that the roughly calculated results and digital computer results are nearly same with each other.(Table 4.I)

Table - 4.I. TRV of CB for resistive load rejection. - Representation by two parameters.

	TRV peak value, U_c p.u.	time coordinate t_3 (μsec)	rate of rise U_c / t_3
Hand calculation	1.2	2000	0.6×10^{-3}
Transient Analysis Program Results	1.2	1500	0.8×10^{-3}

4.2.1.2 Inductive Load Rejection

In this case, Fig. 4.7 defines the system which represents a single line with an inductive load at the receiving end.

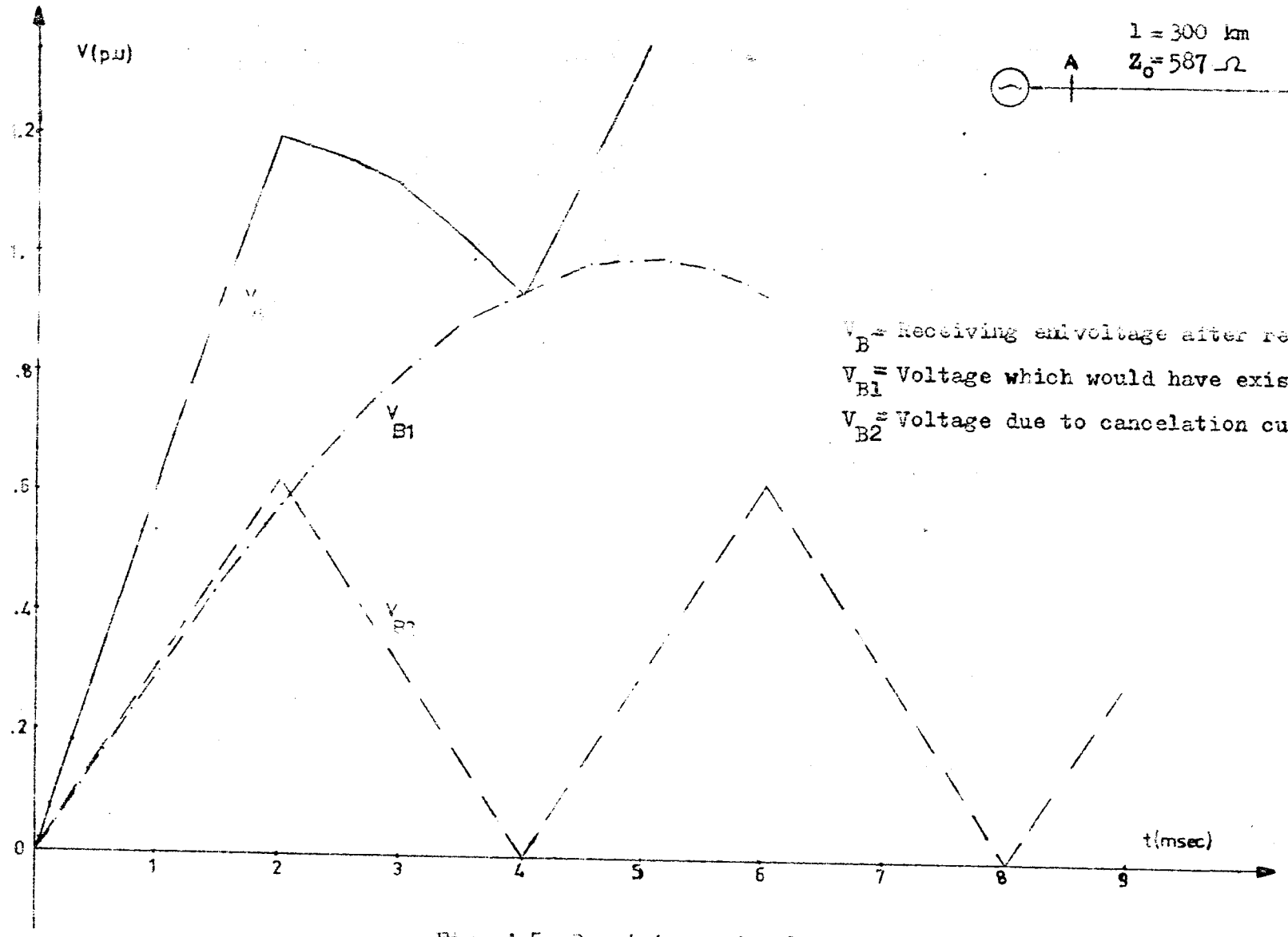

V_B = Receiving end voltage after resistive load rejection

V_{B1} = Voltage which would have existed if the switch was not operated

V_{B2} = Voltage due to cancelation current

Fig. 4.5 Receiving end voltage waveform V_B after resistive load rejection (obtained by Bewley's lattice technique and superposition principle)

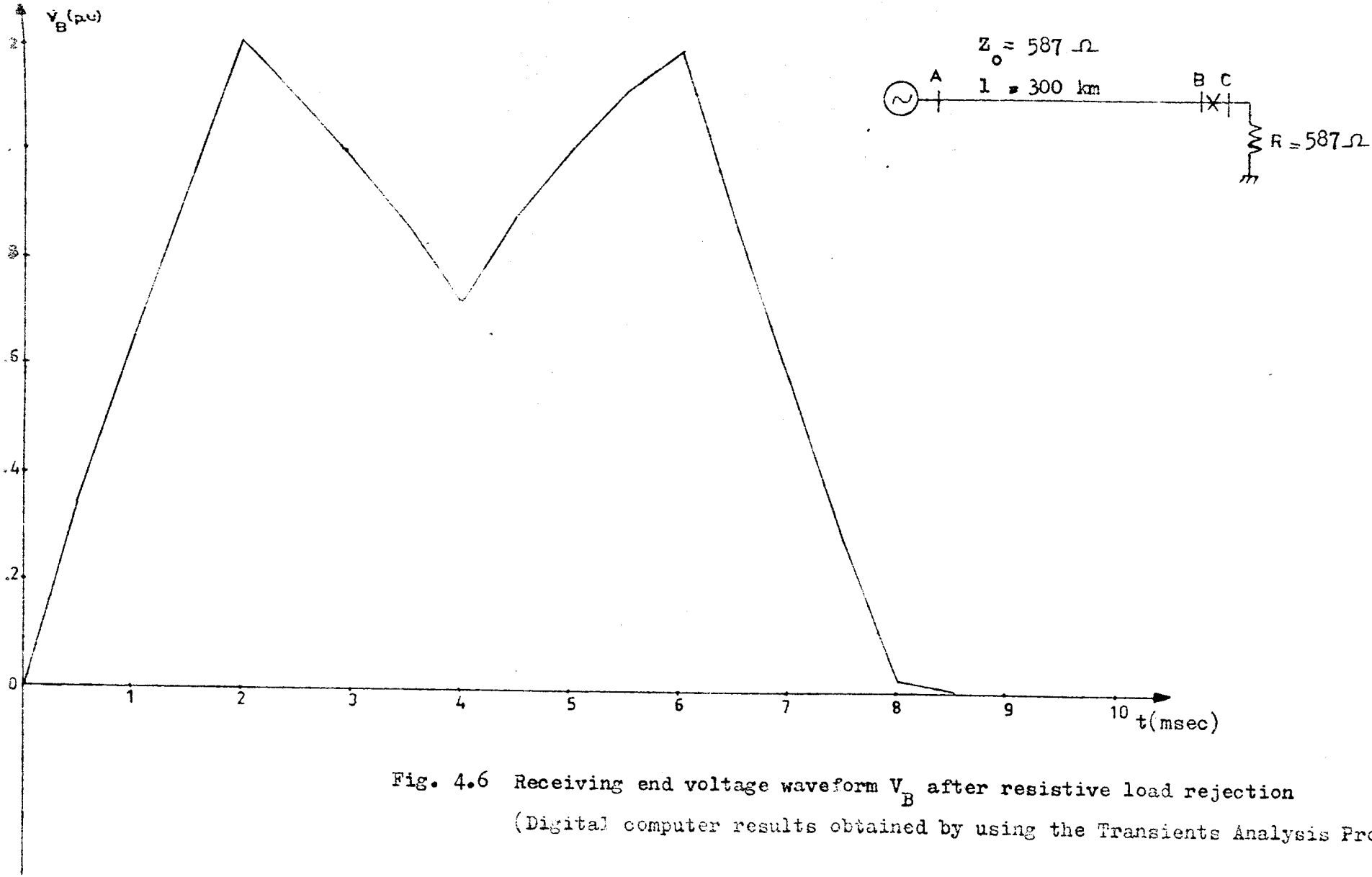

Fig. 4.6 Receiving end voltage waveform V_B after resistive load rejection
(Digital computer results obtained by using the Transients Analysis Program)

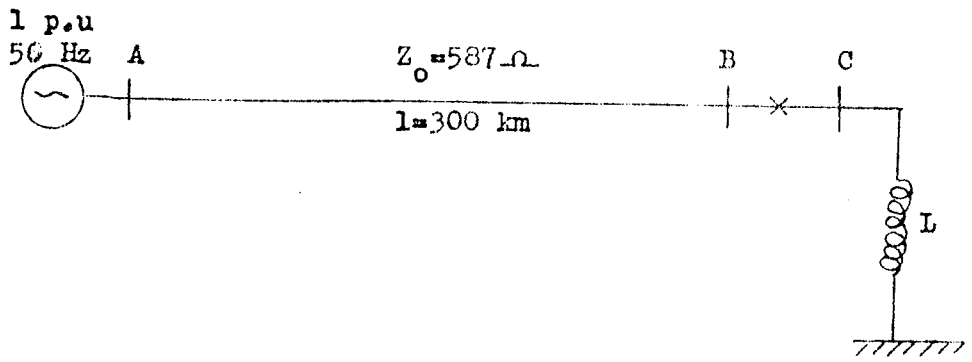

Fig. 4.7 Single phase line with inductive load

Receiving end voltage is smaller than sending end voltage in magnitude and same in the phase.

The voltage waveforms across the CB have been calculated by using superposition principle and the Bewley's lattice technique (Fig.4.8). Voltage waveform V_B in the Fig. 4.8 represents the line side voltage of CB after its opening operation. TRV across the CB contacts $V_B - V_C$ is equal to line side voltage V_B since load side voltage V_C is zero. The terminal voltage waveforms of CB also have been calculated by using the Transients Analysis Program after the inductive load rejection (Fig.4.9). Table 4.II summarises the result for TRV calculated by hand calculation and digital computer study.

Table 4.II TRV of CB for inductive load rejection - Representation by two parameters.

	TRV peak value V_o p.u	Time coordinate t_3 (μsec)	RRV V_o/t_3
Hand calculation	1.08	2000	0.504×10^{-3}
Transients Analysis Program Result	1.08	2000	0.504×10^{-3}

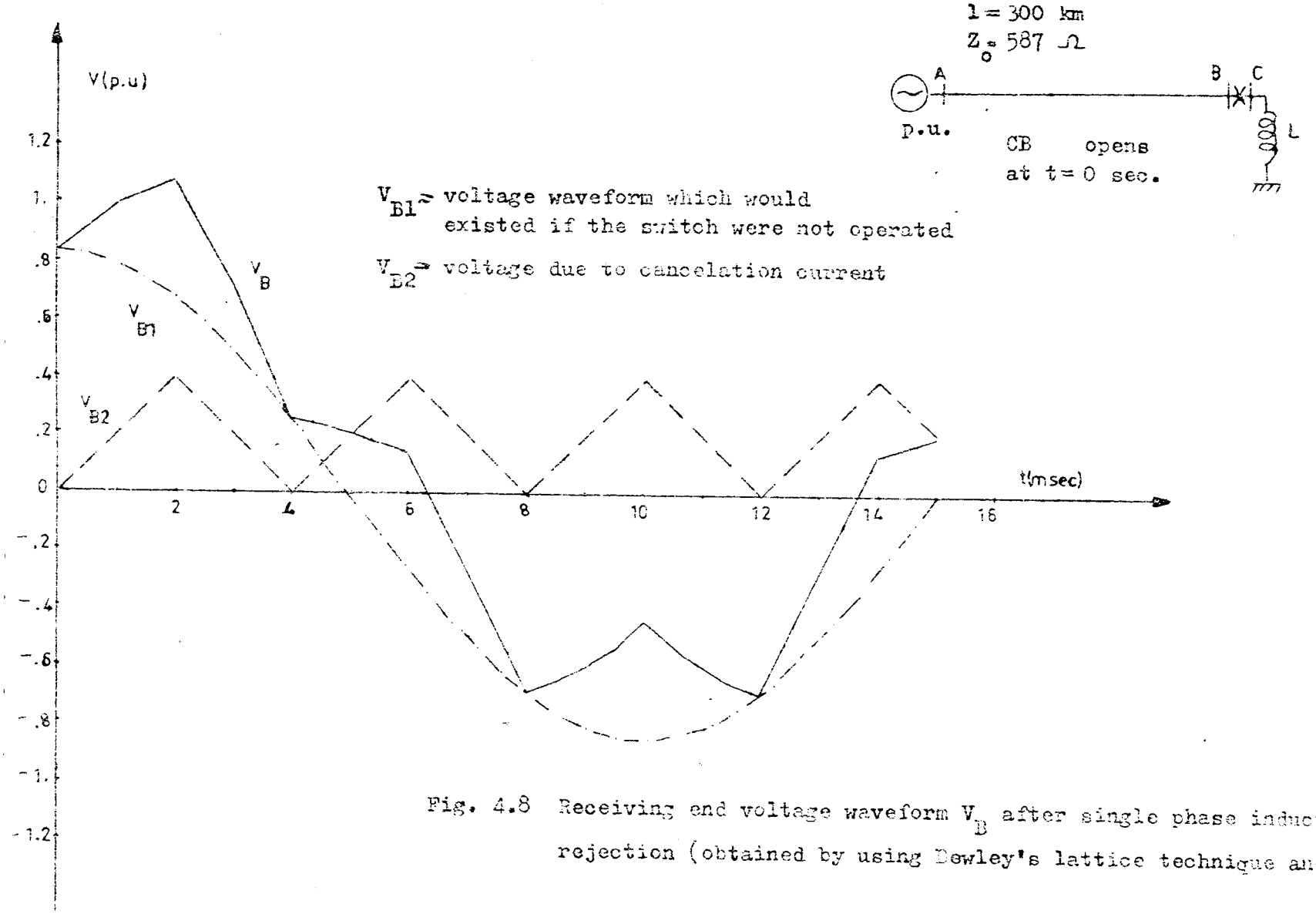

Fig. 4.8 Receiving end voltage waveform V_B after single phase inductive load rejection (obtained by using Dewley's lattice technique and superposition principle)

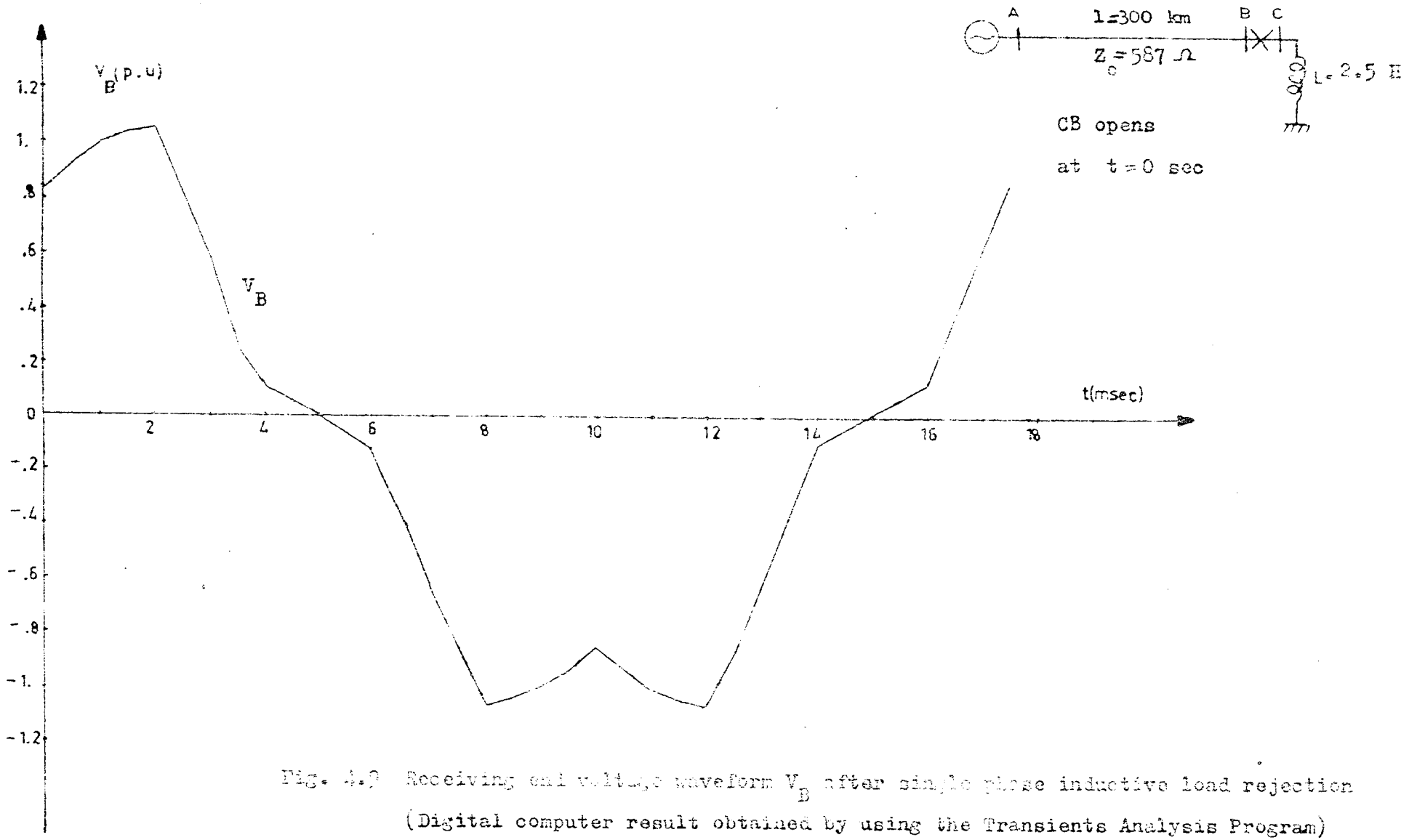

Fig. 4.9 Receiving end voltage waveform V_B after single phase inductive load rejection
(Digital computer result obtained by using the Transients Analysis Program)

4.2.1.3 Capacitive Load Rejection.

Network shown in the Fig. 4.10 represents a single phase transmission line which has a capacitive load at the receiving end.

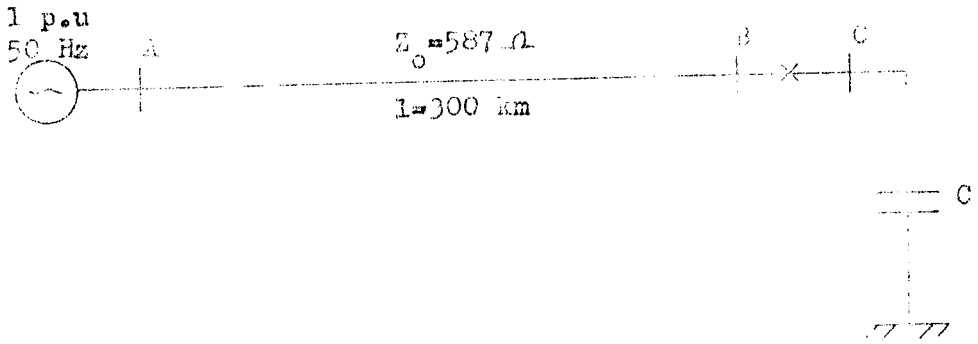

Fig.4.10 Single phase line with capacitive load

As in the previous cases, line is lossless. Sending end and receiving end voltages are same in the phase. Receiving end voltage is greater in the magnitude than sending end voltage due to Ferranti effect and capacitive load.

After the load rejection, the voltage waveforms across the CB have been calculated by using the previous method and procedure (Fig.4.11). The voltage waveforms obtained from digital computer study are shown in (Fig. 4.12). Since the opening occurs at current zero the capacitive load is left charged at peak voltage V_C. The line side voltage than swings away at 50 Hz frequency and the voltage across the contacts builds up sinusoidally, but initially at a very low rate and after 1/2 cycle from current interruption, voltage has its maximum value (Table 4.III).

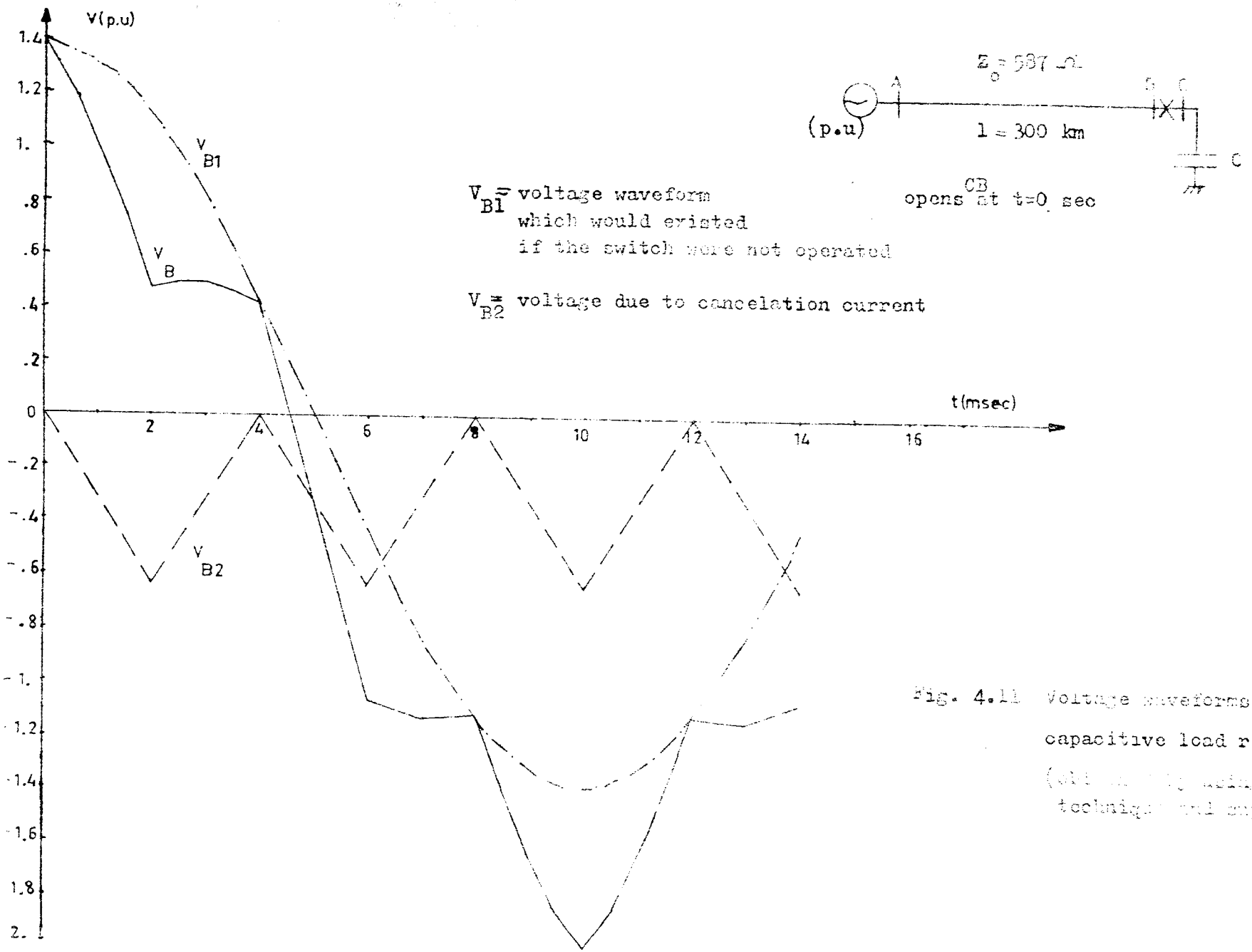

Z_o = 387 Ω

(p.u)

l = 300 km

C

V_{B1} = voltage waveform which would existed if the switch were not operated

V_{B2} = voltage due to cancelation current

CB opens at t=0 sec

Fig. 4.11 Voltage waveforms V_B and V_C after capacitive load rejection at receiving end (with the help of Dowley's lattice technique and superposition principle)

Table 4.III TRV of CB for capacitive load rejection – Representation by two parameters.

	U_c (p.u)	t_3 (μsec)	U_c / t_3
Hand calculation	3.42	10 000	3.42 x 10^{-4}
Computer Results	2.76	10 000	2.76 x 10^{-4}

4. 2.2. Line Opening.

Long lines at no load behaves like a capacitor due to line charging and input impedance can be simulated by an equivalent capacitance as follows

$$Z_{in} = \frac{V_S}{I_S} = \frac{\text{Cosh } \gamma l}{Y_o \text{ Sinh } \gamma l} = Z_o \frac{\text{Cosh } jw\sqrt{LC}\, l}{\text{Sinh } jw\sqrt{LC}\, l}$$

$$Z_{in} = Z_o \frac{\cos w\sqrt{LC}\, l}{j \sin w\sqrt{LC}\, l} = \frac{1}{j w C_{eq}}$$

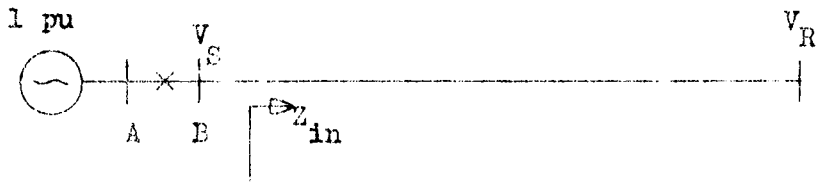

Fig. 4.13 Open ended single line.

After opening of the line, source side voltage V_A follows the source voltage and a non-uniform charge will be trapped on the line. The non-uniformity of the voltage along the line is caused by the Ferranti effect and it will result in waves with amplitudes depending upon the degree of non-uniformity, sloshing up and down the line with a fundamental frequency $1/\sqrt{LC}$ until line loss damp them out (Fig. 4.14).

4.2.3. Fault Clearing.

4.2.3.1. The Terminal Fault Clearing.

Fig. 4.15 shows a power system feeding a fault and its equivalent circuit.

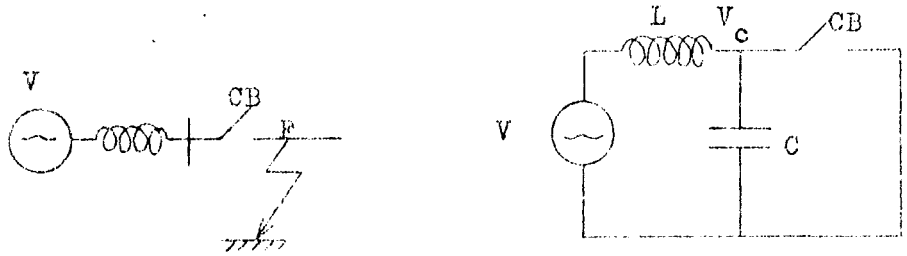

Fig.4.15 Power system feeding a fault and its equivalent circuit when a circuit breaker clears a fault.

L is all the inductance limiting the current to the fault and C is the natural capacitance of the circuit adjacent to the circuit breaker.

Circuit breaker opens at current zero. Since the source voltage is a sinusoidally varying quantity and is at its peak at this moment, it is expressed as V Cosωt. After circuit opening, the circuit equations are as follows:

$$L \frac{dI}{dt} + V_c = V \cos wt \qquad (4.1)$$

$$I = C \frac{dVc}{dt} \qquad (4.2)$$

Solving equations (4.1) and (4.2) for V_c

$$V_c(t) = \frac{w_o^2}{w_o^2 - w^2} V (\cos wt - \cos w_o t) \qquad (4.3)$$

where $w_o^2 = \frac{1}{LC}$

usually $w_o \gg w$, so equation (4.3) reduces to

$$V_c(t) = V (\cos wt - \cos w_o t) \qquad (4.4)$$

It may be concluded from equation (4.4) that when a short circuit **is interrupted** the voltage will swing to twice the system peak in half period of oscillations w_o (Fig. 4.16). For the real systems, the oscillation usually contains several frequencies because of the very complicated network configurations. If L and/or C are high, w_o is low and rate of rise of recovery voltage (RRRV) is low. Therefore, with a large amount of interconnection, the capacitance is high, hence RRRV is low and also RRRV decreases with increase in fault level since L decreases.

The severity of high frequency component which is superimposed on the normal system voltage can be reduced by connecting a resistance R, usually referred as the opening resistor across the contacts of CB (Fig. 4.17). This results in reduction of the TRV which increase the interrupting capability of CB.

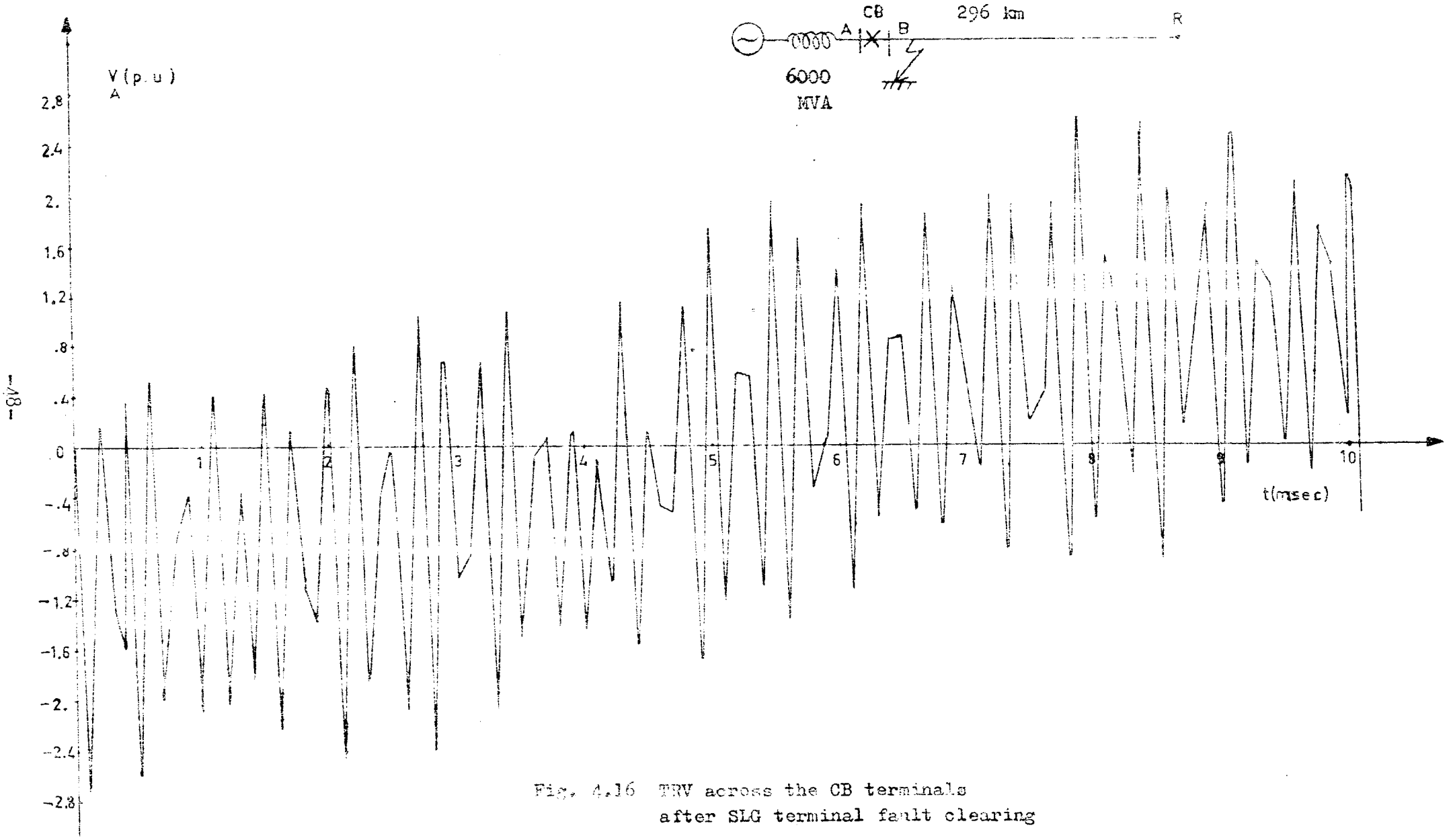

Fig. 4.16 TRV across the CB terminals after SLG terminal fault clearing

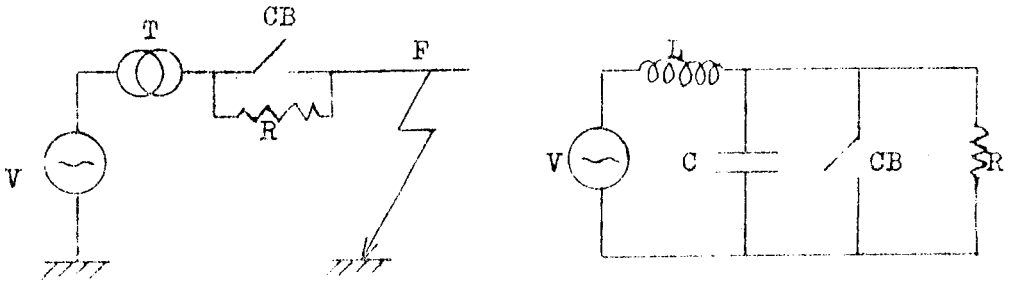

Fig. 4.17 Circuit breaker with shunt resistor clearing a fault

The formula for high frequency is :

$$f = \frac{1}{2\pi}\sqrt{\frac{1}{LC} - \left(\frac{1}{2RC}\right)^2} \qquad (4.5)$$

From this equation, it can be seen that when R is less than $\frac{1}{2}\sqrt{\frac{L}{C}}$ the expression under the square root becomes negative. The high frequency transient is critically damped. Therefore the oscillatory nature of transient ends and it becomes exponential.

Fig. 4.16 shows TRV across the CB which clears the single line to ground fault near the sending end for the system shown in Fig. 4.15. To achieve reduction of TRV, opening resistor R = 3700 Ω which is smaller than $\frac{1}{2}\sqrt{\frac{L}{C}}$ is shunted during the fault clearing of the mentioned system. Fig. 4.18 shows the calculated TRV (Appendix C) waveform which does not contain any oscillatory transients.

4.2.3.2 Short Line Faults.

A short line fault, usually called kilometric fault is a fault occuring a short distance from a CB down a transmission line. This is shown schematically in Fig. 4.19.

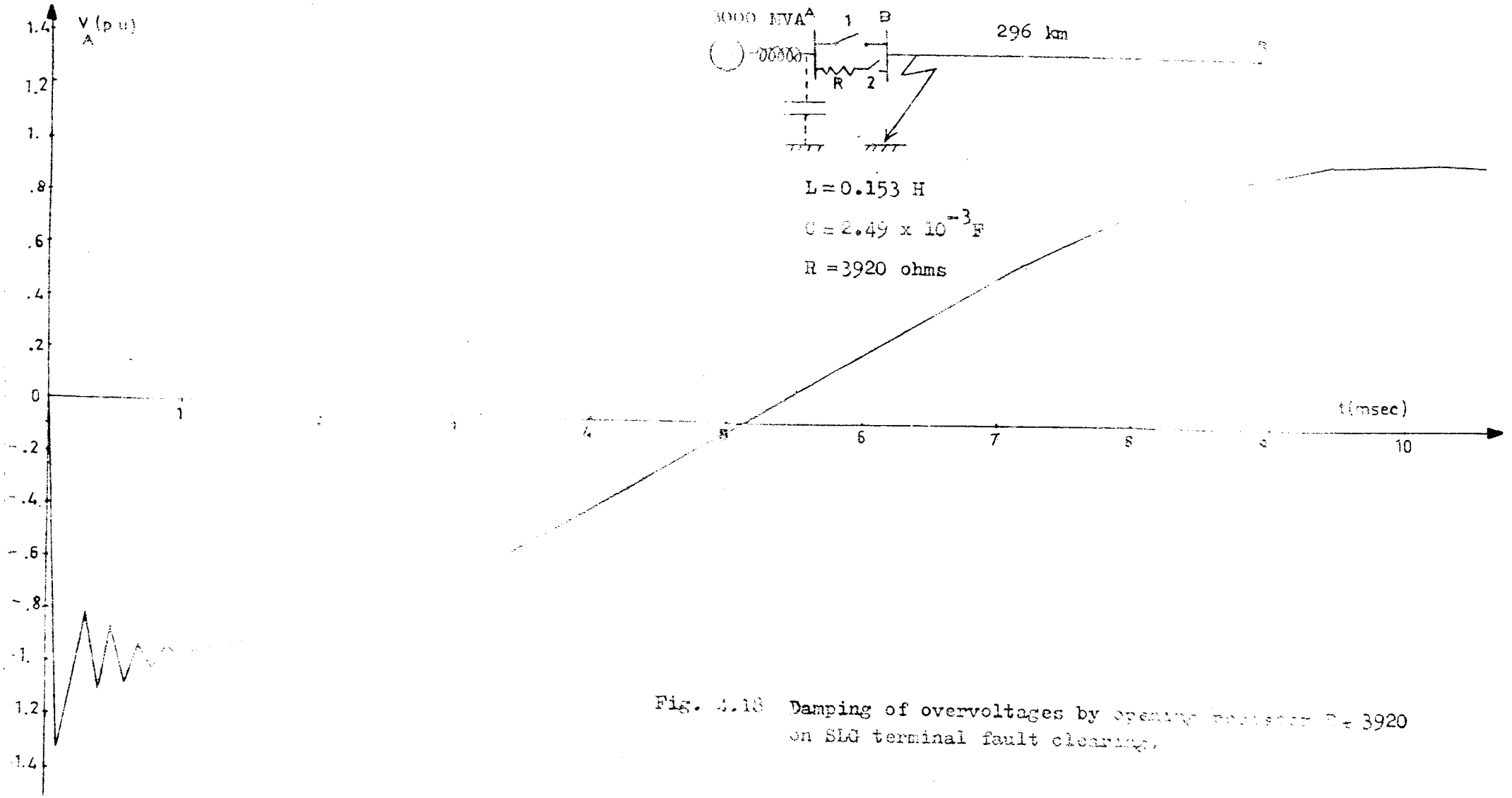

Fig. 4.18 Damping of overvoltages by opening resistor R = 3920 on SLG terminal fault clearing.

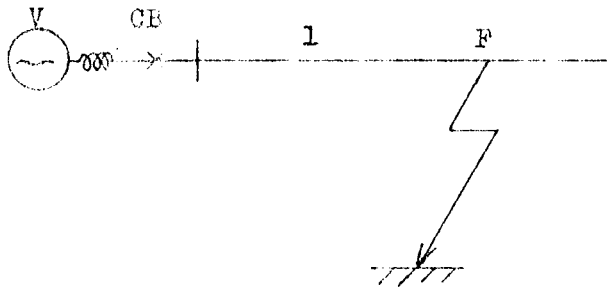

Fig. 4.19 Short-line fault.

After the interruption of current, the voltage on the supply side will oscillate with the network frequency and ultimately approach the open circuit voltage, just as in the case of a terminal fault. The amplitude of the oscillation will be reduced, however because of the reduced voltage drop across the supply network. On the line side the charge left after the interruption will set up waves which travel along the line and back again with the velocity of light being reflected at both ends. These travelling waves will give rise to the voltage on the line side of the CB the sawtooth form as shown in the Fig. 4.20. Since there is no driving voltage on this side the voltage will ultimately become zero because of the line losses. Thus, TRV of the CB has high frequency saw-tooth component. The frequency and the amplitude of this wave is governed by the line length. For short lines this time is very brief, indicating the voltage rise to the first peak is very fast. As the distance to the fault becomes greater, the amplitude of the sawtooth component increases, the rate of rise of the sawtooth component decreases and the fault current decreases.

4.3. Three Phase System Analysis.

The basic system configuration studied are shown by the single line diagrm of Fig. 4.21.

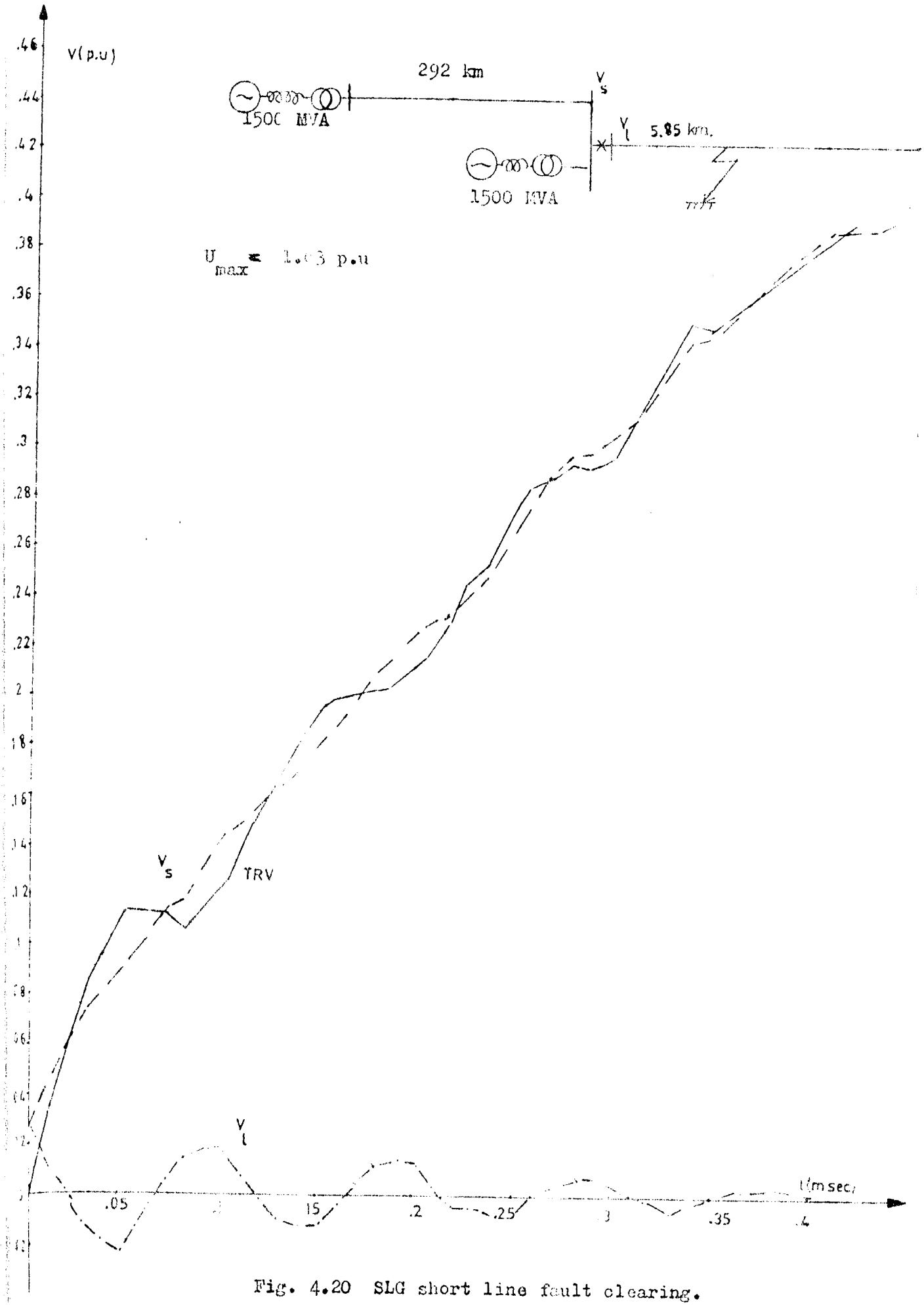

Fig. 4.20 SLG short line fault clearing.

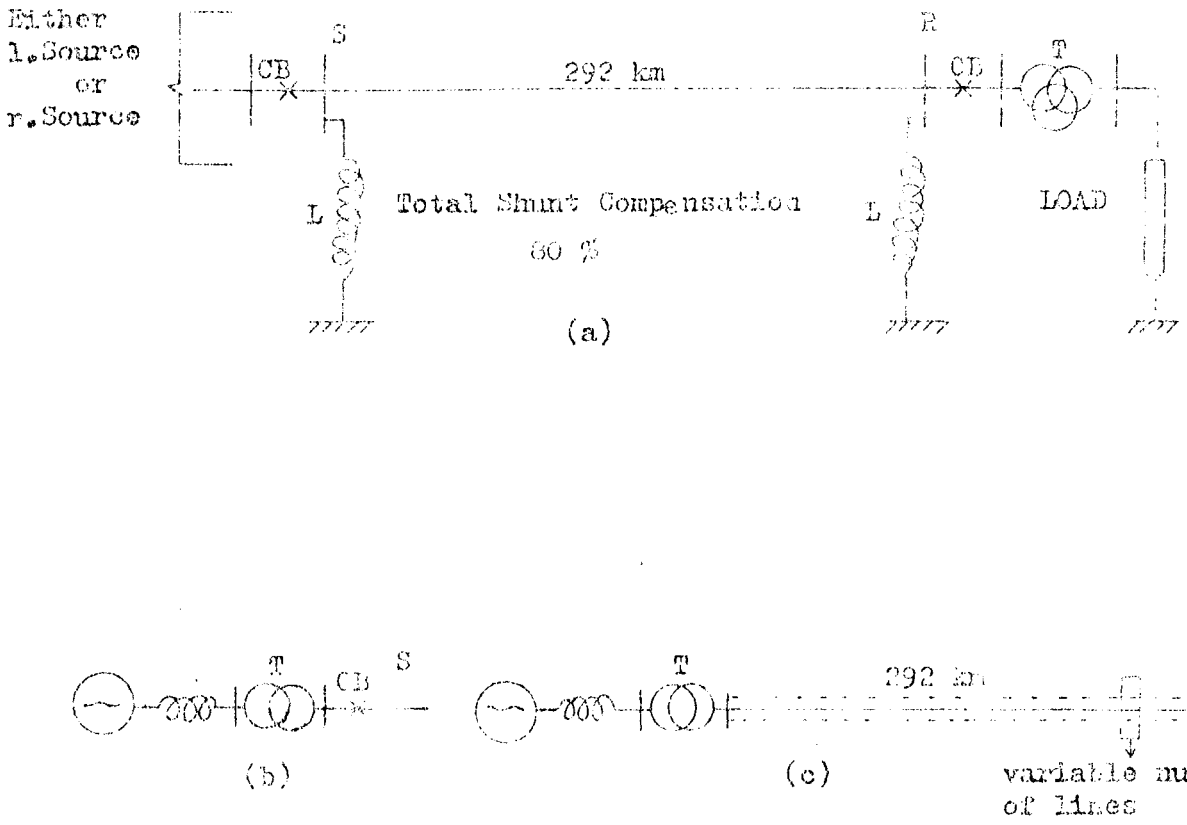

Fig. 4.21 - Single line diagram of system studied
(a) line studied on the Transients Analysis Program,
(b) local source, (c) remote source.

Two different type of sources are used during the study. One type of source (inductive source) represents a source reactance and a 11.3 to 380 kv step-up transformer (Fig. 4.21.b).

The remote source (line source) represents generation supplied through 380 kv transmission lines as in Fig. 4.21.b.

To control the steady state overvoltages, shunt reactors sized to 80 percent of the line charging MVA are used in the study (half at either end).

The data of system parameters to simulate the considered power system on the Transients Analysis Program are listed in Appendix D.

4.3.1. Three Phase Load Dropping at Normal Conditions and Due to Fault on Line[13]

4.3.1.1 Computer Results

Different kinds of load dropping study are studied on computer for different source and fault conditions with compensated and uncompensated lines. Also, a 4k Ω opening resistor is inserted to see its effect in reducing overvoltages for SLG fault clearing case (Fig. 4.2 4).

Table 4.IV summarizes the overall study and gives the receiving end maximum voltage magnitudes after load dropping. Figures (4.22) and (4.23) show an example of three phase load dropping at normal condition and due to SLG fault on the line respectively.

4.3.1.2 Analysis of Computer Results

The voltage rise at the receiving end to 1.6 p.u. after load rejection (Fig. 4.22) is due to Ferranti effect and voltage drop of the capacitive current flowing from line to the generator.[21] Moreover, high frequency transients, caused by switch opening will appear. The overall effect of these dynamical overvoltages and transients will give rise to high voltage crest.

As a consequence of SLG fault near the receiving end of the line

Table 4.IV Receiving end voltages after load rejection for different system conditions.

Source Conditions	Line Conditions	Load Conditions	4 kΩ Opening resistor inserted	Receiving end max. volt. peak (p.u.)		
				A	B	C
inductive source	Uncompensated	Normal	No	1.36	1.32	1.27
inductive source	Uncompensated	1-ϕ-G fault	No	-	1.39	1.58
inductive source	uncompensated	2-ϕ-G fault	No	-	-	1.55
inductive source	Uncompensated	1-ϕ-G fault	Yes	-	1.27	1.41
inductive S. + line source	Uncompensated	1-ϕ-G fault	No	-	1.52	1.73
inductive s. + line source	% 80 shunt compensation	1-ϕ-G fault	No	-	1.46	1.3
inductive s. + line source	uncompensated	2-ϕ-G fault	No	-	-	1.68
inductive source + line source	% 80 shunt compensation	2-ϕ- G fault	No	-	-	1.43

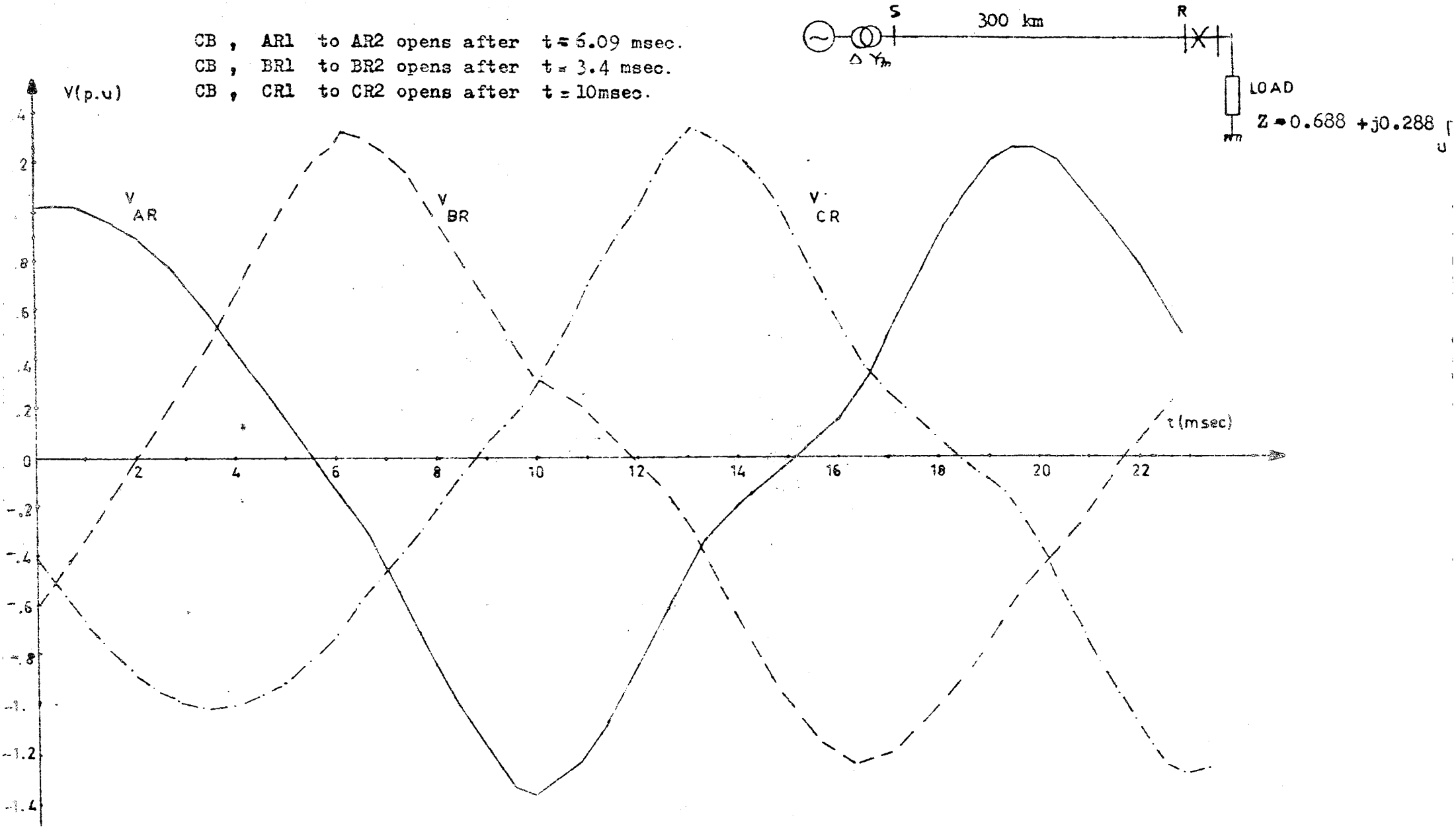

Fig. 4.22 Overvoltages at the receiving end bus following 3 ϕ load rejection

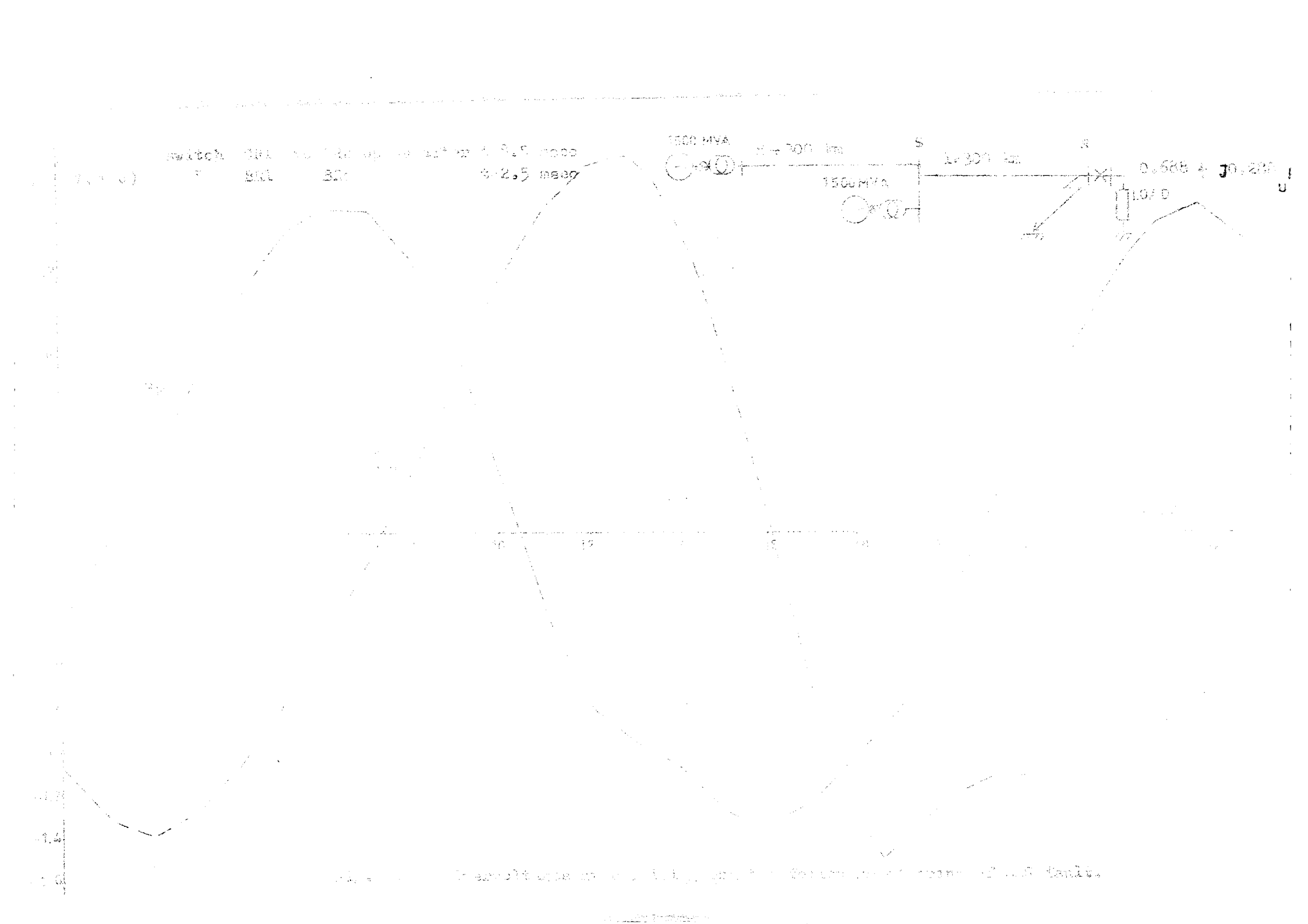
1500 MVA
1500MVA
S
R
1.0/0

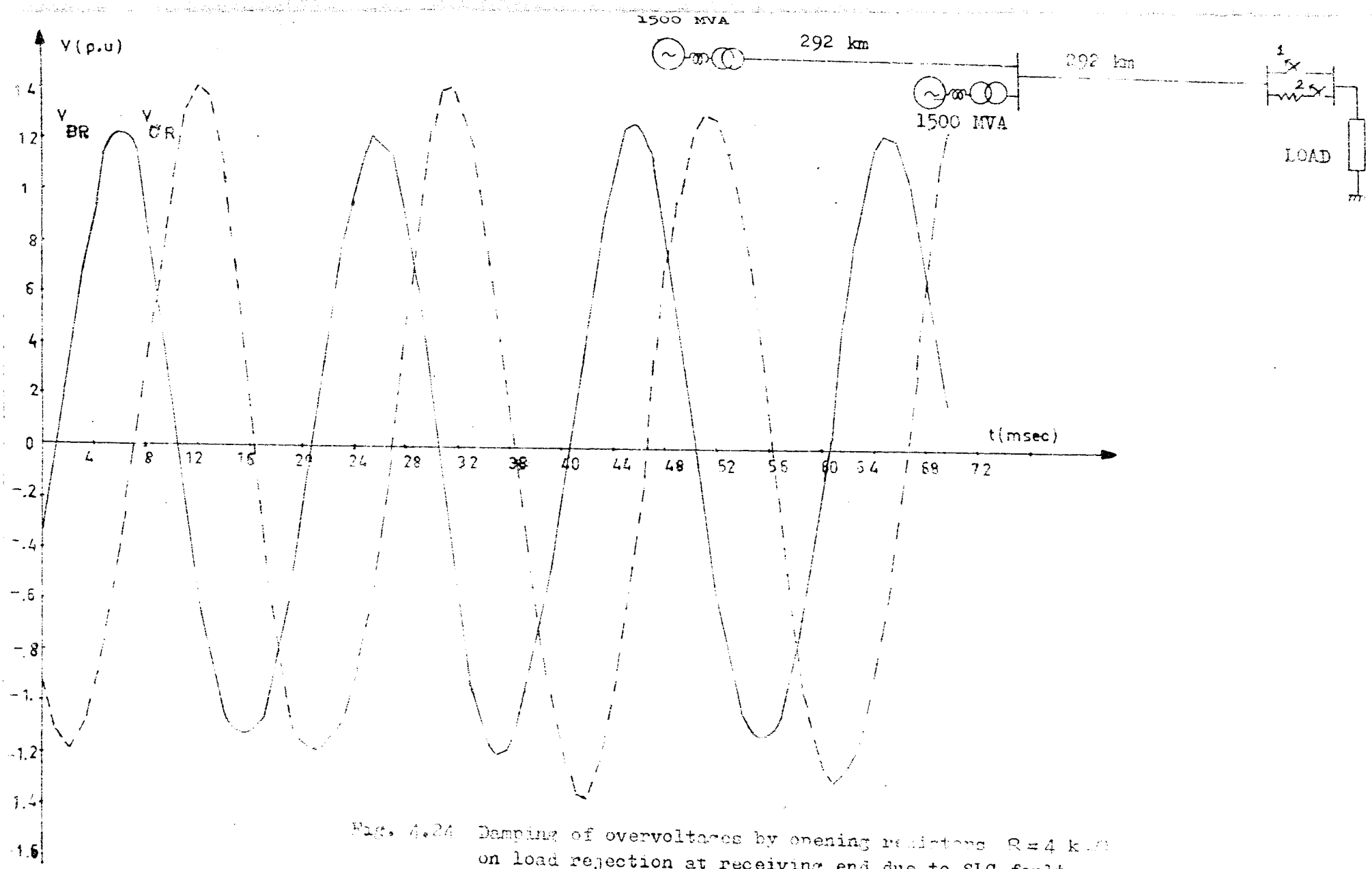

Fig. 4.24 Damping of overvoltages by opening resistors R = 4 kΩ on load rejection at receiving end due to SLG fault (insertion time = 30 msec)

shown in Fig. 4.23 load is disconnected and receiving end voltage rises to 1.73 p.u. since the line is subjected to both load rejection overvoltage and voltage rise of the healthy phases due to neutral point displacement.

If the source short circuit MVA is increased, overvoltage peak is increased at the receiving end after load dropping due to fault there, as the decrease in the terminating impedance at the sending end (high short circuit MVA) results in an increase in the negative reflection there for the travelling waves originated from the CB opening at the receiving end. The worst termination is zero impedance (infinite bus), which is approximated by a bus having several other lines.

For shunt compensated lines overvoltages due to load dropping is less since the line charging is compensated to reduce the dynamicl overvoltages. Moreover, opening resistor inserted across the CB during the opening damps the transient components and overvoltages are reduced.

4.3.2 Fault Clearing Overvoltages[14,15,16]

Because of proposed low insulation design levels of future UHV systems, fault clearing transient overvoltages may exceed the controlled switching-surge levels discussed previously. This part of study is devoted to the investigation and control of these fault clearing transients. Only single line to ground (SLG) fault condition is examined since it has the highest probability of occurrence.[16]

4.3.2.1. Computer Results

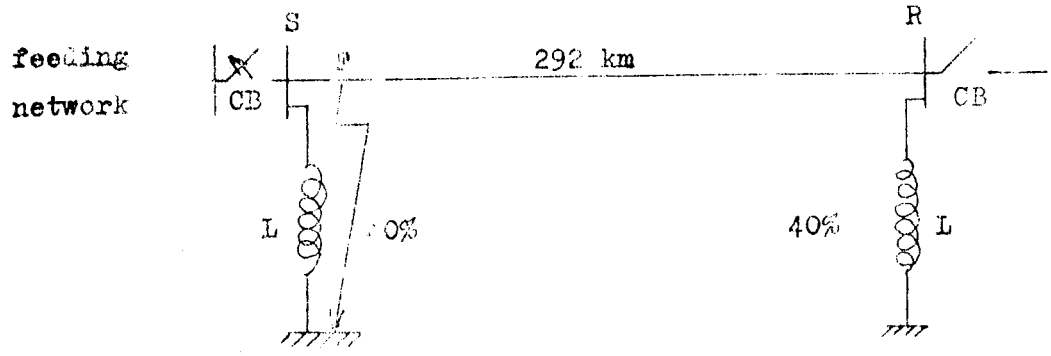

Fig. 4.25 Single diagram of system studied for SLG fault clearing

For the unloaded line in Fig. 4.25, and taking into consideration the various possible combination of feeding networks, the voltage waveforms are calculated for the clearing of SLG faults at the sending end. Example of waves obtained for fault Clearing Overvoltages and TRV across the CB are shown in Fig. 4.26 and Fig. 4.27.

Table 4.V gives the summary of study for overvoltages and TRV after SLG fault clearing. Overvoltages as high as 1.88 p.u. are obtained by clearing faults with breakers not using opening resistors.

The opening resistors in values of 10 kΩ , 4 kΩ , 700 Ω are inserted during the clearing of SLG fault on the local source for the system which has two single source (local and remote). Resistor insertion times were approximately 30 milliseconds. Waveforms shown in Fig.4.28 and Fig. 4.29 give the overvoltage waves and TRV across CB for 200 ohms opening resistors. As can be observed that, the 200 Ω opening resistor reduces the line to ground system overvoltage from 1.68 p.u. to 1.52 p.u and causes damping in TRV. Table 4.IV summarizes the influence of different resistor values on overvoltages and TRV waves for the remaining cases.

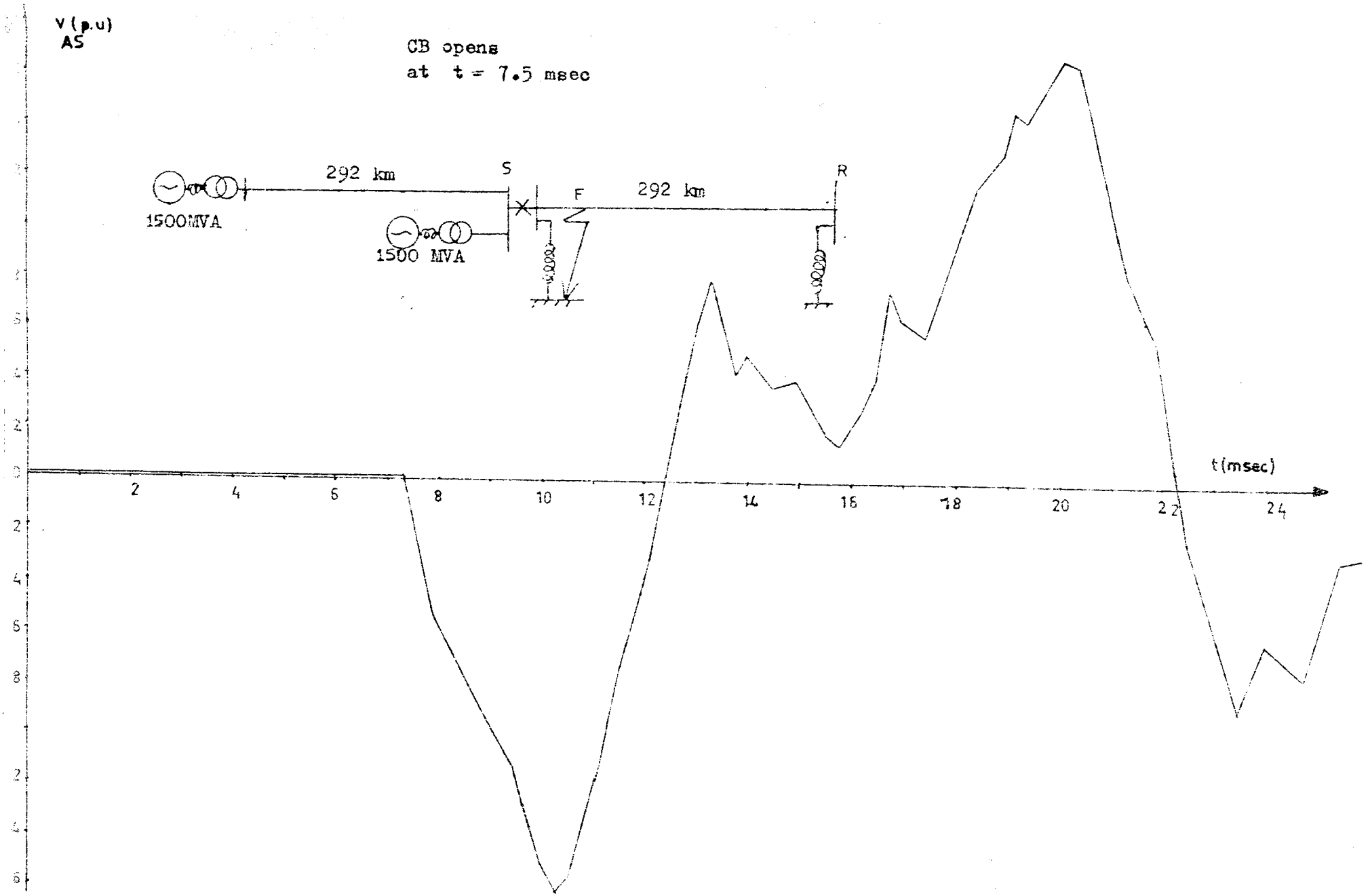

Fig. 4.26 Overvoltages on sending end bus due to SLG fault clearing.

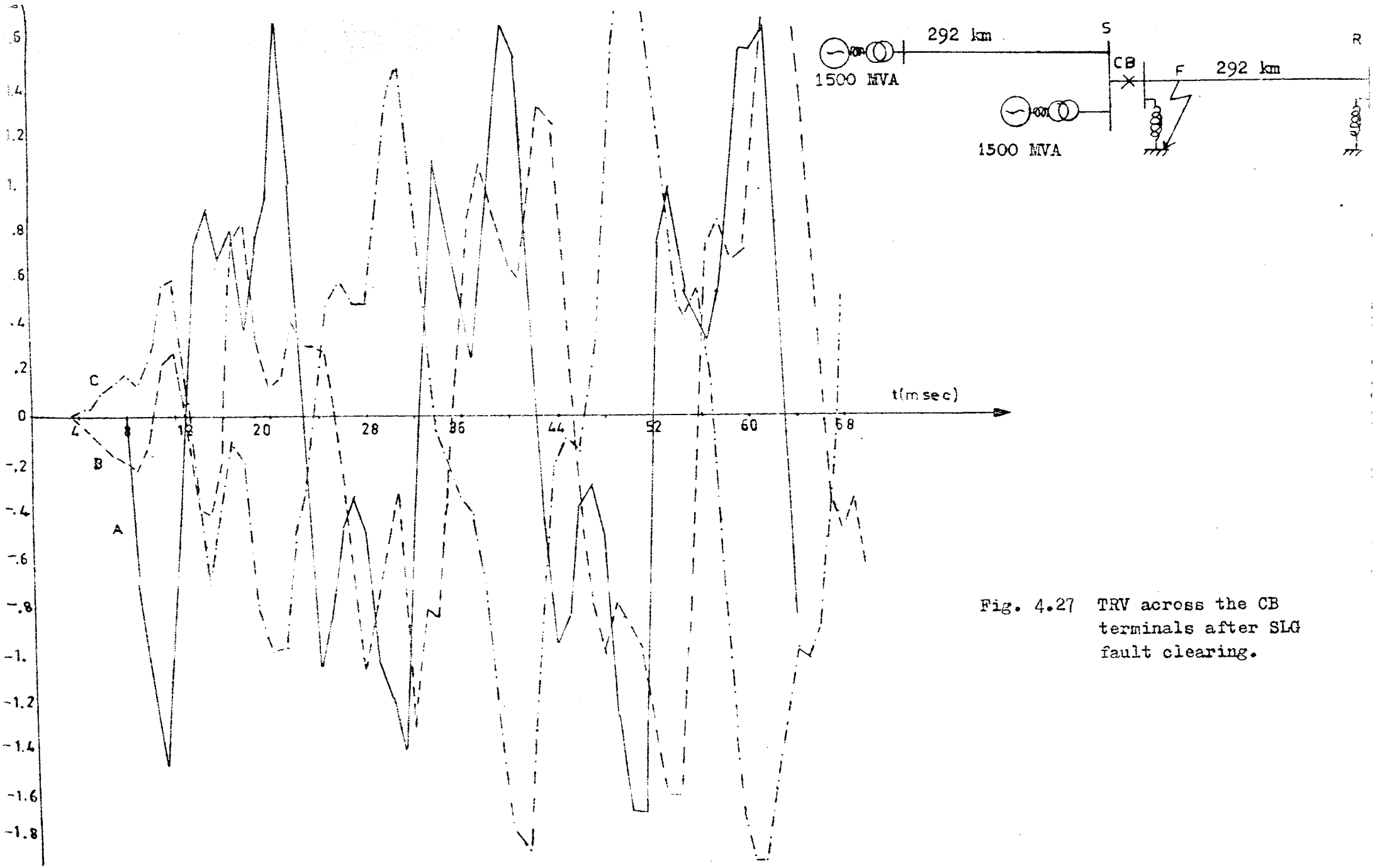

Fig. 4.27 TRV across the CB terminals after SLG fault clearing.

Table 4.V Max. Fault Clearing Overvoltages and TRV for faulted phase across the CB.

Feeding Network	Source MVA line source	Source MVA inductive source	Max. fault C. voltage p.u.	U_{peak} p.u	t_3 μsec	RRRV kv/ μsec
1 short line	6000	-	1.88	1.88	1500	.389
1 short line + inductive s.	3000	3000	1.71	1.71	1200	.442
1 short line + 1 long line	3000 3000	-	1.66	1.57	2200	.2216
1 short line + 1 long line + inductive s.	3000 3000	3000	1.58	1.46	1200	.378
1 long line	3000	-	1.77	1.77	2900	.1899
1 long line	6000	-	1.7	1.7	2500	.21
2 long lines	3000	-	1.75	1.75	3000	.18
2 long lines	6000	-	1.788	1.788	2900	.19
4 long lines	6000	-	1.786	1.786	2900	.191
1 long line + inductive s.	3000	3000	1.6	1.47	2200	.208
2 long lines + inductive s.	3000	3000	1.66	1.56	2300	.210

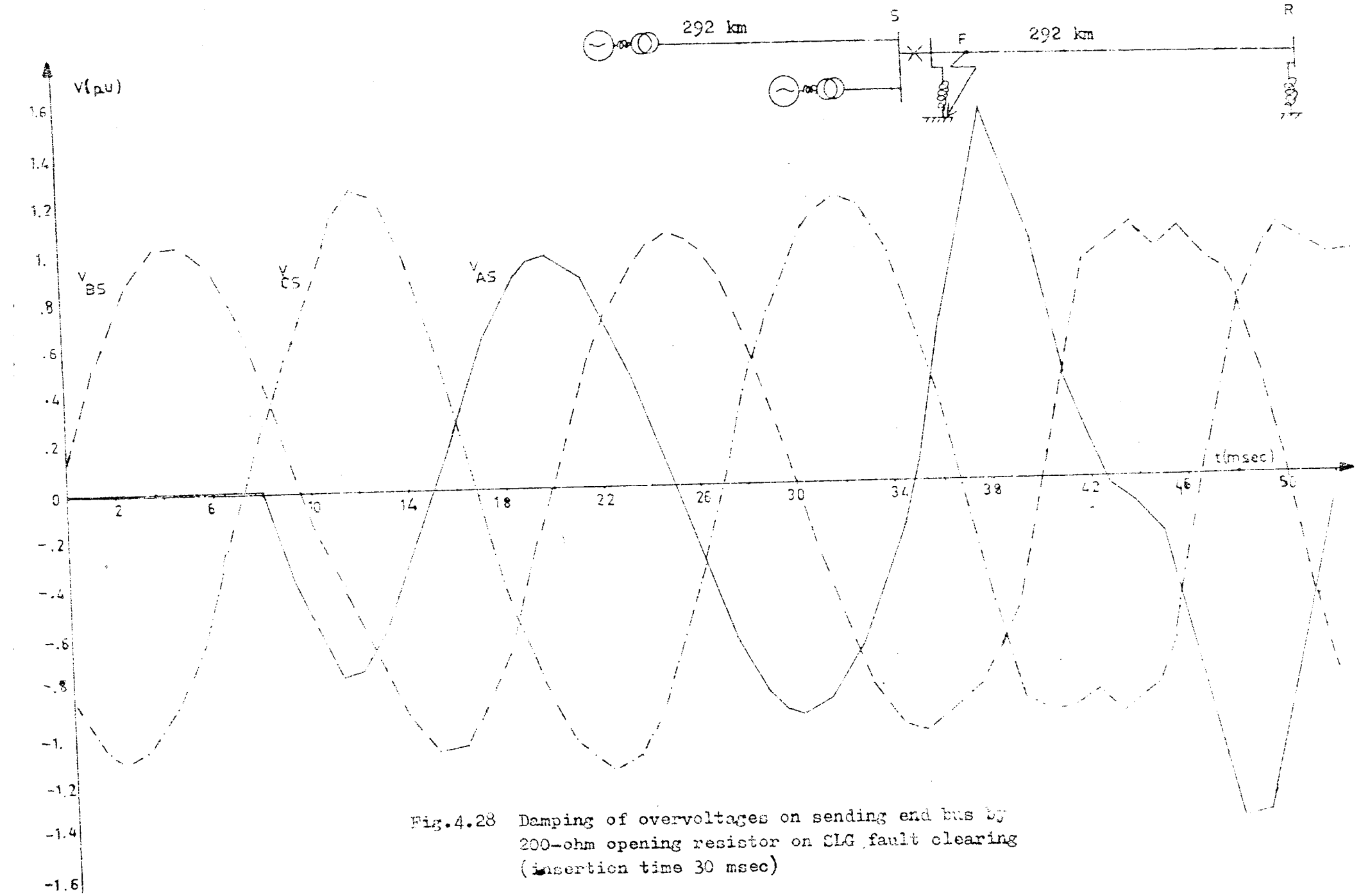

Fig.4.28 Damping of overvoltages on sending end bus by 200-ohm opening resistor on SLG fault clearing (insertion time 30 msec)

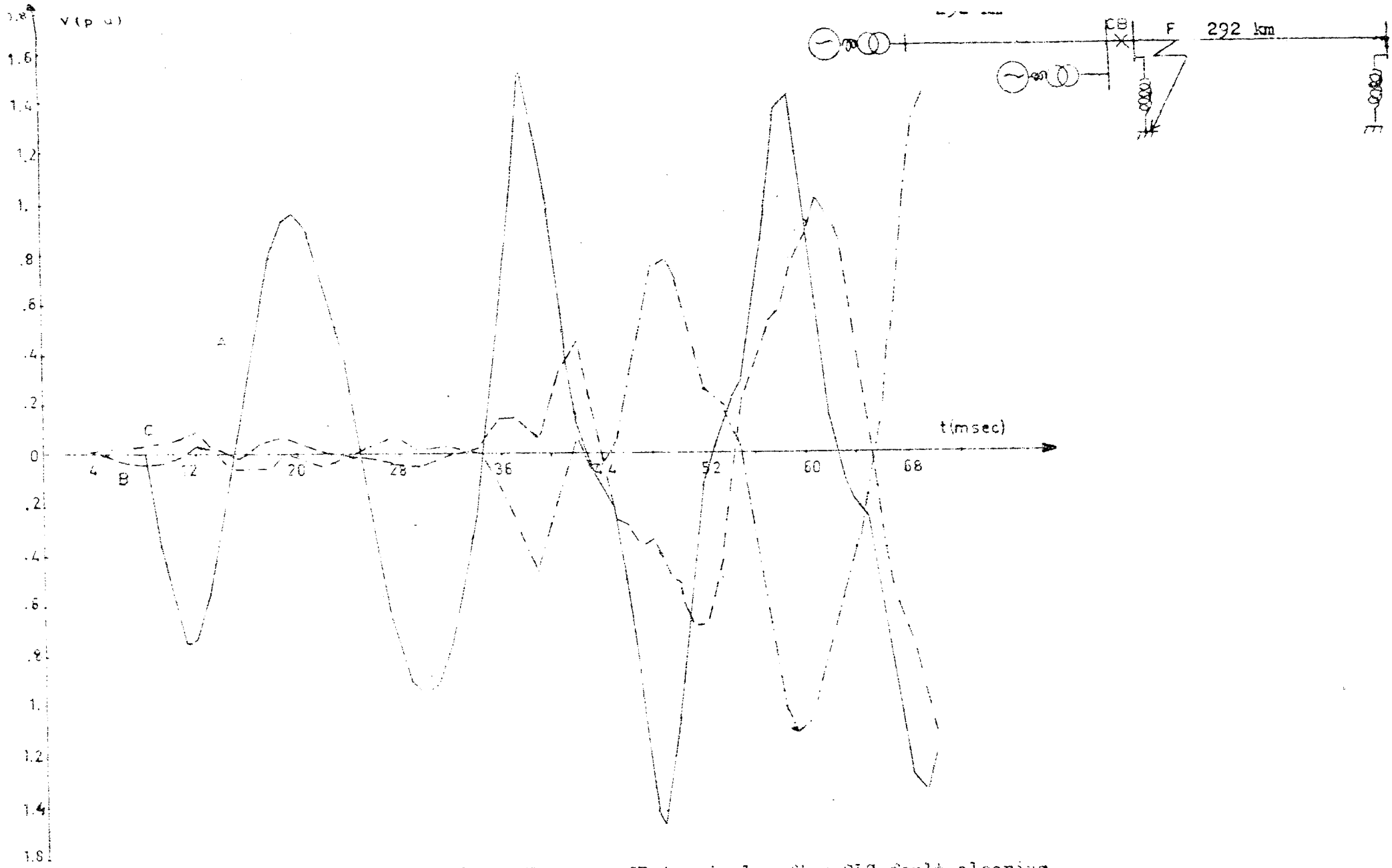

Fig. 4.29 TRV across CB terminals after SLG fault clearing (200-ohm) opening resistor inserted 30 msec during the opening)

Table 4. VI Overvoltages and TRV at sending end of unload line following single line to ground fault clearing versus opening resistors

Circuit Breaker type	Maximum fault clearing voltage (p.u.)	U_{peak} (p.u)	t3 μsec	RRRV kv/μsec
Without opening resistor	1.68	1.604	2900	0.171
10 k Ω opening Resistor	1.63			
4 k Ω opening Resistor	1.55			
200 Ω opening Resistor	1.52	1.52	2900	0.163

4.3.2.2. Analysis of Computer Results

Different system configurations on the source bus have the following influence on the RRRV and the overvoltages produced.

1. As the length of source line is increased, RRRV is decreased and fault clearing overvoltages are decreased because of the following reasons:

   a) Circuit capacitance is increased.

   b) Travel time of surge waves are increased.

2. With the number of lines connected to the source side bus is increased , RRRV is decreased and fault clearing overvoltages are

increased due to:

a) Source side surge impedance is decreased (RRRV $=\sqrt{2}$ I Z_o).

b) Reflection from source line end are increased.

3. When inductive source is connected with line source, RRRV is increased and fault clearing overvoltages are decreased since:

a) Source inductance makes the voltage wave steeper.

b) The reflected waves from the source end will refract through the inductive source at the sending end. In other words, the voltage surge coming from the line source will not be doubled anymore.

4. When the short circuit MVA of line source are increased, fault clearing overvoltages are decreased and RRRV is increased since:

a) Reflection of surge waves from line source end is decreased.

b) Equivalent system capacitance increases.

5. When short circuit MVA of inductive source is increased, RRRV is decreased and fault clearing overvoltages are increased since source inductance decreases.

CHAPTER V

EFFECT OF TRAPPED CHARGE AND ITS DECAY

5.1. Introduction.[13][28][29]

If any phase of an AC transmission line or cable that is not carrying load is interrrupted, the energy stored in the electrostatic dielectrics at the moment of interruption remains trapped on the transmission lines. When the line is compensated with HV reactors, the oscillations of trapped charge take place among the line capacitance and the reactors. However, without reactor, trapped charge on the line may be considered constant.

The magnitude of the trapped charge prevailing at the moment of reenergization of a transmission line materially influences the severity of overvoltages. With a trapped charge equal to the crest of the normal phase to neutral voltage (1 p.u.), the overvoltage at recolusure would reach an amplitude of 3 p.u. as the following single phase line (Fig.5.1) indicates.

In three phase systems, due to coupling between the phases, the overvoltage magnitudes may be as high as 3.5. p.u.[3] The insulation levels in all EHV systems are normally chosen in accordance with the overvoltages generated when closing on trapped charge which could be very high as the above simple analysis shows. However, by simple measures taken during the design of the lines, the effects of trapped

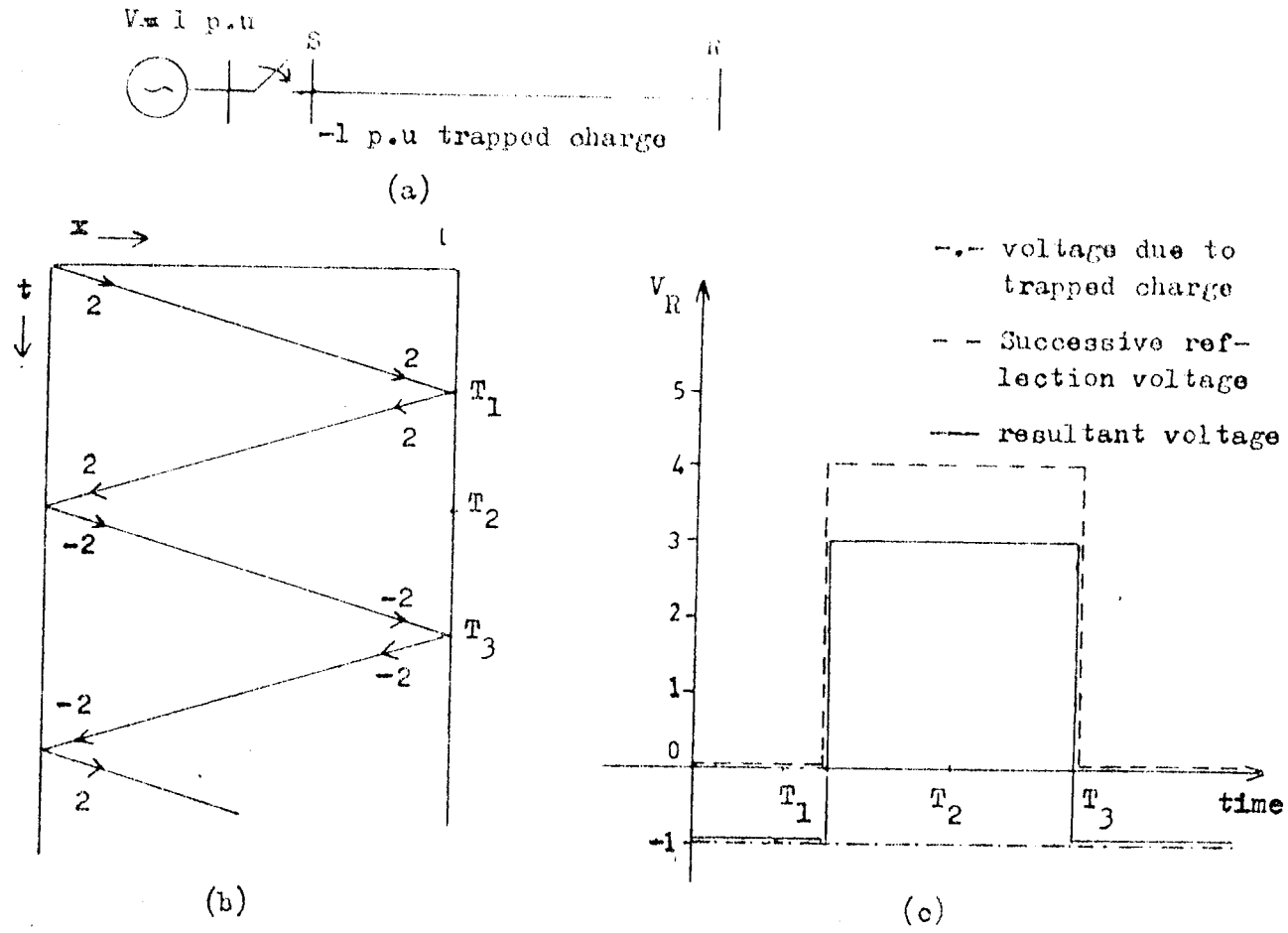

Fig.5.1 Single phase line reenergization

(a) Single phase system, (b) Lattice diagram

(c) Receiving end transient voltage waveform.

charge can be nullified therefore reducing the severity of the overvoltages.

In the following sections the trapped charge and possible voltage oscillations following interruption of charging current of a long unloaded line and measure to discharge the trapped charge will be examined.

5.2. Trapped Charge Decay after Uncompensated Line Dropping

5.2.1. Trapped Charge Due to High Side Switching

The resultant voltages left on the three phases of a transmission line opened by the high voltage breakers are given in Fig. 5.2. The maximum overvoltage occures on phase c which is the first phase to clear, caused by capacitive coupling with the phases still connected to the bus (a function of the switching sequence and of the ratio C_1/C_0). The p.u. overvoltage has a direct and a periodic component with fundamental frequency $1/T_1$ where T_1 is the travelling time of the surges on the line. The periodic component is damped by the line loss while the direct component corresponds to the voltage of the trapped charge.

5.2.2. Discharge Through Opening Resistors.[27]

When an unloaded line is dropped by a circuit breaker equipped with opening resistors, some of the trapped voltage is drained through the opening resistors, the decay being dependent on the size of the resistor as the following single phase analysis shows.

a) Dropping a line fed from an infinite bus:

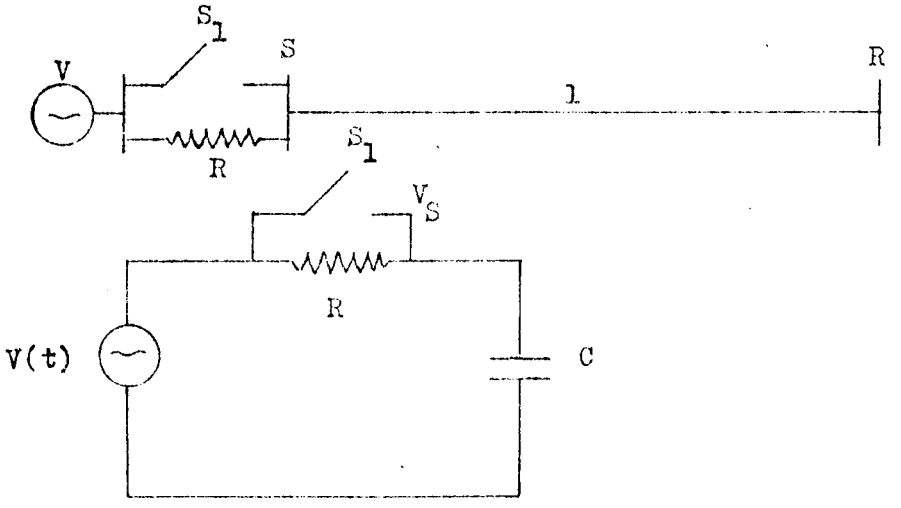

Fig. 5.3. Line dropping scheme and its equivalent circuit.

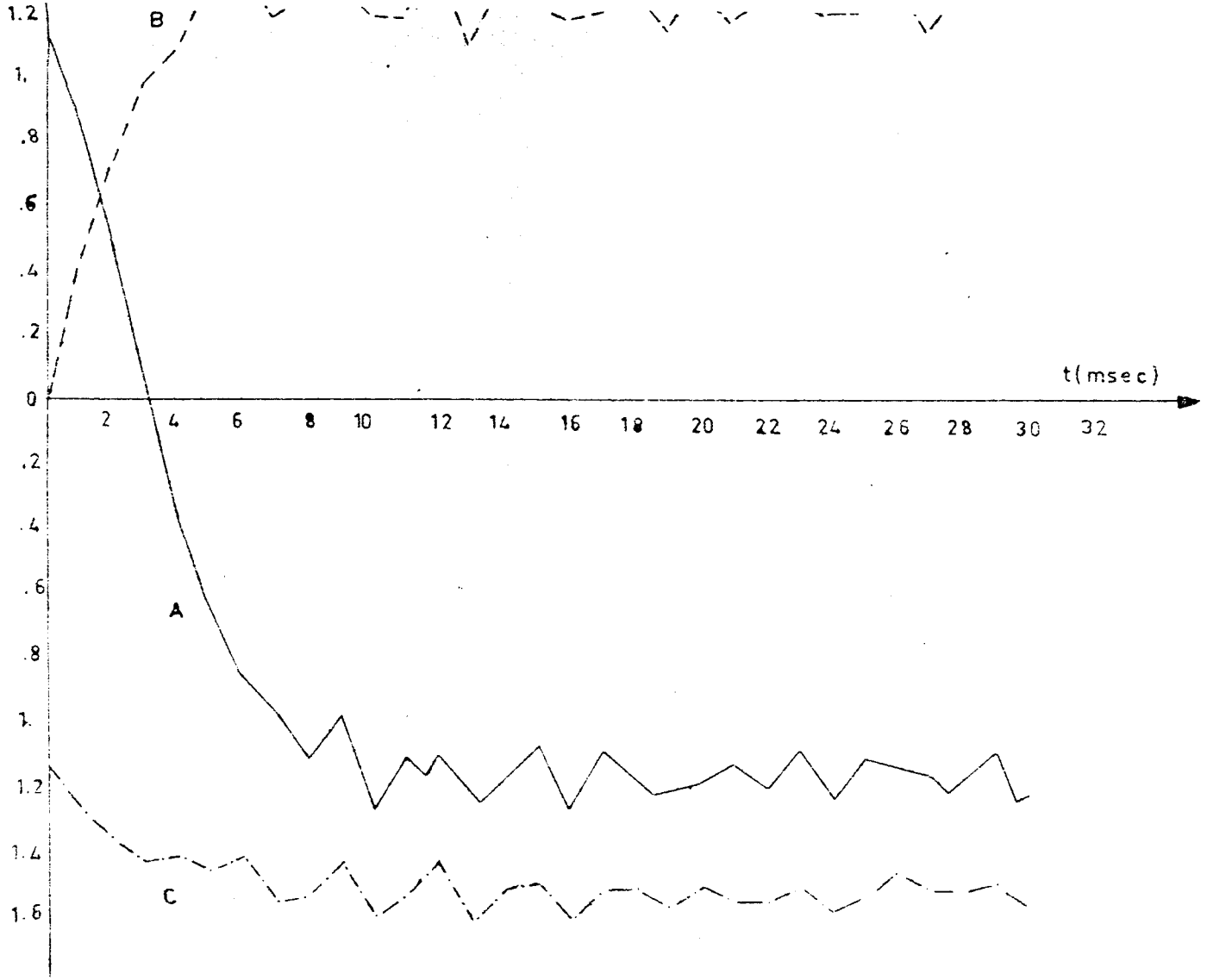

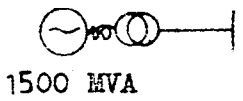

Fig. 5.2 sending end trapped charge voltage waveform after 3ϕ line dropping.

The system analysed is given in Fig. 5.3. The act of opening and the influence of source are treated separately using superposition principle. To obtain the component of V_S due to opening of switch 1, V is set equal to 0 , and a current of fundamental frequency and opposite in sign to the one existing through CB at the time of opening is injected. Then :

$$V_S(s) = \frac{-iR}{sRC+1} = \frac{-IR}{(sRC+1)(s-jw)} \qquad (5.1)$$

where s is the Laplace transform operator.

$$V_S(s) = \frac{-I}{C}\left[\frac{1}{(jw+\frac{1}{RC})(s-jw)} - \frac{1}{(jw+\frac{1}{RC})(s+\frac{1}{RC})}\right] \qquad (5.2)$$

and

$$V_S(t) = \frac{-jEwRC}{jwRC+1}\left[e^{jwt} - e^{-(1/RC)t}\right] \qquad (5.3)$$

Since $V(t)=Ee^{jwt}$ and $I=jEwC$

Adding the voltage due to the influence of the source, the complete solution is obtained as

$$V_S(t) = E\,e^{jwt} - \frac{jEwRC}{jwRC+1}\left[e^{jwt} - e^{-(1/RC)t}\right] \qquad (5.4)$$

b) Dropping of the line fed from an inductive bus :

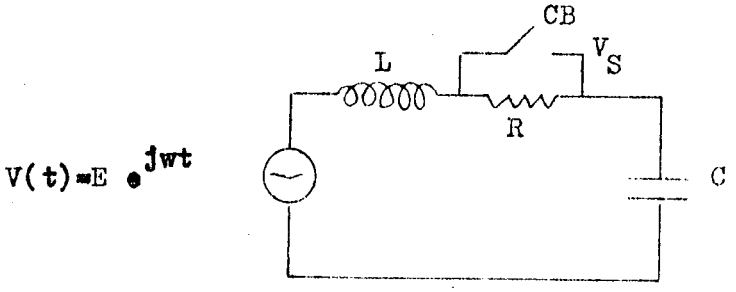

Fig.5.4 Equivalent circuit for line dropping from an inductive source

The analysis given in the preceeding section by including source inductance L as shown in Fig. 5.4

$$V_S(s) = \frac{-jR}{R + sL + 1/sC} \cdot \frac{I}{s} = \frac{-IR}{(RCs + LCs^2 + 1)(s-jw)} \qquad (5.5)$$

letting $\alpha = R/2L$ $\beta^2 = 1/LC - (R/2L)^2 = w_o^2 - \alpha^2$

then

$$V_S(s) = \frac{-IR}{LC(s-jw)\ (s^2+Rs/L+1/LC)} = \frac{-IR}{LC(s-jw)\ (s^2+2\alpha s+\alpha^2+\beta^2)}$$

$$V_S(s) = \frac{-IR(s+\alpha+\alpha+jw)}{LC\ \left[(s+\alpha)^2 - (\alpha+jw)^2\right]\ \left[(s+\alpha)^2+\beta^2\right]}$$

$$V_S(s) = \frac{-IR\ (s+2\alpha+jw)}{LC\left[\beta^2+(\alpha+jw)^2\right]}\ \left[\frac{1}{(s+\alpha)^2 - (\alpha+jw)^2} - \frac{1}{(s+\alpha)^2+\beta^2}\right]$$

$$V_S(s) = \frac{-IR}{LC\left[\beta^2+(\alpha+jw)^2\right]}\ \left[\frac{1}{s-jw} - \frac{s+\alpha+\alpha+jw}{(s+\alpha)^2+\beta^2}\right]$$

and

$$V_S(t) = \frac{-IR}{(1-w^2/w_o^2 + j2\alpha w/w_o^2)}\ \left[e^{jwt} - e^{-\alpha t}(\cos\beta t + (\alpha+jw/\beta)\sin\beta t)\right] \qquad (5.6)$$

The complete solution is given by adding effect of source as:

$$V_S(t) = \frac{E\ e^{jwt}}{1-w^2LC} - \frac{j\ EwCR}{(1-w^2LC)(1-w^2LC+jwRC)}\left[e^{jwt} - e^{-\alpha t}\left(\cos\beta t + \frac{\alpha+jw}{\beta}\sin\beta t\right)\right]$$

(5.7)

5.2.3. The Choice of Opening Resistor Value for Trap Charge Decaying.

The single phase system shown in the Figure 5.5 is simulated on the Transients Analysis Program. Fig. 5.6 shows the resultant waveforms of the trapped charge obtained by inserting different resistors during the opening operation. Fig. 5.7 shows the waveforms for the trapped charge obtained by inserting 4 kΩ opening resistors for different line length after single phase line dropping.

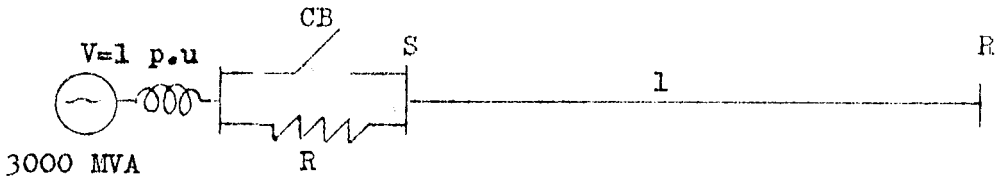

Fig. 5.5 Single phase system
CB is equipped with opening resistor.

Results obtained from the above study can be summarized as follows:

1. As the opening resistor value is increased, the time constant to reach the steady state increases but the trapped charge magnitude left on the line decreases.

2. With the line length increased, the trapped charge magnitude left on the line decreases and the time to reach the steady state increases.

The formulas (5.4) and (5.7) are helpful to understand the above results obtained from the computer study.

From the above results the following conclusion has been arrived.

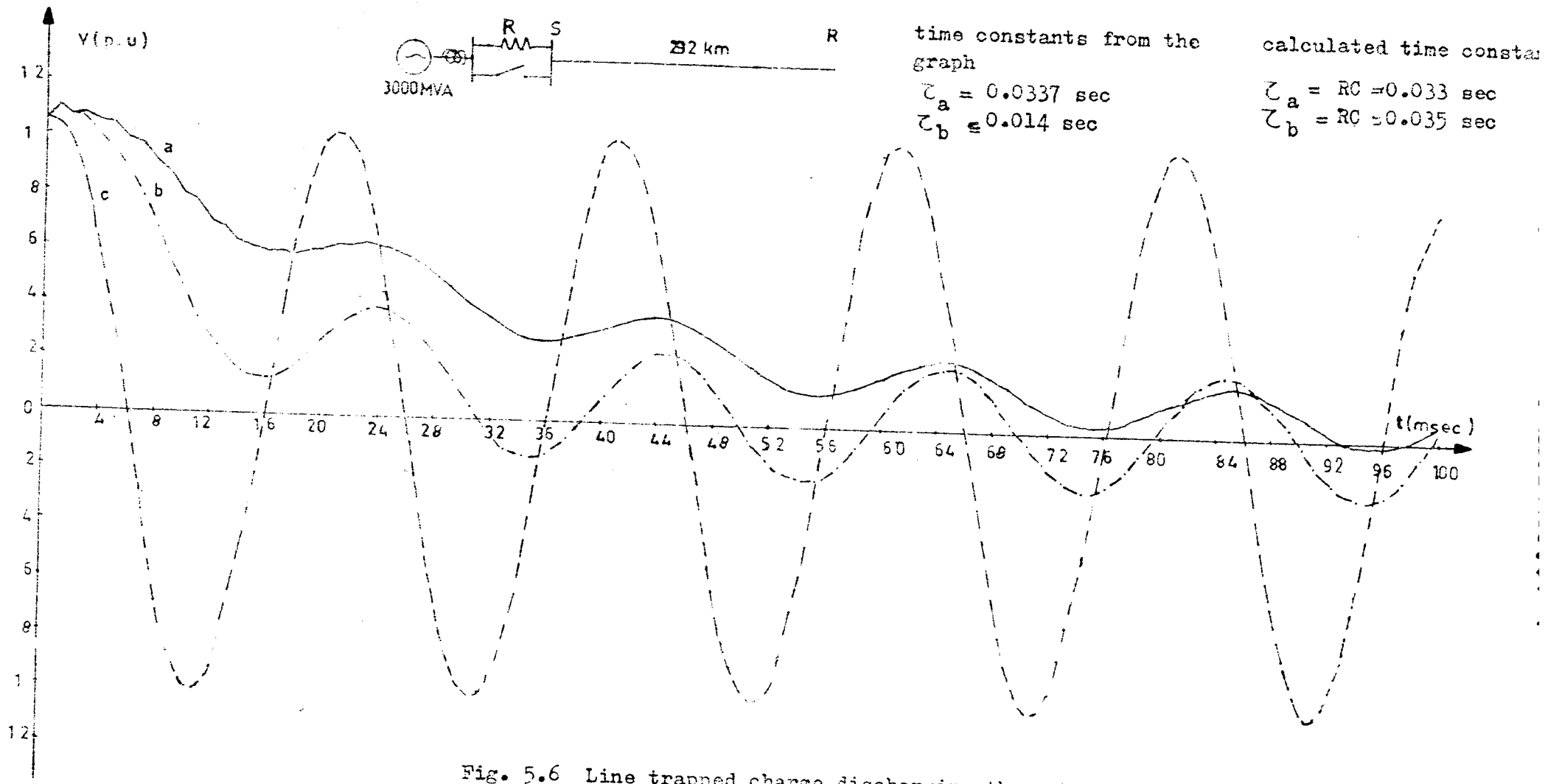

Fig. 5.6 Line trapped charge discharging through the opening resistor R (single phase)

a – R = 10 kΩ b – R = 4 kΩ c– R = 200 Ω

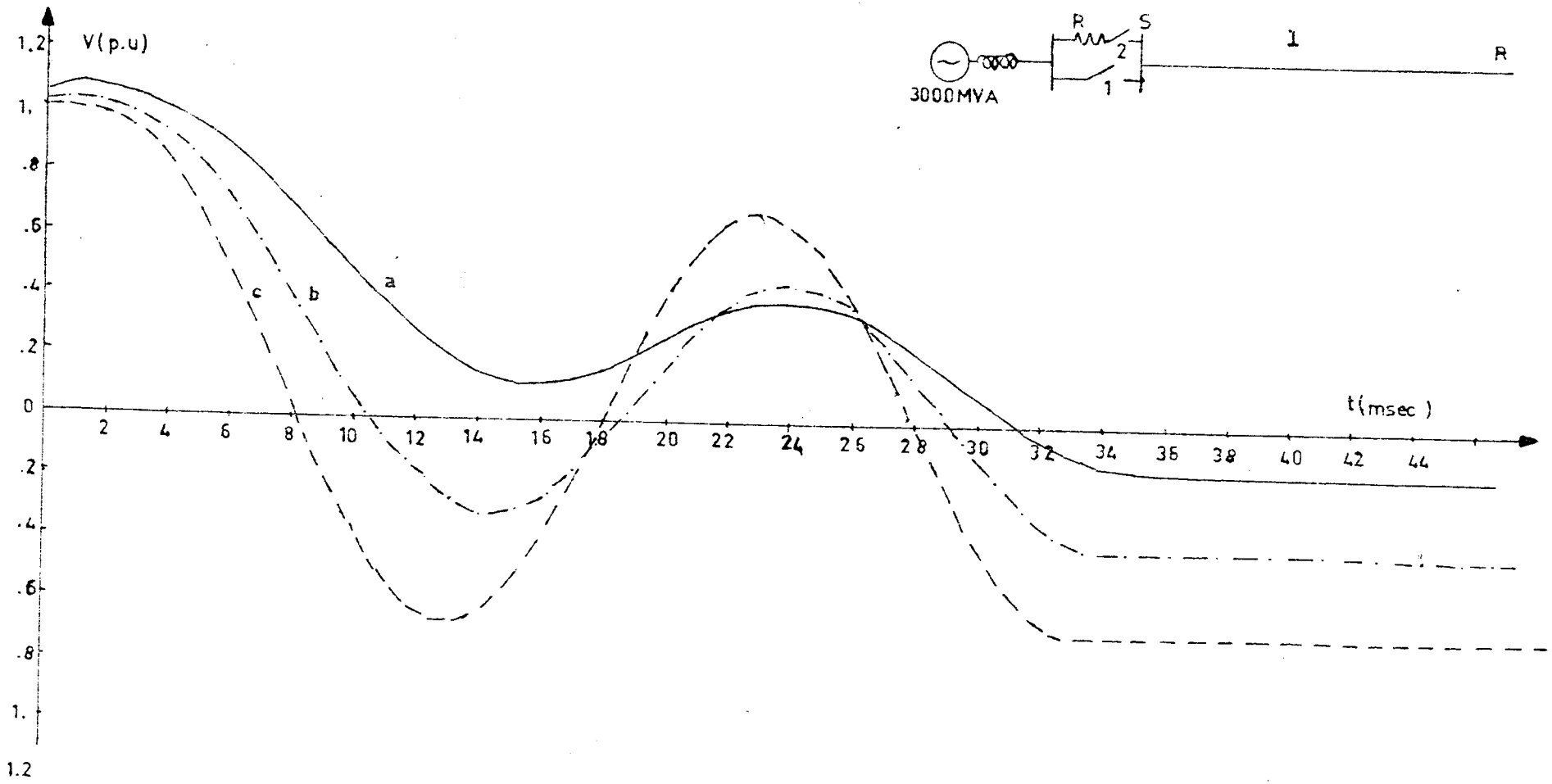

Fig.5.7 Trapped charge discharging through 4 kΩ opening resistor for different line length after single phase line dropping (insertion time = 30 msec)

a- l = 292 km b- l = 146 km c- l = 73 km

- The reduction in the trapped charge depends on the value of resistor, line length, time period of insertion.
- The trapped charge left is less if the resistor value is high. However the insertion time should be made longer.

5.2.4 Three Phase System Study

The three phase line fed from an inductive source with line source shown in the Fig. 5.8 is simulated on the Transients Analysis Program (see Appendix D for its parameters). Line is dropped by opening CB and 4 kΩ, 10 kΩ opening resistors are inserted across the CB breakers for 30 milliseconds. The obtained waveforms are shown in the figures (5.9), (5.10) and the trapped voltage magnitudes are summarized on Table 5.I.

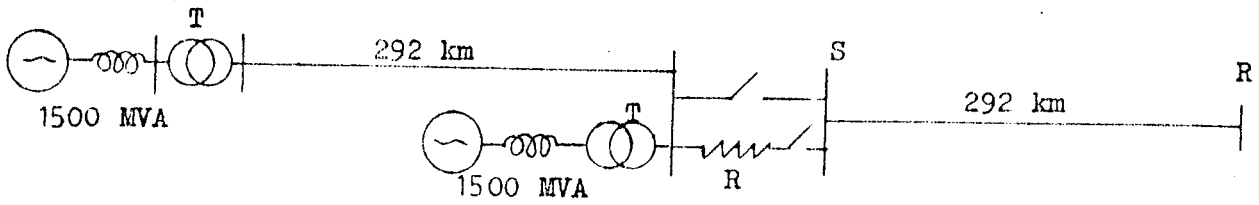

Fig. 5.8. Three phase system studied for the trapped charge decaying.

For 4 kΩ opening resistor inserted 30 msec, less charge is trapped than 10 kΩ opening resistor since the time constant to reach the steady state is less. But, if the insertion time is infinity, the voltage trapped is less in the case of 10 kΩ opening resistor than that of the 4 kΩ resistor case.

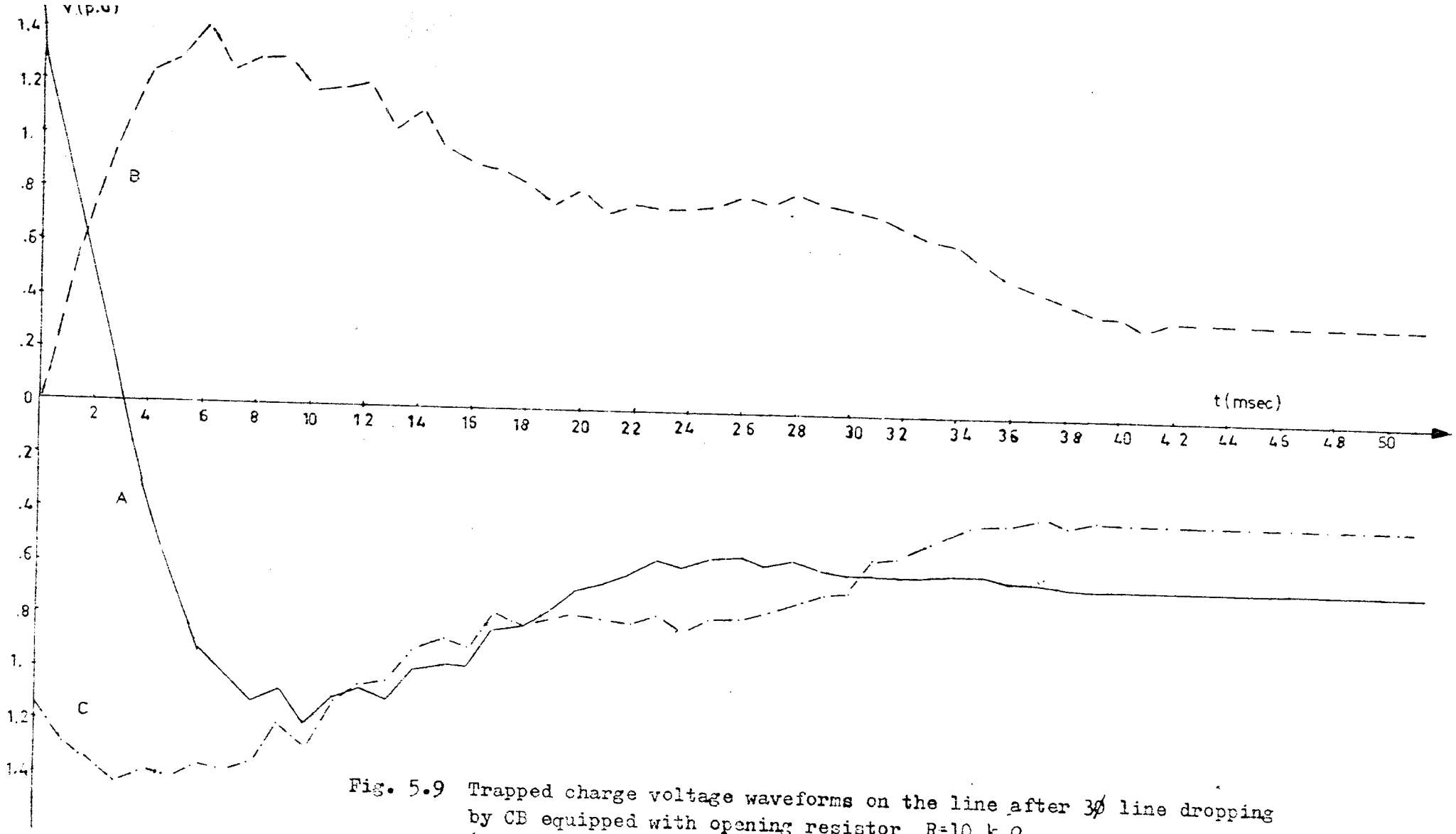

Fig. 5.9 Trapped charge voltage waveforms on the line after 3Ø line dropping by CB equipped with opening resistor R=10 kΩ
(Resistor insertion time 30 mseo)

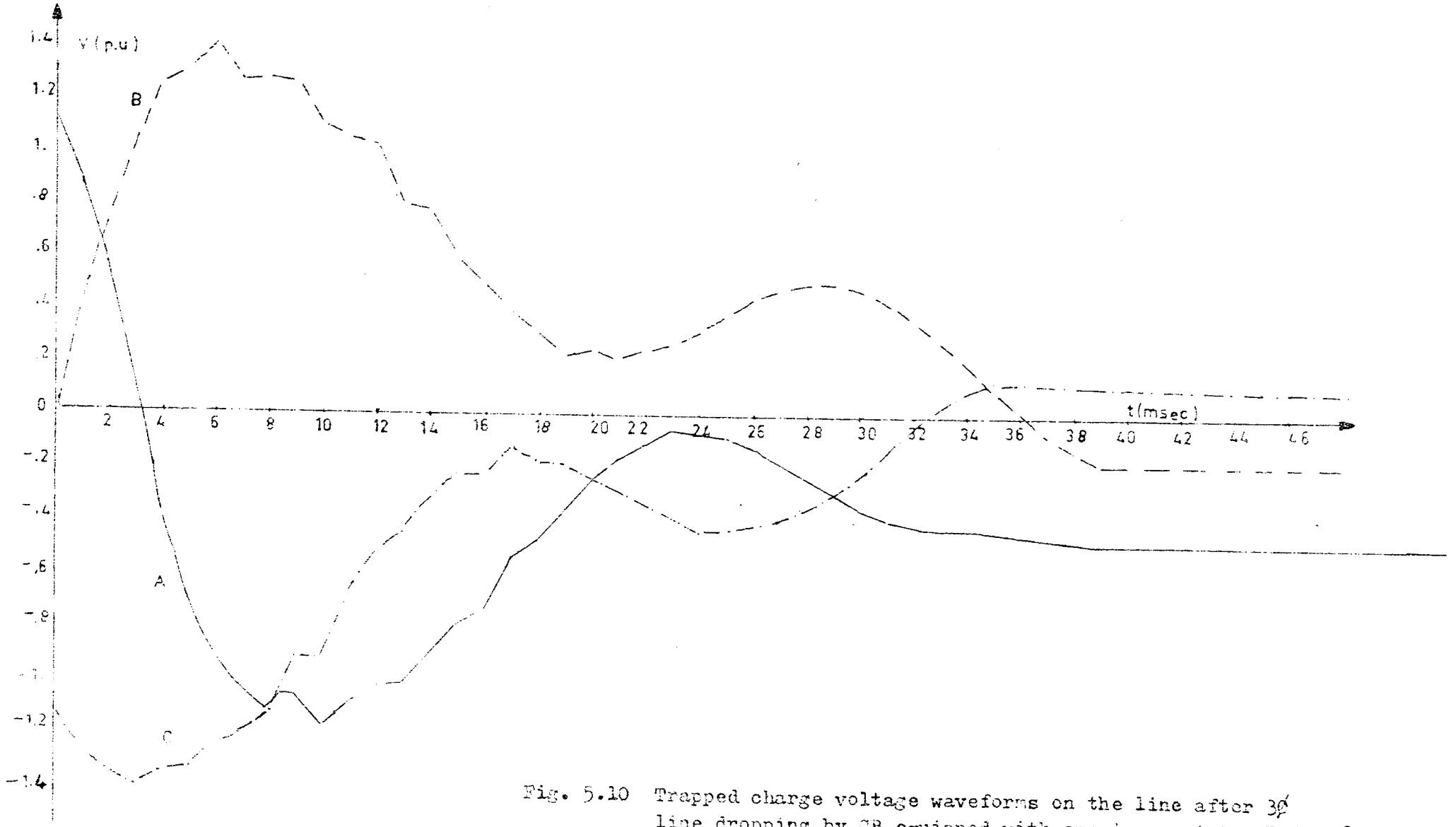

Fig. 5.10 Trapped charge voltage waveforms on the line after 3ϕ line dropping by CB equipped with opening resistor R=4 k Ω (Resistor insertion time 30 msec)

Table 5.I Trapped charges on the phases after 3ϕ no load uncompensated line dropping.

Phases	A	B	C
Without opening resistor	1.1	1.2	1.5
With 10 kΩ opening resistor 30 msec. insertion time	0.63	0.41	0.39
With 4 kΩ opening resistor 30 msec. insertion time	0.46	0.41	0.39

5.2.5 Low-Side Switching[8][30]

As the following analysis indicates, when low side switching is used as opposed to the high side switching, a completely different case is obtained as there is now a path available for the draining of trapped charge.

Several cases of low-side opening have been analysed with different line length, ground resistance and winding loss. The resultant waveforms of one of the cases is shown in Fig. 5.11.

As the line length decreases, trapped charge decaying is fast and frequency of oscillation decreases since lesser electromagnetic energy is trapped and frequency of oscillation is inversely proportional to the total line capacitance. Change in the ground resistance in range 1 Ω to 4 Ω does not result considerable effect on decaying time of the trapped charge. The oscillations of the trapped charge can be explained

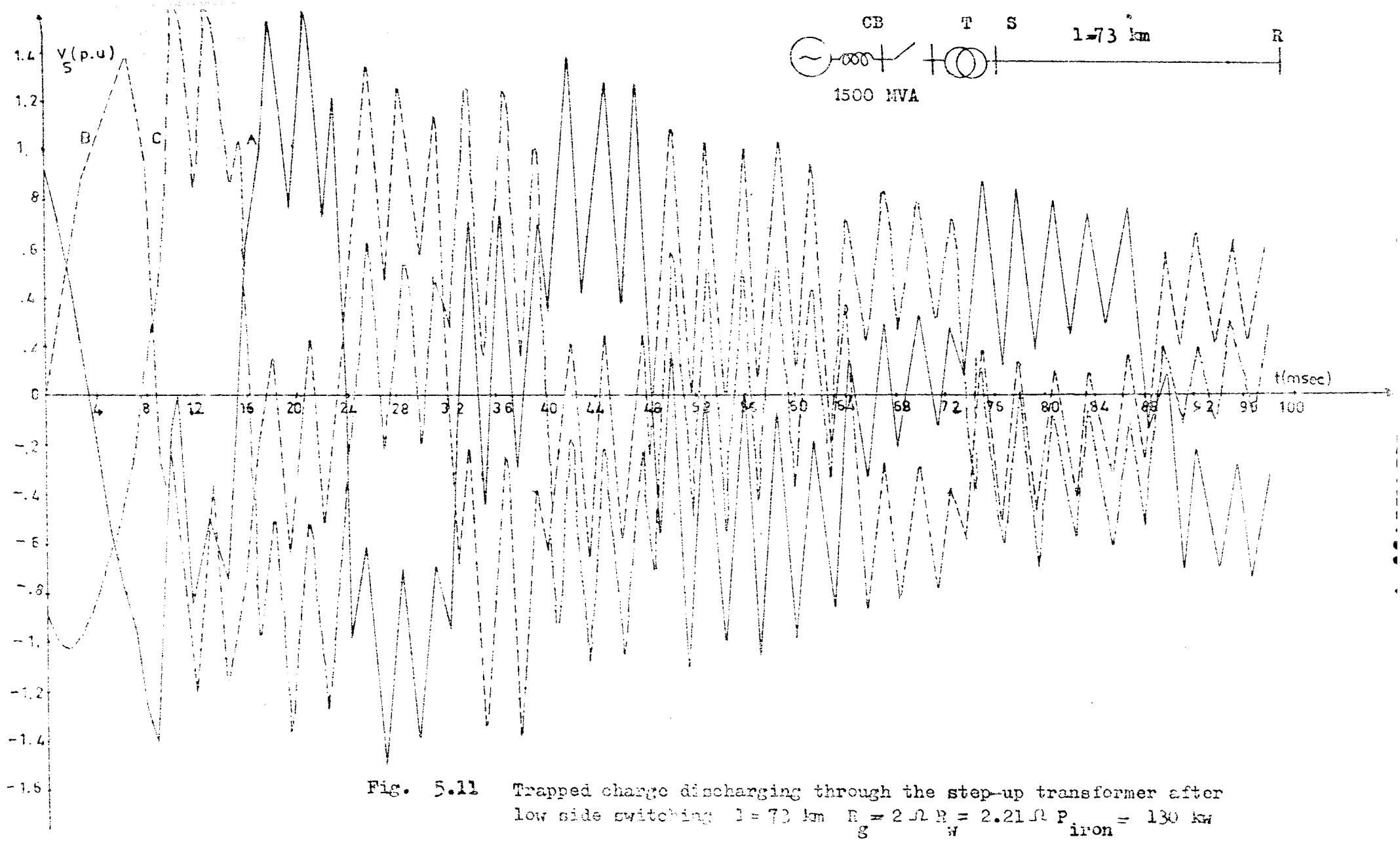

Fig. 5.11 Trapped charge discharging through the step-up transformer after low side switching $l = 73$ km $R_g = 2\ \Omega$ $R_w = 2.21\ \Omega$ $P_{iron} = 130$ kW

as follows: When the line is dropped, the electromagnetic energy trapped on the line has a path through the magnetizing impedance of the transformer, by which it can discharge. However, as long as the core is unsaturated, this represents a high impedance and the discharge is very slow. While the transformer is in the non-saturated state the oscillation frequency is usually much lower than the power frequency. Thus, the transformer will enter saturation a few millisecond after switching, increasing the frequency of oscillations and their damping. The oscillation frequency with the transformer in the saturated state is several times the power frequency and the damping time constant is of the order of some tenths of a second. When the amplitude of the voltage oscillations is low enough the transformer will return to the non-saturated state, the low frequency oscillations will start again and the process described above may repeat itself until the amplitude is such that the transformer will remain in the non-saturated state.

5.3. Trapped Charge Phenomena for Shunt Compensated Lines.[24]

When a line with shunt reactors is switched off, the trapped voltage will start oscillations similar to those appearing when the line is loaded with power transformers. However, because of the characteristics of the reactors used the oscillation frequency will be quite close to the power frequency.

The simplified circuit for a compensated line has two natural frequencies,

$$w_o = 1/\sqrt{LC_o} \qquad \text{and} \qquad w_1 = 1/\sqrt{LC_1}$$

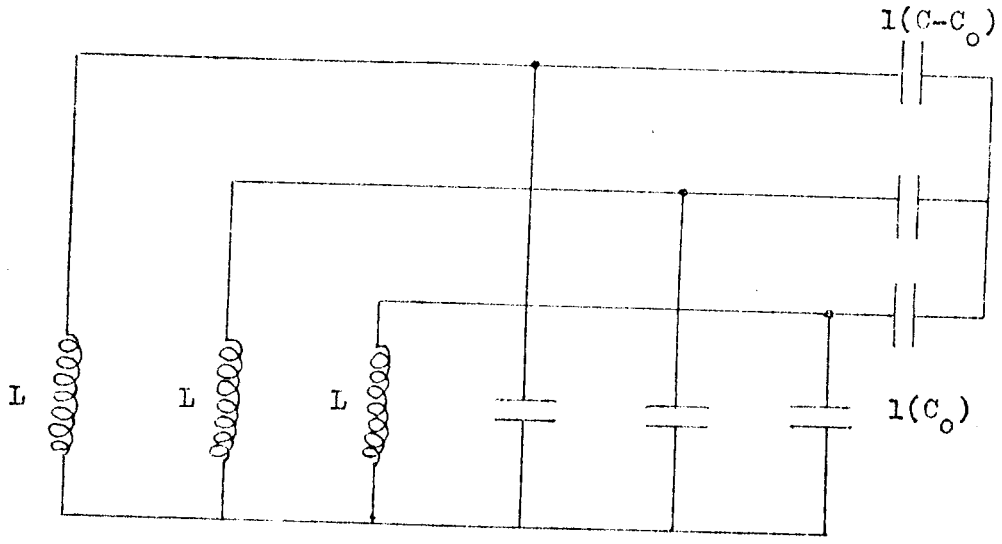

Fig.5.12 The equivalent circuit for shunt compensated lines.

Therefore, if a no-load shunt compensated and transposed line is opened, two main natural frequencies appear in the oscillation of phase to ground line voltages. However the amplitude of w_1 is approximately equal to the feeding phase to ground peak voltage whereas the frequency w_o is negligible for many cases.(24)

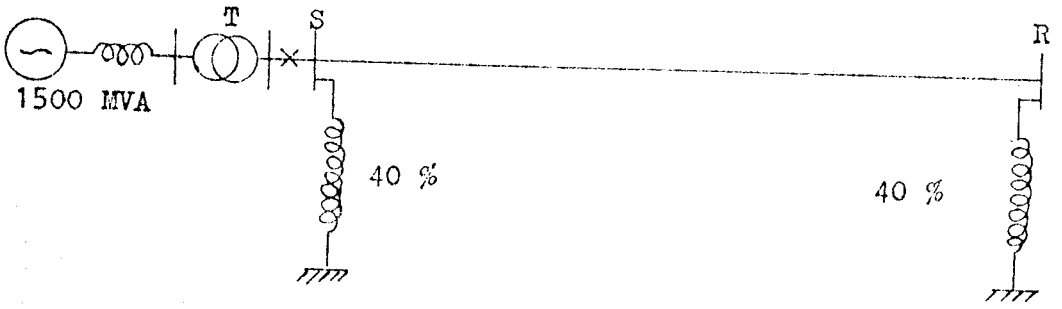

Fig. 5.13 Shunt compensated unloaded line.

Fig. 5.14 gives the phase to ground voltages by opening at subsequent current zeros of no load fully transposed line shown in Fig. 5.13. The oscillation frequency is 1/22 and is approximately equal to $f_1 = 1/2\pi\sqrt{LC_1}$ c/msec.

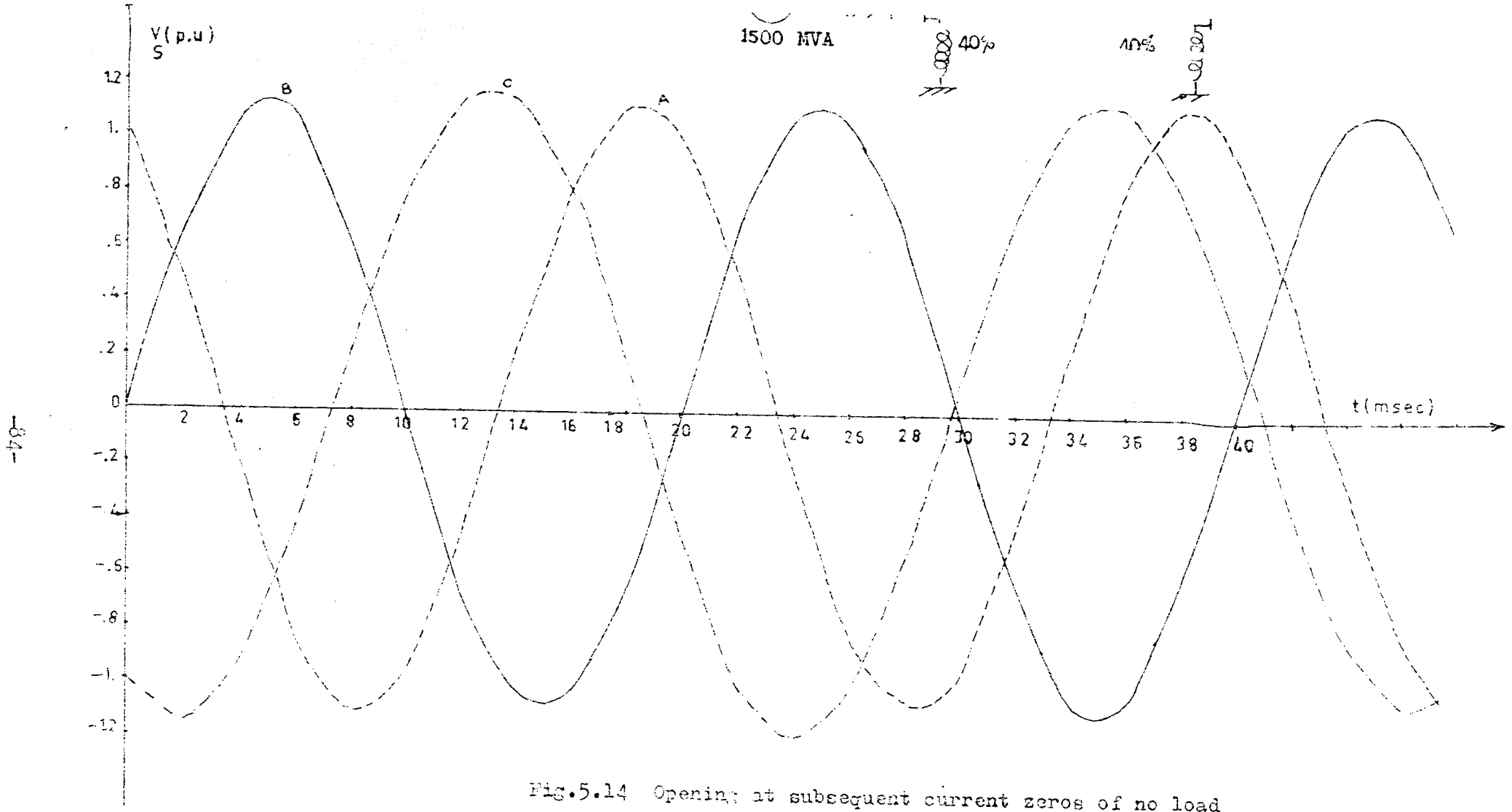

Fig.5.14 Opening at subsequent current zeros of no load fully transposed and shunt compensated line. Phase to ground voltages on phases A-C of the line.

5.3.1. Influence of Line Loss on the Decay of Trapped Charge.[24]

The results of computer study for the system given are shown in Fig. 5.15 indicating the effect of line loss on decay of trapped charge voltages. The time constant for the decay of trapped charge voltages are calculated from the related figures by using formula (Table 5.I)

$$V_{A1} = e^{-t/\tau} \sin w_o t \qquad (5.8)$$

The mathematical computation of the time constant of decay of trapped charge voltages due to line loss can be made by refering to Fig. 5.15. The distribution of the current along the line can be assumed to be approximately linear (origin at the end without shunt reactor)(Fig.5.16).

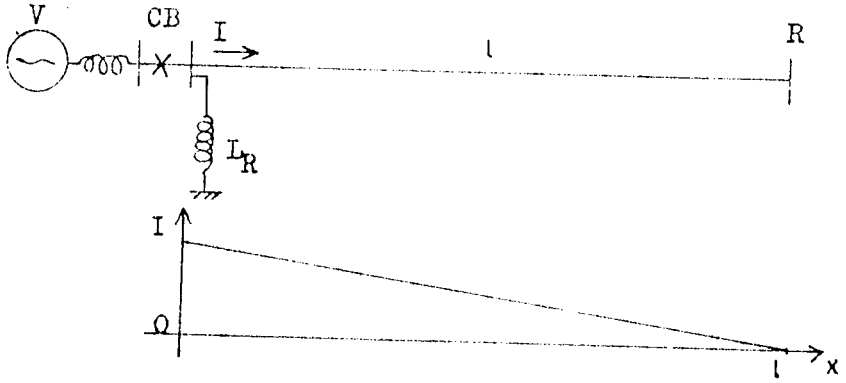

Fig. 5.16. Current distribution along the line.

The equivalent line resistance is given by the power consideration:

$$R_L = \frac{1}{I^2} \int_0^l r \left(I \frac{x}{l}\right)^2 dx = r \frac{x^3}{3\,l^2}\Big|_0^l = \frac{rl}{3} \qquad (5.9)$$

where R_L : equivalent resistance of the line

I : r.m.s. Current in the shunt reactor

r : unit length line resistance

l : line length

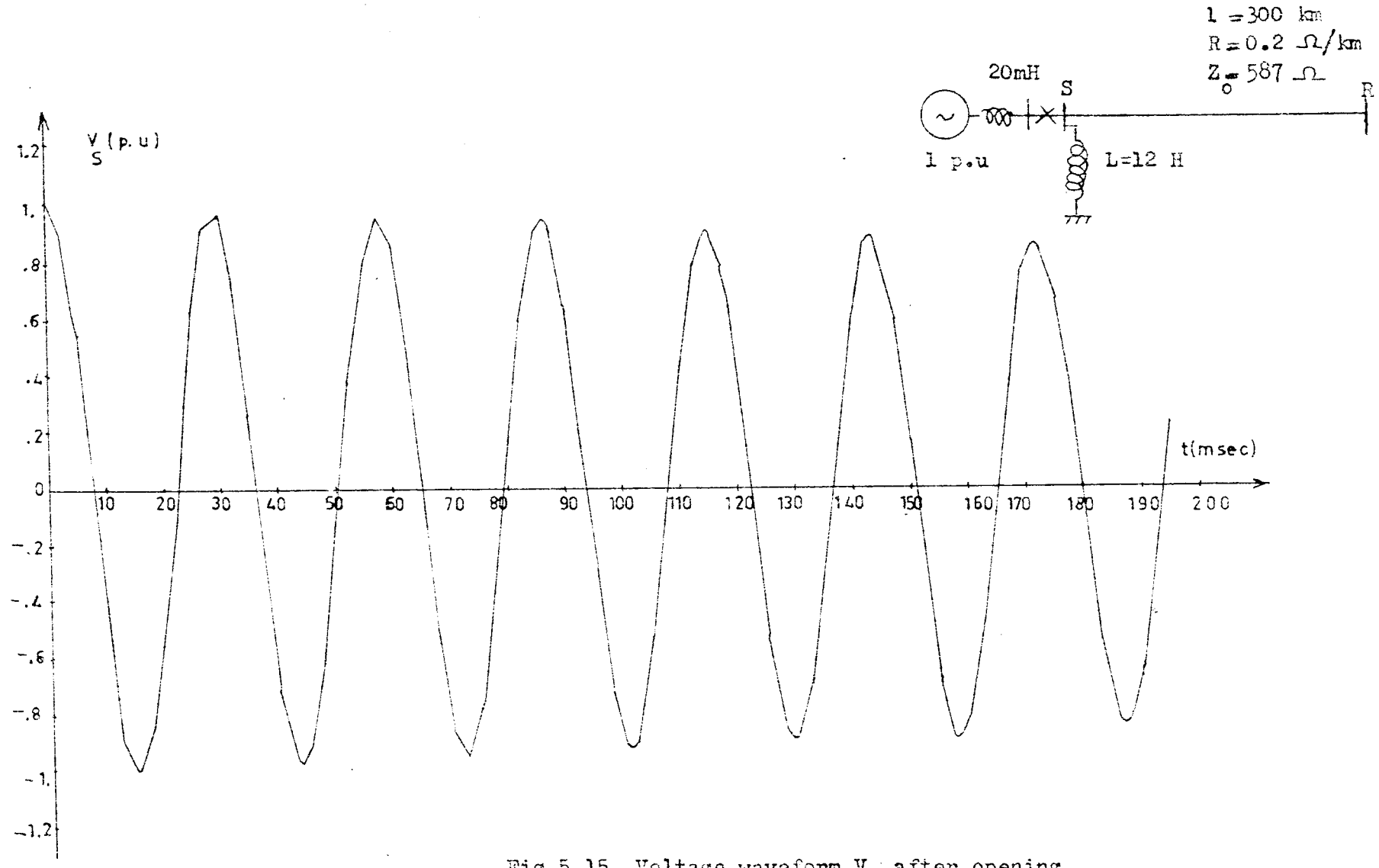

Fig.5.15 Voltage waveform V_S after opening of single phase noload shunt compensated line.

ıeglecting the line inductance

$$\tau_L \approx \frac{2L_R}{R_L} \qquad (5.10)$$

ı the help of formulas (5.9) and (5.10), the expression for τ_L becomes

$$\tau_L = \frac{6L_R}{r\ell} \qquad (5.11)$$

the system under study, the calculated time constant for decay of ped charges due to line loss by using the derived formula is given able 5.II.

e 5.II. The time constant for decay of trapped charge due to line loss at shunt compensated lines for different percentage.

(H) ctance of ıt reactor	τ_L (sec) The time constant calculated from computer results	τ_L (sec) Time constant calculated from $\tau_L = \frac{6L_R}{r\ell}$
.33	0.121	0.133
	0.27	0.3
	1.2147	1.2
.5	4.31	2.75

As it can be seen the results of τ_L calculated from the result ıomputer study and formula 5.11 are same. The line loss does not ıngly effect of the values of the decay and time constant decreases he percentage of shunt compensation increases.

5.3.2 Influence of the Reactor Loss on the Decay of Trapped Charge Voltage

Shunt reactor losses are, in many cases, a dominant factor for the decay of trapped charge voltages. For instance, according to a report,[24] in a 800 kv system (60 Hz, 300 km line length, h= .31 (percent of shunt compensation), Q= 350), it results:

τ_R = 3.7 sec. due to reactor losses

τ_L = 5.38 sec. due to line losses

In the computation, the reactor is simulated by a constant inductance L_R with a constant resistance R_R computed at $R_R = \frac{2\pi f L_R}{Q}$ where f is rated frequency and $Q = \frac{\omega L_R}{R_R}$ is the quality factor at rated voltage and frequency.

The decay time constant due only to the reactor losses is

$$\tau_R = \frac{2L_R}{R_R} = \frac{2Q}{2\pi f} \qquad (5.12)$$

if the reactors are equipped with series resistor; i.e. if they have an equivalent Q = 20, the effect of the line loss is not appreciable. The total time constant of the circuit can be evaluated by synthesizing time constants due to line loss and reactor loss as

$$\tau = \frac{1}{\frac{1}{\tau_R} + \frac{1}{\tau_L}} \qquad (5.13)$$

where τ_R : time constant in case of no line loss

τ_L : time constant in case of no reactor loss

.3.3 Opening Resistors

Fig. 5.17 shows the effect of opening resistor inserted 1.5 cycles f rated frequency on line discharging of three phase shunt compensated ine given in Fig. 5.13.

It can be observed that there is negligible effect of opening esistor on the trapped charge voltage contrary to the uncompensated ines. The reasons are:

a) The line input impedance is greatly increased by the high degree of shunt compensation, and therefore the transients at the opening resistor is lowered.

b) The main time constant of the transient current through the resistor when it is inserted is doubled if shunt reactors are connected to the line.

.3.4 Resistors Inserted in the Neutral of Shunt Compensation Reactors.[13][25][26][27]

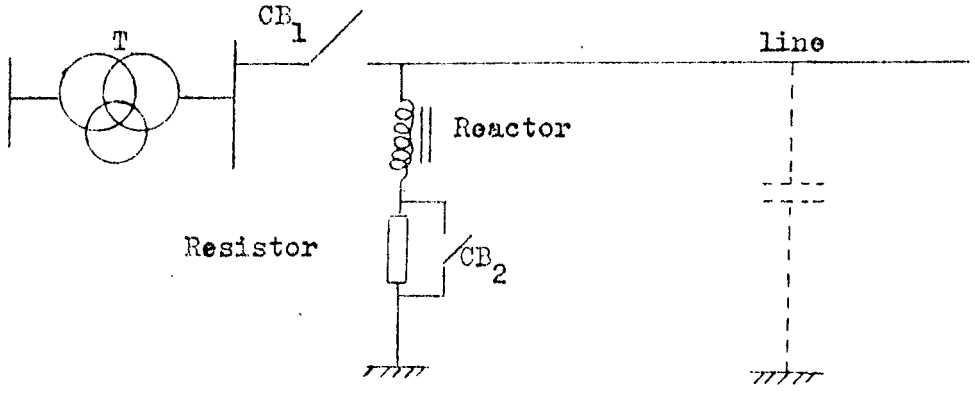

Fig. 5.18 Shunt Compensation reactors with resistors inserted in the neutral of it.

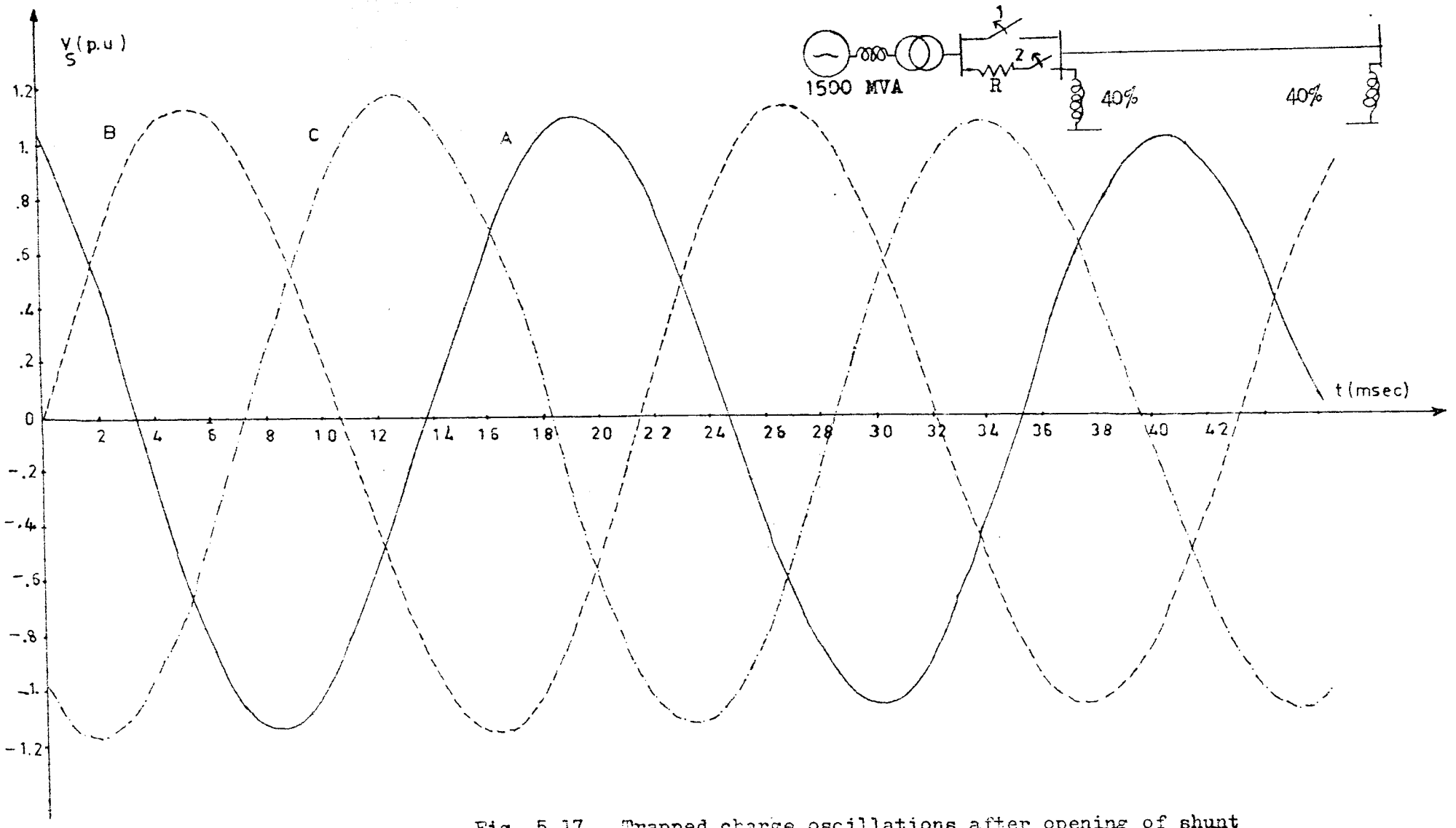

Fig. 5.17 Trapped charge oscillations after opening of shunt compensated line with opening resistor R = 4kΩ inserted for 30 msec.

For transmission lines compensated with shunt reactors, a damping resistor may be breifly inserted in the reactor circuit in order to damp the voltage oscillation produced by the capacitance of the interrupted line and the inductance of reactors, when the line is disconnected (25) (Fig.5.18). The resistors may be connected to the system permanently. But this is very costly one in terms of system losses (section 2.4.2). Therefore, the resistor would be inserted in the circuit immediately after the main breaker opens and short circuited just before it recloses as it is explained in section 2.4.2.

By considering the damping effect and resistive power loss during the normal times, an optimum value of resistor should be selected. For the power system shown in Fig. 2.6 which has characteristics given in Appendix D, a grounding resistor is inserted in the reactor circuit in order to damp the voltage oscillation (trapped charge oscillation) between the line capacitance and reactor inductance when the line is disconnected on no load.

To reduce the closing overvoltage factor in EHV systems to values less than 2.5 p.u, the trapped charge should be completely decayed during the dead time (400 millisecond) before the line reenergization.(3) By neglecting the decaying due to line loss, the value of resistor by which the reactor is grounded can calculated as follows:

$$\tau = \frac{2L}{R+R_R} \qquad (5.14)$$

where τ = decaying time constant (sec.)

L = Reactor inductance (Henry)

R_R = Reactor winding resistor (ohm)

R = Series resistor (ohm)

for the complete decaying in 400 millisecond

$$4\tau = 4\ \frac{2L}{R + R_R} = 0.4\ \text{s. with} \quad L = 7.6\ \text{H}, \quad R_R = 7.2\ \text{ohms.}$$

Hence

R = 153 ohms.

Waveforms calculated by the Transients Analysis Program for the trapped charge decaying on the line with 153 ohms resistor inserted between reactor and earth are shown in Fig. 5.19. The time constants calculated from the waveform is nearly equal to 0.1 sec.

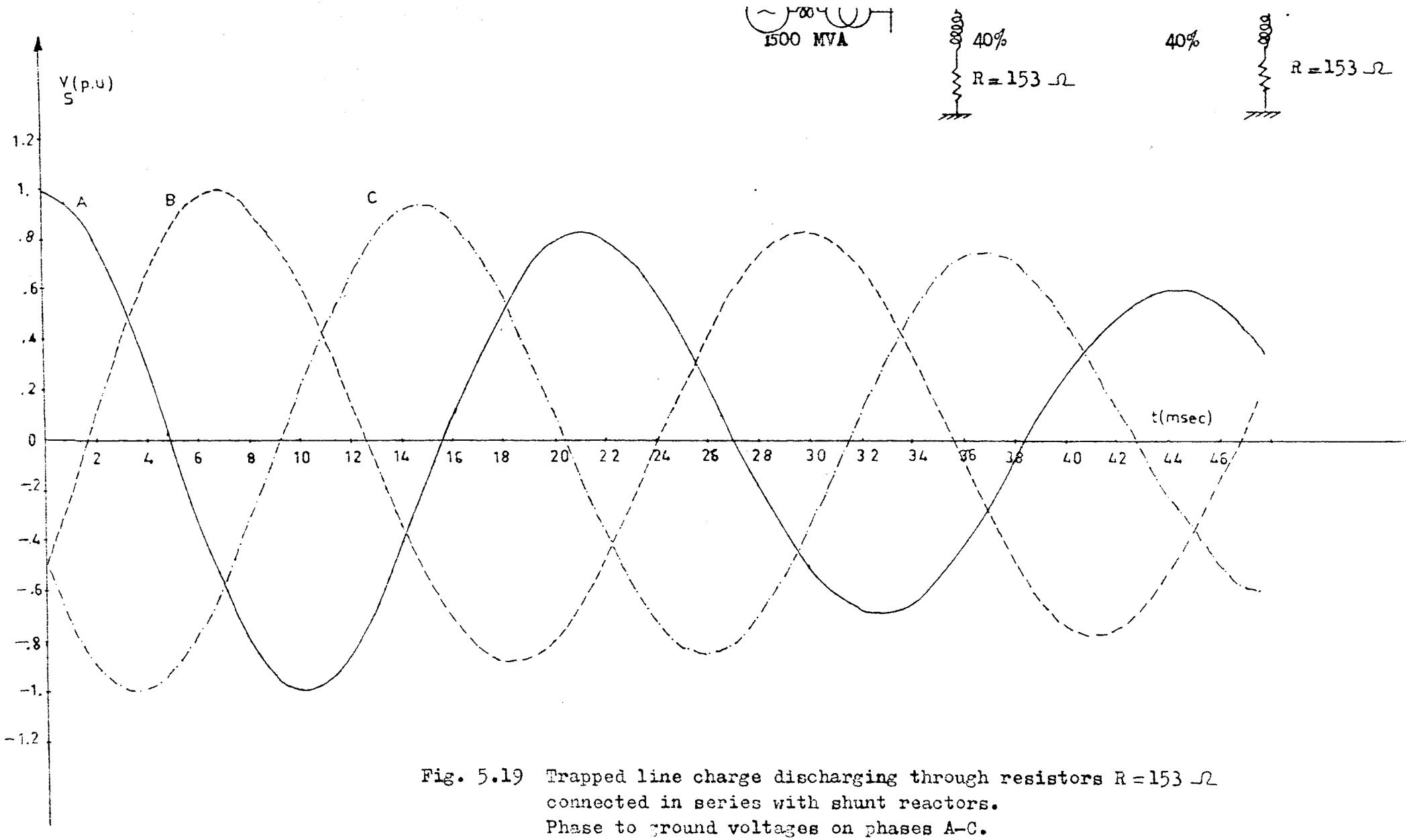

Fig. 5.19 Trapped line charge discharging through resistors R = 153 Ω connected in series with shunt reactors.
Phase to ground voltages on phases A-C.

CHAPTER VI

CONCLUSIONS

For the future EHV and UHV power systems insulation design, the insulation requirements are determined by overvoltages occuring on the system. If the line energization overvoltages are controlled and reduced to below 2.0 p.u, then the other sources of overvoltages should be investigated for proper insulation design.

Steady state overvoltages occur on the systems when the line is loaded below its surge impedance loading during the initial stages of operation which is not a problem in the long range. When the voltage rise across the system reactance due to loading below SIL is high enough to make the transformer operate above the knee of its magnetization curve, the nonlinearity of the curve generates harmonics which can result in increased overvoltages. Raising the knee of saturation curve (may be done by the transformer manufacturer) or reducing system voltage below the knee of saturation curve by application of shunt reactors, the steady state overvoltages can be controlled.

For the power system shown in Fig.3.5, maximum overvoltages were evaluated for SLG faults initiating at various points along the line (Table 3.II). From the results obtained, following conclusions have been arrived:

1. SLG fault may produce an overvoltage on an unfaulted phase as high as 1.87 p.u.

2. The worst fault location from this standpoint is at the midpoint of the line as the maximum overvoltage occurs at this point.

3. The worst termination condition is zero impedance which is approximated by a bus having several other lines. Therefore, as the UHV system increases in complexity, the transient overvoltages is generally higher.

In Chapter IV, switching conditions with particular reference to CB design and overvoltages due to load rejections and fault clearing have been studied.

1. For resistive load rejection, the CB must be capable of withstanding the peak value of system voltage within 1/4 cycle after extinction of the current, and it must develop the required dielectric strength at sinusoidal rate.

2. A CB for opening capacitive load and dropping unloaded line must be capable of withstanding appreciably higher peak values of recovery voltage (2 p.u) than are encountered in resistive switching within 1/2 cycle from current interruption. The RRRV is at sinusoidal rate of the power frequency.

3. After inductive load rejection at the receiving end of a line, voltage across CB reaches to 1 p.u in times less than 1/4 cycle of rated frequency.

4. After clearing of a terminal fault, TRV across the CB rises to ? p.u in the form of a damped oscillation superimposed on the system voltage with the natural frequency $1/\sqrt{LC}$ (Fig. 4.4). Hence, to interrupt a fault current, CB must have a high rate of rise of dielectric strength, and it must be capable of withstanding, in the single-phase case, peak recovery voltage up to twice the peak value of system voltage almost instantenously after interruption. Opening resistor inserted during opening and has a value less than $\frac{1}{2}\sqrt{\frac{L}{C}}$ damps the transient oscillations after fault clearing.

In three phase study, system parameters and different type of its onfigurations affecting on the value of transient overvoltages due to oad rejection and fault clearing have been observed.

After load is dropped at normal conditions, maximum overvoltage peak .36 p.u is obtained. This voltage rise is due to Ferranti effect and ransients caused by CB opening. Overvoltages following load dropping ue to fault on line rise to 1.73 p.u due to neutral point displacement. hunt reactors connected to the HV lines reduces the overvoltage magnitudes ince the line charging current is compensated. Moreover, opening resistor = 4 kΩ across the CB terminals during the opening damps the transient omponents and overvoltages are reduced from 1.58 p.u to 1.41 p.u Table 4.IV).

Overvoltages as high as 1.88 p.u were obtained by clearing SLG fault ith breakers not using opening resistors. As the complexity of UHV system s increased (fault fed by infinite bus) RRRV is decreased and overvoltage s reduced (Table 4.V). Low ohmic value resistors (less than 1 kΩ) limits ue overvoltages. For instance for 200 Ω opening resistor, maximum over-oltage is reduced from 1.68 p.u. to 1.52 p.u (Table 4.VI).

In Chapter IV trapped charge phenomena which is important as far as energization is considered has been studied. If an uncompensated line s droped from low voltage side, trapped charge decays through the step-up ransformer (Fig. 5.11). However, after line dropping by high side witching a d.c trapped charge stays on the line (Fig.5.2). Bu using uitable opening resistors ($R \gg \frac{1}{wC} > 4000\ \Omega$) during the opening, some f the trapped charge decays through the resistors (Table 5.I).

If the line is compensated by using shunt reactors, trapped charge oscillation occurs between line capacitance and reactor inductance. In order to prevent any unfavourable conditions that might arise when the voltage across the terminals of the CB are at full opposition at the instant of closure, the trapped charge should be drained out of the line. Opening resistor has negligible influence on the trapped charge voltage decaying (Fig. 5.17). On the other hand, resistors connected in series with reactors cause decaying of trapped charge at very high rate (Fig.5.19). However, due to large power loss under normal conditions this solution is very expensive. These series resistors should be inserted after line is disconnected and shorted before line closing by the use of a medium voltage CB.

These conclusions are based on the system constants and configurations used in this thesis. When specific EHV and UHV systems are being designed, however, it is very important that these type of transient overvoltages should be investigated using the methods discussed. This will insure discovery of any combination not covered by this thesis that may produce higher overvoltages.

REFERENCES

(1) A.Hauspurg, G.S.Vassell, G.I. Stillman, J.H.Charkow, J.C.Haahr, "Overvoltages on the AEP 765-kV System," IEEE Trans. Power Apparatus and Systems, vol. PAS-88, pp. 1329-1342, September 1969.

(2) "Transmission Line Reference Book 345 kv and Above," Electric Power Research Institute, 1975, Ch. 10.

(3) Ş.Şener, "Determination of risk of failure in EHV systems", M.S. Thesis, METU, 1978.

(4) "Consulting service on abnormal outages on external insulation of TEK 380 kv lines," CESI, report AT-2723, October 1975.

(5) "Economics and applications of shunt capacitors on utility systems," McGraw-Edison power system division, Reference No. 71011.

(6) W.Diesendorf, "Insulation Co-ordination in High Voltage Electric Power System," Butterworths, 1974.

(7) R.Gerth, H.Glavitsch, N.N. Tikhodeyev, S.S. Shur, B.Thoren, "Temporary overvoltages, their classification, magnitude, duration, shape and frequency of occurance," (CIGRE 1972, rep. 33-12).

(8) A. Greenwood, "Electrical Transients in Power Systems," John Wiley, 1971.

(9) D.D. Wilson, J.W. Yetter, "Application of Shunt reactors to EHV systems."

(10) T.R.Hoke, R.L. Shafford, "Voltage and VAR control on the SCEC ehv system," IEEE, Conference paper, No. 31PP 66-517, 1966.

(11) A.Capasso, F. Iliceto, "On the voltage control and transient over-voltages of extra-long-distance AC transmission lines," L'Eenegia Elettrica, volume LIII, 1976.

(12) G.W. Alexander, J.N. Hopkinson, A.V.Welch, "Design and application of ehv shunt reactors," IEEE, vol. PAS-85, pp. 1287-1298, December, 1966.

(13) E.F. Roynham, "Discussions on major aspects in the equipment requirements, design and construction of ESCOM's 400-kv distribution stations." H.R.Müthrich, Spreeler and Schuh Aarau, Switzerland.

(14) E.W. Kimbark, A.C. Legate, "Fault Surge versus switching surge, a study of transient overvoltages caused by line-to-ground faults," IEEE, vol. PAS-87, pp. 1762-1769, September, 1968.

(15) A.Clerici, A. Taschini, "Overvoltages due to line energization and reenergization versus overvoltages caused by fault and fault clearing in ehv systems," IEEE, vol. PAS-89, pp. 932-941, May, June, 1970.

(16) R.G.Colcloaser, Jr., C.L. Wagner, D.E.Buettner, "Transient overvoltages caused by the initiation and clearance of faults on a 1100-kv system," vol. PAS-89, November/December, 1970.

(17) J.Zaborsky, J.W.Mittenhouse, "Some Fundamental Aspects of Recovery Voltages," AIEE transactions, PAS, Feb. 1963, pp. 815-822.

(18) Application guide for transient recovery voltage for a.c. high voltage circuit breakers rated on symmetrical current basis, ANSI C37.0721-1971.

(19) Requirements for transient recovery voltage for a.c. high voltage circuit breakers rated on a symmetrical current basis, ANSI, c37.072-1971.

(20) IEC Recommendation, Pub. 56-2, High Voltage Alternating-Current Circuit Breakers, 1971/72.

(21) Glovitsch, J, "Power frequency overvoltages in EHV systems," Brown Boveri Rev. (1964), No. 1-2, pp. 21-32.

(22) TEK-PKD, "hat ve iletgenlerin taşıma kapasiteleri ve birim karakteristikleri," Ocak 1976, No. 19.

(23) TEK-Şebekeler Dairesi Başkanlığı, "Seyitömer, Seydişehir, İzmir ve Gökçekaya'daki bazı teçhizatla ilgili karakteristikler."

(24) A.Clerici, G.Ruckstuhl, A.Vian, "Influence of Shunt Reactors on Switching Surges," IEEE, vol. PAS-89, No. 8, November/December 1970. pp.1727-1736.

(25) G.Köppl, E. Russ, "Switching Overvoltages in EHV and UHV Networks," Brown Baveri Rev. 12-70, pp. 554-561.

(26) J.K. Dillard, J.M. Clayton, L.A.Kilar, "Controlling Switching Surges on 1100 - kv transmission systems," IEEE, vol. PAS-89, pp.1752-1762,1970.

APPENDIX A

DERIVATION OF TRANSMISSION LINE EQUATIONS[32]

The transmission lines are represented according to their length and the accuracy required. If high degree of accuracy is required in calculating 50 Hz lines more than approximately 150 miles long, the parameters of the line are not lumped but are distributed uniformly through the lenght of the line.

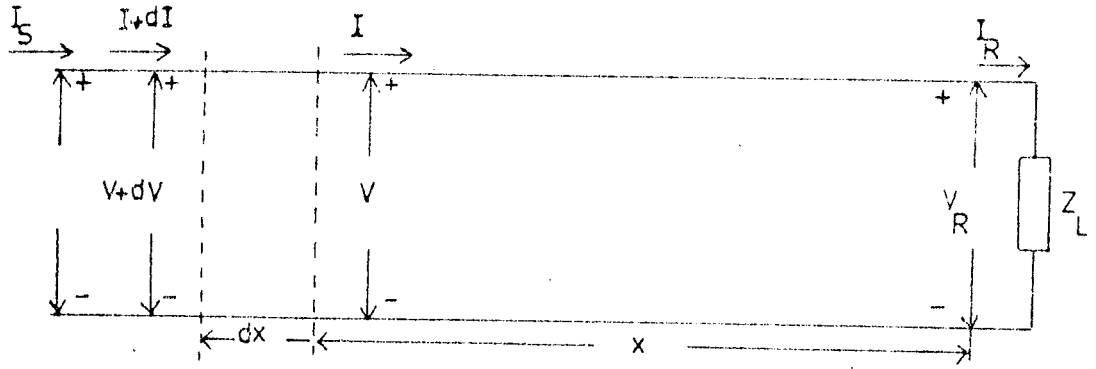

Fig.A.1 Transmission line represnetation showing differential line elements.

Fig. A.1 shows one phase and neutral connection of three phase line.Let us consider a very small element in the line and calculate the difference voltage and difference in current between the ends of the element.

Let x = distance measured from the receiving end.

dx = elemental length

zdx = series impedance of elemental length

ydx = shunt admittance of the elemental length

The rise in voltage in the direction of increasing x is the product of the current in the element flowing opposite to the direction of increasing x and the impedance of the element or $Izdx$. Thus

$$dV = Izdx$$

or
$$\frac{dV}{dx} = Iz \qquad (A.1)$$

$$V_R = V_i + V_r \tag{A.9}$$

and $$I_R = \frac{1}{z} \left.\frac{dV}{dx}\right|_{x=0}$$

$$\left.\frac{dV}{dx}\right|_{x=0} = z\, I_R \tag{A.10}$$

Taking the derivative of V with respect to x in Eqs. (A.7) and substituting the righthand side of Eqs. (A.10) for dV/dx when x = 0.

$$\left.\frac{dV}{dx}\right|_{x=0} = z\, I_R = V_i \sqrt{yz} - V_r \sqrt{yz} \tag{A.11}$$

solving Eqs. (A.9) and (A.11) for V_i and V_r give

$$V_i = \frac{V_R + I_R Z_o}{2} \tag{A.12}$$

and $$V_r = \frac{V_R - I_R Z_o}{2} \tag{A.13}$$

where $$Z_o = \sqrt{z/y}$$

Then substituting the values for V_i and V_r in Eqs. (A.7) and (A.8) and letting $\gamma = \sqrt{yz}$ we obtain

$$V(x) = \frac{V_R + I_R Z_o}{2} e^{\gamma x} + \frac{V_R - I_R Z_o}{2} e^{-\gamma x} \tag{A.14}$$

and $$I(x) = \frac{V_R/Z_o + I_R}{2} e^{\gamma x} - \frac{V_R/Z_o - I_R}{2} e^{-\gamma x} \tag{A.15}$$

At receiving end load current is equal to

$$I_R = \frac{V_R}{Z_L}$$

Hence, Eqs. (A.15) becomes

$$V(x) = \frac{1}{2} V_R \left(1 + \frac{Z_o}{Z_L}\right) e^{\gamma x} + \frac{1}{2} V_R \left(1 - \frac{Z_o}{Z_L}\right) e^{-\gamma x} \tag{A.16}$$

$\gamma = \sqrt{yz}$ is called the propogation constant and is a complex quantity

$$\gamma = \alpha + j\beta \qquad (A.17)$$

where

α: attenuation constant

β : phase constant

for lossless line $\alpha = 0$

(for longlines $X \gg R$ i.e. $\alpha \cong 0$)

thus,

$$V(x) = \frac{1}{2} V_R \left[\left(1 + \frac{Z_o}{Z_L}\right) e^{j\beta x} + \left(1 - \frac{Z_o}{Z_L}\right) e^{-j\beta x} \right] \qquad (A.18)$$

By substituting trigonometric functions for exponential terms in Eqs. (A.18) ad new equation is found.

$$V(x) = V_R \left[\cos\beta x + j \frac{Z_o}{Z_L} \sin\beta x \right] \qquad (A.19)$$

APPENDIX B

PROPOGATION OF TRAVELLING WAVES

B.1 The Wave Equations

If the line losses are negligible (R = 0) and

$$\gamma = \sqrt{zy} = p\sqrt{LC} = \frac{p}{v}$$
$$Z_o \simeq \sqrt{z/y} = \sqrt{\frac{L}{C}}$$

than Eqs. (A.14) and (A.15) give

$$V = e^{x\,p/v}\ f_1(t) + e^{-xp/v}\ f_2(t) \qquad (B.1)$$

$$i = -\frac{1}{Z_o}\left(e^{xp/v}\ f_1(t) + e^{-xp/v}\ f_2(t) \right) \qquad (B.2)$$

where

$$f_1(t) = \frac{V_R + I_R Z_o}{2} \quad \text{and} \quad f_2(t) = \frac{V_R - I_R Z_o}{2}$$

Now by Taylor's theorem

$$f(t+a) = e^{ap}\ f(t) \qquad (B.3)$$

if Eqs. (B.3) is compared with Eqs. (B.1) and (B.2) their solutions are immediately apparent as

$$V = f_1\left(t + \frac{x}{v}\right) + f_2\left(t - \frac{x}{v}\right) \qquad (B.4)$$

$$i = -\frac{1}{Z_o}\ f_1\left(t + \frac{x}{v}\right) + f_2\left(t - \frac{x}{v}\right) \qquad (B.5)$$

Any function of the form

$$f\left(t \mp \frac{x}{v}\right) \tag{B.6}$$

represents a rigid distribution, or travelling wave, because for any value of t a corresponding value of x can be found such that $\left(t \mp \frac{x}{v}\right)$ has a constant value, and therefore defines a fixed point on $f\left(t \mp \frac{x}{v}\right)$. Corresponding values of x and t which define the same point on a wave are given by

$$\begin{aligned} t - \frac{x}{v} &= C_2 \qquad \text{for the forward wave} \\ t + \frac{x}{v} &= C_1 \qquad \text{for the backward wave} \end{aligned} \tag{B.7}$$

Their velocities of propogation are found by differentiating Eqs. (B.7) as shown

$$\begin{aligned} \frac{dx}{dt} &= v = \frac{1}{\sqrt{LC}} \qquad \text{for the forward wave} \\ \frac{dx}{dt} &= v = -\frac{1}{\sqrt{LC}} \qquad \text{for the backward wave} \end{aligned} \tag{B.8}$$

Thus, it is seen that the voltage and current distribution of Eqs. (B.4) and (B.5) are propogated as travelling waves, and each may be consist of a forward wave f_2 moving in the direction of positive x and a backward wave f_1 moving in the direction of negative x, both wave having the same velocity. It is also noticed upon comparing Eqs. (B.4) and (B.5) that

$$\frac{V}{i} = \sqrt{\frac{L}{C}} = Z_o = \frac{1}{Y_o} \qquad \text{for a forward wave } f_2 \tag{B.9}$$

$$\frac{V}{i} = -\sqrt{\frac{L}{C}} = -Z_o = -\frac{1}{Y_o} \qquad \text{for a backward wave } f_2 \tag{B.10}$$

that is, the ratio of voltage to current - the surge impedance - is constant.

B.2. Reflection of Travelling Waves

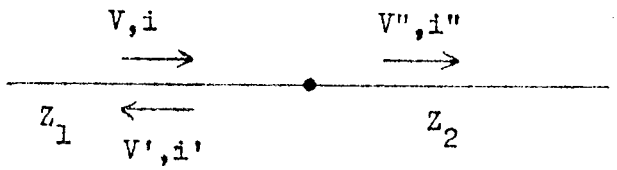

Fig.B.1. Junction of two lines or cables of different surge impedance.

A travelling wave V, i, which encounters a discontinuity (change of surge impedance), generates a reflected wave V' , i', travelling in the opposite direction. (Fig. B.1)

Beyond the discontinuity propogates a transmitted wave V" , i" so that

$$V'' = V + V' \qquad (B.11)$$

$$i'' = i + i' \qquad (B.12)$$

If the surge impedance before the discontinuity is Z_1 and the surge impedance beyond the discontinuity is Z_2 , in accordance with equations (B.9) and (B.10) the voltage and current wave are related by the surge impedance of the line.

$$\frac{V}{i} = Z_1 \qquad (B.13)$$

$$\frac{V'}{i'} = Z_1 \qquad (B.14)$$

$$\frac{V''}{i''} = Z_2 \qquad (B.15)$$

Substituting Eqs. (B.13), (B.14), (B.15) into Eqs. (B.11) , (B.12) and solving for the various quantities, there result

$$V' = V \frac{Z_2 - Z_1}{Z_2 + Z_1} \qquad \text{the reflected voltage} \qquad (B.16)$$

$$i' = -i \frac{Z_2 - Z_1}{Z_2 + Z_1} \qquad \text{the reflected current} \qquad (B.17)$$

$$V'' = V \frac{2Z_2}{Z_2 + Z_1} \qquad \text{the transmitted voltage} \qquad (B.18)$$

$$i'' = i \frac{2Z_1}{Z_2 + Z_1} \qquad \text{the transmitted current} \qquad (B.19)$$

The factor in Eqs. (B.16) is the reflection coefficient, in eq. (B.18) it is called the transmission coefficient.

For $Z_2 = Z_1$ (matched termination), there is long line. For open circuited, $Z_2 = \infty$; reflection coefficient $= +1$; voltage is doubled at incidence, current reduced to zero. For short-circuited, $Z_2 = 0$, reflection coefficient $= -1$, voltage reduced to zero, current doubled on incidence.

B.3. Mutually Coupled Circuits

The travelling wave equations for a conductor earth loop, enlarged for three parallel conductors 1, 2 and 3 are (all voltages to ground): -

$$V_1 = Z_{11} i_1 + Z_{12} i_2 + Z_{13} i_3 \qquad (B.20$$

$$V_2 = Z_{21} i_1 + Z_{22} i_2 + Z_{23} i_3 \qquad (B.21)$$

$$V_3 = Z_{31} i_1 + Z_{32} i_2 + Z_{33} i_3 \qquad (B.22)$$

where Z's are self and mutual surge impedances. It can be shown that

$Z_{12} = Z_{21}$ and $Z_{23} = Z_{32}$, $Z_{13} = Z_{31}$

Eqs. (B.20) to (B.22) apply to the forward waves and the transmitted (refracted) waves beyond the junction point. Similar equations are valid for the reverse waves generated at points of discontinuity.

$$V_1' = -Z_{11}\, i_1' - Z_{12}\, i_2' - Z_{13}\, i_3'$$

$$V_2' = -Z_{12}\, i_1' - Z_{22}\, i_2' - Z_{23}\, i_3'$$

$$V_3' = -Z_{13}'\, i_1' - Z_{23}'\, i'_2 - Z_{33}'\, i'_3$$

(Reflected wave quantities have one prime, transmitted quantities have double prime. The positive direction for voltage and currents is the direction of travel of the forward wave.)

$$V_1'' = V_1' + V_1$$

$$V_2'' = V_2' + V_2$$

$$V_3'' = V_3' + V_3$$

3.4. The Reflection Lattice (Bewley's Lattice Diagram)[33]

Before the days of digital computers, Bewley proposed a schem of space time diagrams, called lattice diagrams. This is a graphical methods of determining the voltages at any point in a transmission system and is an effective way of illustrating multiple reflexions which take place. Two axes are established, a horizontal one scaled in distance along the system and a vertical one scaled in time.

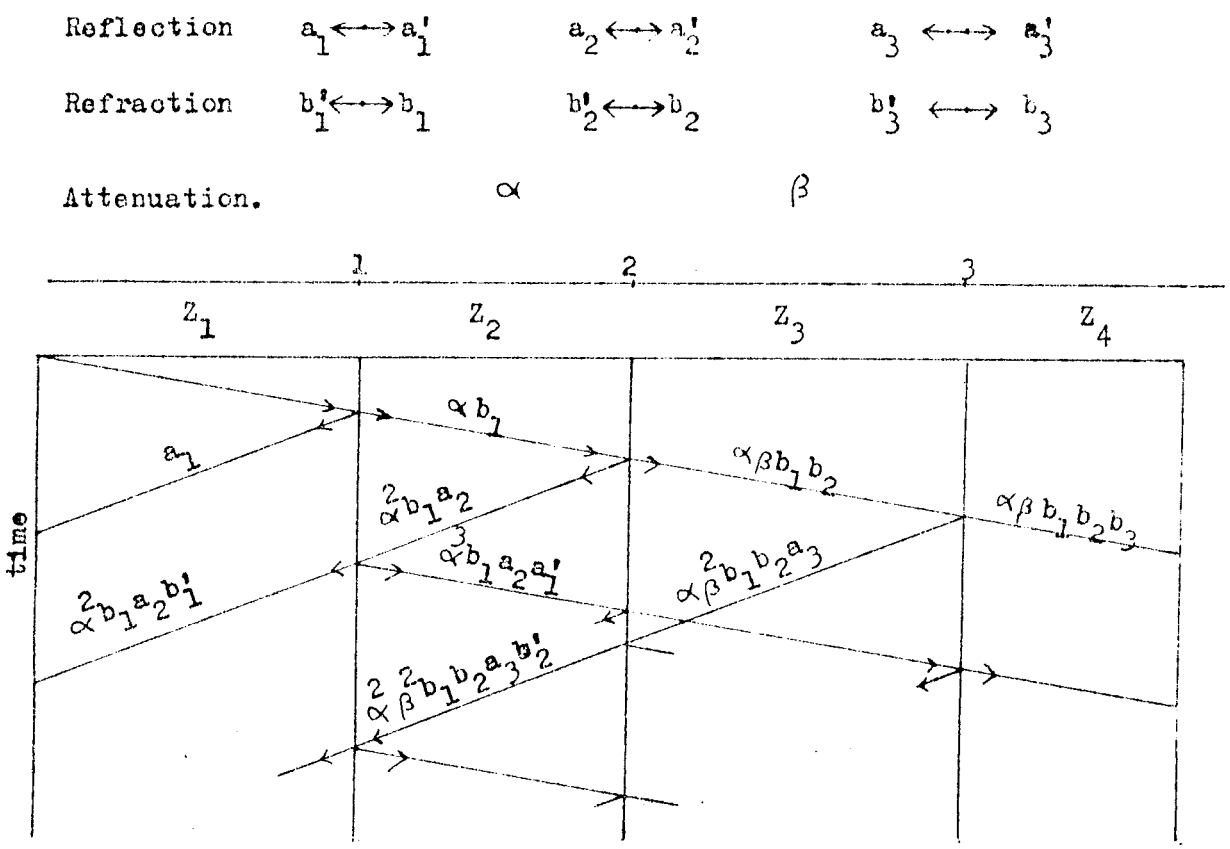

Fig.B.2 The reflection lattice.

The principle of reflection lattice is illustrated in Fig. B.2. Three junction, Nos 1,2,3 placed at unequal intervals along the line, are shown. These junctions may consist of any combination of impedances in series with the line or shunted to ground. In fact, no restrictions are placed on the generality of the impedances at the junctions as far as the lattice is concerned. The circuit between junctions may be either overhead lines or cables having, in general, different surge impedances, velocity of wave propogation and attenuation factors.

Now starting at the origin of the initial incident wave at the upper left hand corner of the lattice, obtain the coefficients for the reflected and refracted waves at each junction to the incident waves arriving there

from both the left and the right, and proceed until the lattice is completed. The coefficients labelled as follows:

a : reflection coefficient for waves approaching from the left.

a': reflection coefficient for waves approaching from the right.

b : refraction coefficient for waves approaching from the left.

b': refraction coefficient for waves approaching from the right.

α, β: attenuation factors for section between junction.

it will be observed that[33]

1. All the waves travel downhill
2. The position of any wave at any time is given by the time scale at the left of the lattice.
3. The total potential at any point at any instant of time is the superposition of all the waves which have arrived at that point up until that instant of time, displaced in position from each other by intervals equal to the differences in their time of arrival.
4. The previous history of any wave is easily traced; that is one can find where it came from and just what other waves went into its composition.
5. Attenuation is included so that the amount by which a wave is reduced in travelling between junctions is taken into account.

APPENDIX C

TRANSIENTS ANALYSIS PROGRAM[34,35]

C.1 Introduction

The Transients Analysis Program, originally developed by Dr.Dommel of the Bonneville Power Administration, calculated the overvoltages resulting from switching operations in a specific power system network.

The program can handle systems with a maximum of 400 buses, 500 branches, 20 switches, 100 sources (current or voltage), and 25 non-linear elements. The system to be studied may have distributed or lumped parameter element and arbitrary excitations.

The input data required are:

- Branch data (distributed or lumped parameter)
- Switch data
- Characteristics of non-linear elements
- Standard excitation sources
- Externally defined excitations
- Time step and total time.

The printed or plotted output can be obtained for

- Node voltages
- Maximum and minimum overvoltage magnitudes
- Switch current
- Branch current
- TRV across the CB

C.2. Used Solution Technique[34]

Electromagnetic transients in arbitrary single or multiphase networks are solved by nodal admittance matrix method.

The method of characteristics and the trapezoidal rule are combined into a generalized algorithm capable of solving transients in any network with distributed as well as lumped parameters. The method of characteristics is used for lines and trapezoidal rule of integration is used for lumped parameters.

A digital computer solution for transients is necessarily a step by step procedure that proceeds along the time axis with a variable or fixed step width Δt. The latter is assumed here. Starting from initial conditions at $t=0$, the state of the system is found at $t = \Delta t$, $2\Delta t$, $3\Delta t$, ..., until the maximum time t_{max} for the particular case has been reached. While solving for the state at t, the previous states at $t-\Delta t$, $t-2\Delta t$, ..., are known.

A limited portion of this "past history" is needed in the method of characteristics, which is used for lines, and in the trapezoidal rule of integration, which is used for lumped parameters. With a record of this past history, the equations of both methods can be represented by simple equivalent impedance networks. A nodal formulation of the problem is then derived from these networks.

C.3. Solution for Single Phase Network

C.3.1 Lossless Line

Although the method of characteristics is applicable to lossy lines, the ordinary differential equations which it produces are not directly integrable. Therefore loss is neglected at this stage.

terminal a ——————————————————— terminal b

I

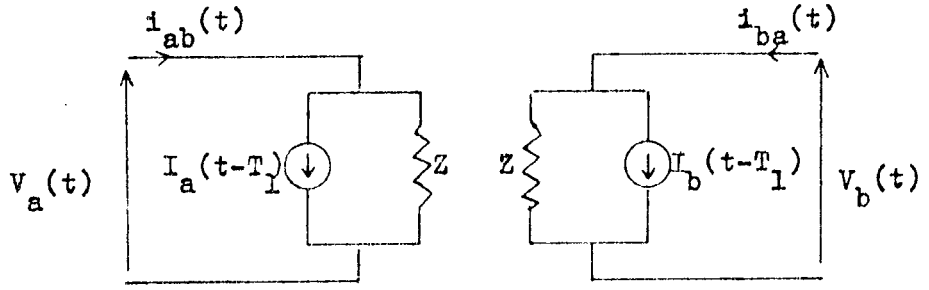

II

Fig.C.1. I) lossless line II) Equivalent impedance network.

As we have explained in Appendix B, surge travels along the line. If the travel time to get from one end of the line to the other is $T_1 = \frac{1}{v} = l\sqrt{LC}$ (l is the length of the line). Then, the voltages and current in Fig. C.1 can be related as

$$V_b(t - T_1) + Z_o\, i_{ba}(t-T_1) = V_a(t) + Z_o\,(-i_{ab}(t)) \qquad (C.1)$$

From this equation follows the simple two part equations for i_{ab}

$$i_{ab}(t) = \frac{1}{Z_o}\, V_a(t) + I_a(t-T_1) \qquad (C.2)$$

and analogous

$$i_{ba}(t) = \frac{1}{Z_o}\, V_b(t) + I_b(t-T_1) \qquad (C.3)$$

with equivalent current sources I_a and I_b which are known at state t from the past history at time $t-T_1$.

$$I_a\ (t-T_l) = -\left(\frac{1}{Z_o}\right) V_b\ (t-T_l) - i_{ba}\ (t-T_l) \qquad (C.4)$$

$$I_b\ (t-T_l) = -\left(\frac{1}{Z_o}\right) V_a\ (t-T_l) - i_{ab}\ (t-T_l) \qquad (C.5)$$

Fig. C.2 shows the corresponding equivalent impedance network, which fully describes the lossless line at its terminal. Topologically the terminals are not connected; the conditions at the other end are only seen indirectly and with a time dealy T_l through the equivalent current sources I.

C.3.2 Inductance

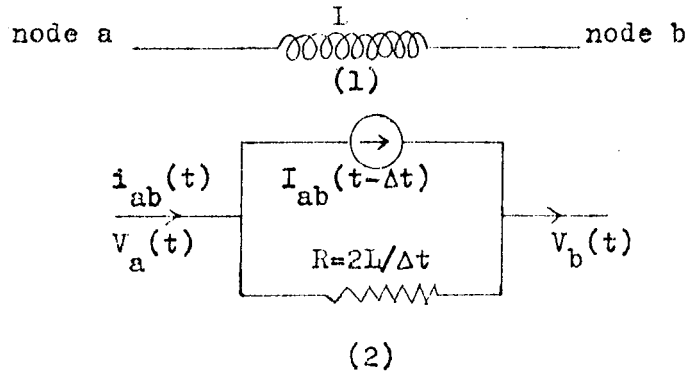

Fig.C.2 (1) Inductance. (2) Equivalent impedance network.

For the inductance L or a branch a,b, (Fig. C.2) we have

$$V_a - V_b = L\frac{di_{ab}}{dt} \qquad (C.6)$$

which must be integrated from the known state at $t-\Delta t$ to the unknown state at t

$$i_{ab}(t) = i_{ab}\ (t-\Delta t) + \frac{1}{L}\int_{t-\Delta t}^{t} V_{ab}\ (t)\ dt \qquad (C.7)$$

using the trapezoidal rule of integration yields the branch equation

$$i_{ab}(t) = \frac{\Delta t}{2L} \left(V_a(t) - V_b(t)\right) + I_{ab}(t-\Delta t) \qquad (C.8)$$

where the equivalent current source I_{ab} is again known from the past history.

$$I_{ab}(t-\Delta t) = i_{ab}(t-\Delta t) + (\Delta t/2L)\left(V_a(t-\Delta t) - V_b(t-\Delta t)\right)$$

The equivalent impedance network corresponding to equation (C.8) is shown in Fig. C.2

C.3.3 Capacitance

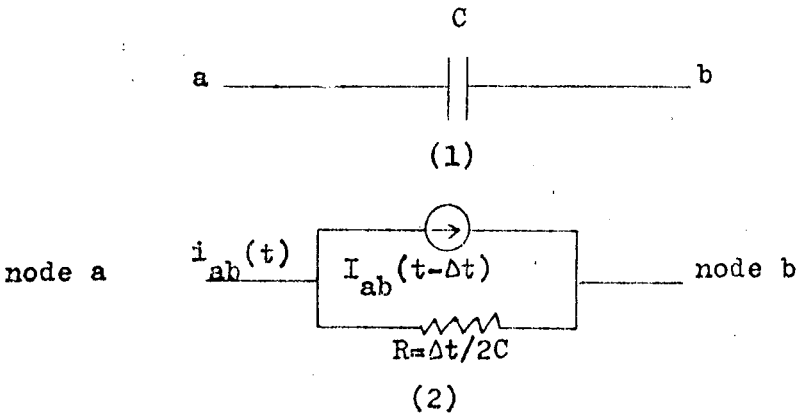

Fig.C.3 (1) Capacitance. (2) Equivalent impedance network.

For the capacitance C of a branch a, b (Fig.C.3) the equation

$$V_a(t) - V_b(t) = \frac{1}{C} \int_{t-\Delta t}^{t} i_{ab}(t)\, dt + V_b(t-\Delta t) \qquad (C.9)$$

can again be integrated with the trapezoidal rule, which yields

$$i_{ab}(t) = \left(\frac{2C}{\Delta t}\right)\left(V_a(t) - V_b(t)\right) + I_{ab}(t-\Delta t) \qquad (C.10)$$

with the equivalent current source I_{ab} known from the past history

$$I_{ab}(t-\Delta t) = - i_{ab}(t-\Delta t) - \frac{2C}{\Delta t} (V_a(t-\Delta t) - V_b(t-\Delta t)) \qquad (C.11)$$

An equivalent impedance network is shown in Fig. C.3. Its form is identical with that for the inductance.

C.3.4 Resistance

For the completeness the branch equiation is added for the resistance.

$$i_{ab}(t) = \frac{1}{R} (V_a(t) - V_b(t)) \qquad (C.12)$$

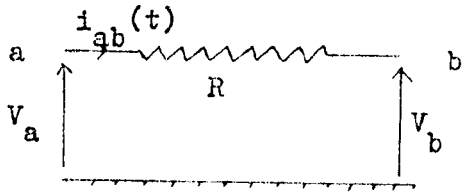

Fig.C.4. Resistance

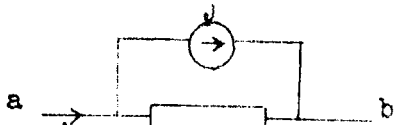

type of branch	y	j
transmisson line	$\frac{1}{Z_o}$	$I_{ab}(t-\Delta t)$
L	$\frac{\Delta t}{2L}$	$I_{ab}(t-\Delta t)$
C	$\frac{2C}{\Delta t}$	$I_{ab}(t-\Delta t)$
R	$\frac{1}{R}$	-

Fig.C.5 General impedance network.

C.3.5 Nodal Equation:

Performance equation of each device can be written as

$$i - j = y\ V \qquad (C.13)$$

Also a matrix equation at time t :

$$[Y]\ [V(t)] = [i(t)] - [j] \qquad (C.14)$$

with

$[Y]$ nodal conductance matrix which remains unchanged as long as t remains unchanged.

$[V(t)]$ column vector of node voltage at time t .

$[i(t)]$ column vector of injected node currents at time t .

$[j]$ known column vector, which is made up of known equivalent current sources I.

In Eqs. (C.14) part of the voltages will be known (specified excitations) and the others will be unknown. Let the nodes be subdivided into a subset A of nodes with unknown voltages and subset B of nodes with known voltages. Subdividing the matrices and vectors accordingly it is obtained from Eqs. (C.14)

$$\begin{bmatrix} Y_{AA} & Y_{AB} \\ Y_{BA} & Y_{BB} \end{bmatrix} \begin{bmatrix} V_A(t) \\ V_B(t) \end{bmatrix} = \begin{bmatrix} i_A(t) \\ i_B(t) \end{bmatrix} - \begin{bmatrix} j_A \\ j_B \end{bmatrix} \qquad (C.15)$$

from which the unknown vector $V_A(t)$ is found by solving

$$\left[Y_{AA}\right] \left[V_A(t)\right] = \left[I_{total}\right] - \left[Y_{AB}\right] \left[V_B(t)\right] \qquad (C.16)$$

$$\left[I_{total}\right] = \left[i_A(t)\right] - \left[j_A\right] \qquad (C.17)$$

The equation (C.16) is best solved by triangular factorization of the augmented matrix $\left[Y_{AA}\right]$, $\left[Y_{AB}\right]$ once and for all before entering the time step loop. The same process is then extended to the vector $\left[I_{total}\right]$ in each time step in the so-called forward solution, followed by back substitution to get $\left[V_A(t)\right]$ as indicated in Fig.C.6.

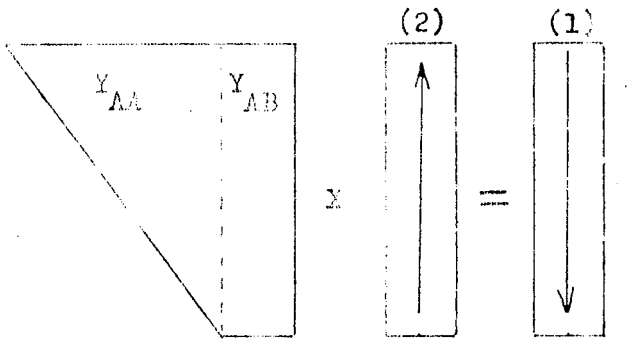

INITIALLY:

TRIANGULAR FACTORIZATION

IN EACH TIME STEP:

(1) FORWARD SOLUTION

(2) BACK SUBSTITUTION

Fig.C.6 Repeat solution of linear equations.

C.4 Switches:

The network may include any number of switches, which may change their positions in accordance with defined criteria. They are represented as ideal ($R=0$ when closed and $R=\infty$ when open); however, any branches may be connected in series or parallel to simulate physical properties (e.g time varying current dependent resistance).

When switching position has changed some modifications must be made on the calculation.

C.5 Lossless Multiphase Line:

Equations (A.5) (A.6) are also valid for the multiphase lines if the scalars are replaced by vectors V, I and matrices Z, Y.

$$\left[\frac{d^2 V(x,t)}{dx^2}\right] = \left[Z\right]\left[Y\right]\left[V(x,t)\right]$$
$$\left[\frac{d^2 I(x,t)}{dx^2}\right] = \left[Y\right]\left[Z\right]\left[I(x,t)\right] \qquad (C.18)$$

The solution of Eqs.(C.18) is complicated by the presence of off-diagonal elements in the matrices which occur because of mutual coupling between the phases. This difficulty is overcome if the phase variables are transformed into mode variables by similarity transformations that produce diagonal matrices in the modal equations. This is well known eigen value problem. Each of the independent equations in the modal domain can then be solved with the algorithm for the single phase line by using its modal travel time and its modal surge impedance.

Multiphase lines with distributed parameters are assumed to be balanced (uniformly transposed transmission lines). This shall be defined as follows: The self-impedances of all phases are equal among themselves and all mutual impedances are equal among themselves. i.e.

$$Z = \begin{bmatrix} Z_s & Z_m & Z_m \\ & Z_s & Z_m \\ & & Z_s \end{bmatrix} \qquad Y = \begin{bmatrix} Y_s - Y_m & - Y_m \\ & Y_s - Y_m \\ & & Y_s \end{bmatrix}$$

where $Z_s = \dfrac{Z_{11} + Z_{22} + Z_{33}}{3}$ $\qquad Z_m \dfrac{Z_{31} + Z_{21} + Z_{32}}{3}$

For "balanced" lines transformation is defined by

$$\left[V_{phase}\right] = \left[Q\right]\left[V_{mode}\right] \qquad (C.19)$$

$$\left[i_{phase}\right] = \left[S\right]\left[i_{mode}\right] \qquad (C.20)$$

with $$\left[Q\right] = \begin{bmatrix} 1 & 1 & \cdots & 1 \\ 1 & 1-M & \cdots & 1 \\ & 1 & & \\ & & & \\ 1 & 1 & \cdots & 1-M \end{bmatrix}$$, with M = number of phases

let's define

$$\left[S\right] = \left[Z\right]\left[Y\right]$$

with $$\left[S\right] = \begin{bmatrix} S_s & S_m & S_m \\ & S_s & S_m \\ & & S_s \end{bmatrix}$$

where $$\left[Q\right]^{-1}\left[S\right]\left[Q\right] = \Lambda = \begin{bmatrix} Z_o & & & \\ & Z_1 & & \\ & & Z_1 & \\ & & & \ddots \\ & & & & Z_1 \end{bmatrix}$$

with $Z_o = S_s + (M-1)\, S_m$ M = number of phases

$Z_1 = S_s - S_m$

and $\gamma_1 = \gamma_2$ = aerial mode $= (S_s - S_m)^{1/2}$

γ_3 = ground mode $= (S_s + (M-1)\, S_m)^{1/2}$

It can be shown that the phase current vector (i_{ab}) entering nodes at terminal a toward b can again be written as a linear vector equation

$$\left[i_{ab}(t)\right] - \left[G\right]\left[V_a(t)\right] + \left[I_a\right] \qquad (C.21)$$

and analogous for $\left[i_{ba}\right]$. Equation (C.21) is derived from a set of modal equations, subjected to the transformations (C.19). In building $\left[Y_{AA}\right]$, $\left[Y_{AB}\right]$ in (C.16), a matrix $\left[G\right]$ is entered instead of a scalar value $1/Z$. The vector $\left[I_a\right]$, which enters $\left[I_A\right]$, is calculated from the past history of the modal quantities. Since the span $(t-T_1)$ for picking up the past is different for each mode, a time argument was deliberately omitted in writing $\left[I_a\right]$. Even though the nodal equations are in phase quantities, the past history must be recorded in modal quantities.

C.6. Lumped Series Resistance in Line

To approximate losses in the lossless line representation, the transient program lumps R/4 at both end and R/2 at the middle of the line where

$$R = r\,l$$

where r = resistance per unit length

l = length of the line

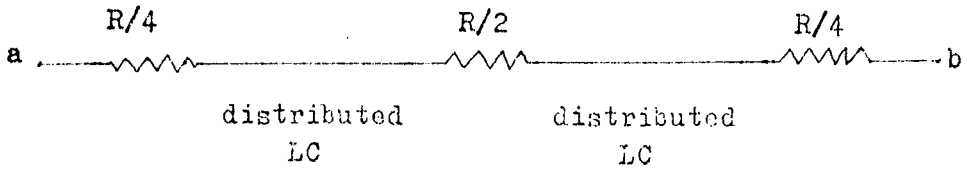

Fig.C.7 Lumped Series resistance in line.

APPENDIX D

SYSTEM PARAMETERS USED IN STUDIES[22,23]

Generators

Rating : 180 MVA

Rated voltage: 15 kv

Zero sequence impedance: 4.4 % p.u

Negative sequence impedance: 12.1 % p.u

Set-up transformers

Nominal rating: 135/180 MVA

No load voltage ratio: 380/15 kv

Short circuit reactance: 12% p.u

No load current at base voltage: 0.42 % p.u.

Per unit voltage at knee point: 1.117

Magnetization curve slope ratio: 0.00063

d.c magnetization curve is used

Autotransformers

Nominal rating: 180/180/44 MVA

No load voltage ratio:

HV : 380 kv IV: 154 kv LV: 15.8 kv

Short circuit reactances:

X(HV/IV) = 11 % p.u , X(HV/LV) = 27.8 % p.u

X(IV/LV) = 14.7 % p.u

No load current at base voltage: 0.49 %

Per unit voltage at knee point: 1.111 p.u

Magnetization curve slope ratio: 0.00166

d.c magnetization curve is used.

380 kv transmission lines

Positive and negative sequence system

$R_1 = 0.0315$ Ω/km

$L_1 = 1.009$ mH/km

$C_1 = 11.6$ nF / km

Zero sequence system

$R_o = 0.314$ Ω/km

$L_o = 3.1258$ mH/km

$C_o = 7.75$ nF/km

Shunt Reactors

$Z_R = 7.22 + j\ 2406.6$

Q = 334 L = 7.66 H

Saturation curve-linear.

Load

S = 145 + j 178 MVA

Bus capacitance

C = 2500 pF

System freguency

50 Hertz